

Contributions to Gemology

No.9 May 2009

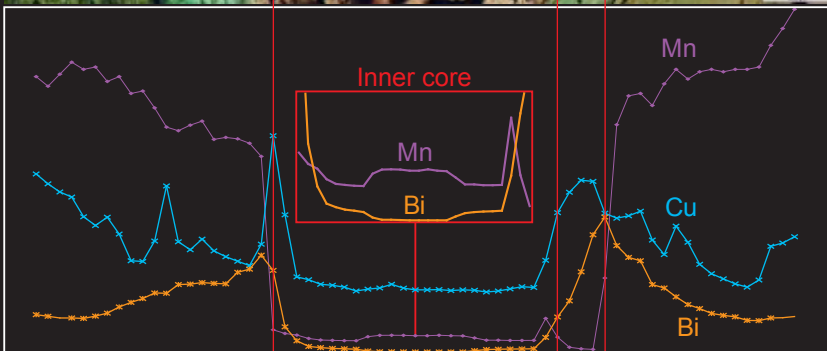
Chemical Variations in Multicolored "Paraíba"-Type
Tourmalines from Brazil and Mozambique:
Implications for Origin and Authenticity Determination



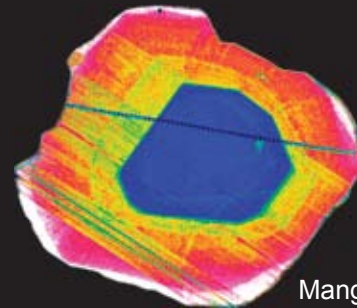
"Cuprian-Elbaite"-Tourmaline from Mozambique



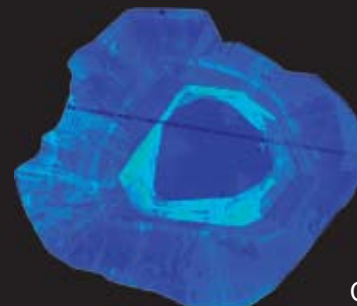
"Paraíba"- Tourmaline from Brazil



Chemical Variation in "Paraíba"-Tourmaline



Manganese



Copper

Chemical Distribution Mapping

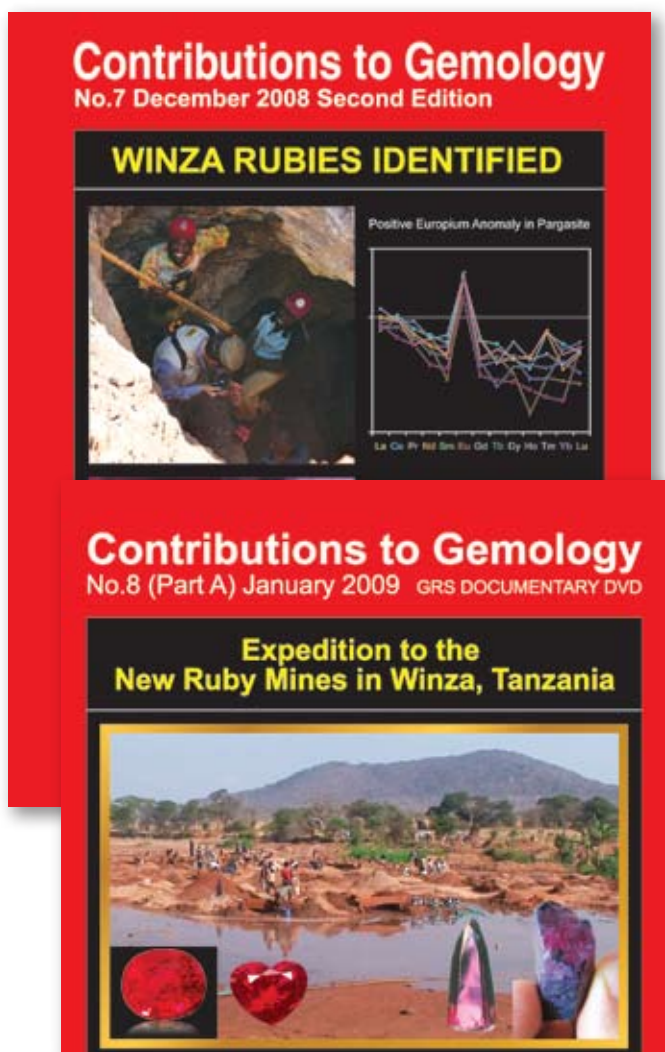
GRS

**GEMRESEARCH
SWISSLAB**

Editor

Dr. A. Peretti, FGG, FGA, EurGeol
GRS Gemresearch Swisslab AG, P.O.Box 4028,
6002 Lucerne, Switzerland
adolfo@peretti.ch

Previous Journal and Movie



This journal follows the rules of the Commission on New Minerals and Mineral Names of the IMA in all matters concerning mineral names and nomenclature.

Distributor

GRS (Thailand) Co., LTD
257/919 Silom Rd., JTC Building
Bangkok 10500, Thailand.

Journal and Website Copyrighted by GRS (Thailand) Co. LTD, Bangkok, Thailand and GRS Gemresearch Swisslab AG, Lucerne, Switzerland

This report is available online at
www.gemresearch.ch

ISBN 978-3-9523359-9-4



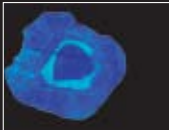
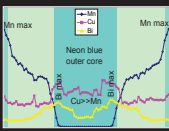
Message from the Editors Desk: When trace element research matters most

When copper bearing tourmalines were found 20 years ago in the state of Paraíba in Brazil, they intrigued by their “neon”-blue color and soon became known as “Paraíba” tourmalines in the trade. In the years before and into the new Millennium, these tourmalines have emerged to become one of the most valuable and demanded gems, comparable to prestigious rubies and sapphires. In the last couple of years an unprecedented tourmaline boom has occurred due to the discovery of new copper-bearing tourmaline deposits. The name “Paraíba” tourmaline was originally associated only with those copper-bearing tourmalines (or “cuprian-elbaïtes”), which were found in the state of Paraíba (Brazil). New mines were subsequently encountered in Rio Grande do Norte in Brazil, as well as in Nigeria and in Mozambique. The market and the laboratories were split on the issue whether to call the newly discovered neon-blue colored tourmalines “cuprian-elbaïtes” or “Paraíba tourmaline” regardless of origin. While this controversy initiated the first high-profile law suite in the USA (currently dropped), the debate on Paraíba tourmalines progressed into a new direction. A first theory emerged on the Internet and in a seminar at the Tucson show in 2009, arguing that Paraíba tourmaline may have been diffusion-treated.

In 2006, GRS has announced on its website, that it had achieved to apply a chemical testing procedure which enables to distinguish “Cuprian-Elbaïtes” from different origins, based on an extensive research program. In the light of the new controversy, GRS and the laboratory of Inorganic Chemistry and Applied Biochemistry from the ETH Zurich decided to publish this specialized research report in full length.

Although some chemical data on the origin of Paraíba tourmalines have been published elsewhere, we have chosen a different approach in our research and combined the capabilities of different analytical techniques. We concentrated on the analysis of element variations within single crystals of copper-bearing tourmalines, which contain pronounced color zoning and extensive chemical variability. Fortunately, it was possible to solve two different issues at the same time: Establish criteria for origin determination of “Paraíba tourmalines” as well as to characterize natural chemical zoning patterns within these tourmalines. We are confident that our research will prevent further confusion between “chemical fingerprints” induced by nature and those claimed to be potentially inflicted by treatment techniques.

Adolf Peretti

	<i>Introduction</i>	1		<i>The "Quintos" -Tourmaline Mine in the State of Rio Grande Do Norte (Brazil)</i>	15
	<i>World-Wide Occurrence of Copper-Bearing Tourmalines</i>	2			
	<i>Jewelry Sets with High Valuable "Paraiba"-Type Copper-Bearing Tourmalines</i>	3		<i>Underground Mining and Occurrence of Copper-Bearing Tourmalines in the Host Rock at the Quintos Mine in Brazil</i>	16
	<i>Different Types of Faceted Copper-Bearing Tourmalines from Mozambique</i>	4		<i>Multicolored Copper-Bearing Tourmaline in the Host Rock at the Quintos Mine (Rio Grande Do Norte, Brazil)</i>	17-18
	<i>Materials and Statistic</i>	5			
	<i>Statistics of Size, Color and Enhancement of Cuprian-Elbaite (-Tourmaline) from Mozambique</i>	6		<i>Electron Microprobe Profile Analysis of Paraiba Tourmalines</i>	19-20
	<i>Copper-Bearing Tourmalines From Brazil</i>	7		<i>Backscattered Electron Images and Element Distribution Mapping of Paraiba Tourmaline EMPA</i>	21
	<i>Statistics of Size, Color and Enhancement of Copper-Bearing Tourmaline from Brazil</i>	8		<i>Electron Microprobe Analysis: Element Distribution Mapping</i>	22
	<i>Type Locality of "Paraiba"-Tourmalines in Brazil: The Batalha Mine</i>	9		<i>Electron Microprobe (EMPA) and LA-ICP-MS Analysis</i>	23
	<i>Underground Mining of "Paraiba"-Tourmalines</i>	10		<i>LA-ICP-MS, LIBS and ED-XRF Analysis (Methods)</i>	24
	<i>Archive Pictures from the "Paraiba"-Tourmaline Mining Operation at the Batalha Mine (Batalha, Paraiba, Brazil)</i>	11		<i>LA-ICP-MS Chemical Analysis Profiles of Paraiba Tourmaline, Batalha Mine Sample No. GRS-Ref2976</i>	25-32
	<i>The Recent "Paraiba"-Tourmaline Mines at Batalha (Paraiba, Brazil)</i>	12		<i>LA-ICP-MS Chemical Analysis Profiles of Paraiba Tourmaline, Batalha Mine Sample No. GRS-Ref 2976.2</i>	33-34
	<i>Multicolored Tourmaline Rough Crystals from Paraiba (Brazil)</i>	13		<i>LA-ICP-MS Chemical Analysis Profiles of Paraiba Tourmaline, Batalha Mine Sample No. GRS-Ref2965</i>	35-36
	<i>Paraiba Tourmalines in the Host Rock (Batalha Mine, "Heitor"-Shaft)</i>	14		<i>LA-ICP-MS Chemical Analysis Profiles of Paraiba Tourmaline, Batalha Mine 1988, Pavlik Collection Sample No. GRS-Ref3111</i>	37-38

Contents of Contributions to Gemology No.9



LA-ICP-MS Chemical Analysis Profiles of "Paraiba"-Tourmaline, Rio Grande Do Norte, Quintos Mine (P. Wild), Sample No. GRS-Ref2079 39-40

Inclusion Research Case Study of a Copper-Bearing Tourmaline from Mozambique: Materials 41



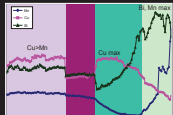
Inclusion Research Case Study of a Copper-Bearing Tourmaline from Mozambique 42-45

Inclusion Research Case Study of a Copper-Bearing Tourmaline from Mozambique: Summary and Interpretation 46



Color-Zoning in Copper-Bearing Tourmalines from Mozambique 47

LA-ICP-MS Analysis Profiles of Multicolored Tourmaline from Mozambique 48-50
Sample No. GRS-Ref3134.



LA-ICP-MS Analysis Profiles of Multicolor Tourmaline from Mozambique 51-52
Sample No. GRS-Ref7782

Ga-Pb

Comparison of Chemical Analysis Profiles: Ga- and Pb-Concentrations LA-ICP-MS Analysis 53

Ga-Pb and Cu-Ga

Diagram for Origin Determination of Tourmalines LA-ICP-MS Analysis 54-55

Cu/Ga

Diagram for Origin Determination of Tourmalines Comparison of ED-XRF with LA-ICP-MS Analysis 56

Origin Determination of Copper-Bearing Tourmalines: Flow Chart of Methods 57

Pb, Be

Comparison of Variation of Pb- and Be-Concentrations in Multicolored Copper-Bearing Tourmalines from Brazil and Mozambique 58

Be-(Mn+Cu) Be-Mn-Cu

Diagram for Origin Determination of Copper-Bearing Tourmalines 59-60

Cu+Mn Pb/Be

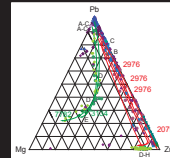
Diagram for Origin Determination of Copper-Bearing Tourmalines 61-62

Cu+Mn Pb/Be

Diagram for Origin Determination of Copper-Bearing Tourmalines: Different Color Groups 63-64

Classification of Copper-Bearing Tourmalines Using Mn- and Bi-Concentrations (LA-ICP-MS and ED-XRF Analysis) 65

Conclusions 66



Chemical Evolution Trends in Copper-Bearing Tourmalines 67-68

About the Authors, Acknowledgment and Literature 71-72

Analyses

Chemical Compositions from Brazil. Sample No. GRS-Ref3111, 2079, 2965 73

Chemical Compositions from Brazil. Sample No. GRS-Ref2976 74

Chemical Compositions from Mozambique. Sample No. GRS-Ref7782, 3134 75

Chemical Compositions from Mozambique. Sample No. GRS-Ref2939, 2942, 2943, 3138, 3143 76

Chemical Compositions from Nigeria 77

CHEMICAL VARIATIONS IN MULTICOLORED “PARAIBA”-TYPE TOURMALINES FROM BRAZIL AND MOZAMBIQUE: IMPLICATIONS FOR ORIGIN AND AUTHENTICITY DETERMINATION

Adolf Peretti (1,2,3), Willy Peter Bieri (2,3), Eric Reusser (4), Kathrin Hametner (5) and Detlef Günther (5)

(1) GRS Gemresearch Swisslab AG, Sempacherstr. 1, CH-6003 Lucerne, Switzerland

(2) GRS Gemresearch Swisslab AG, Rue du Marché 12, CH-1204 Geneva, Switzerland

(3) GRS (Thailand) CO LTD, Bangkok, Silom 919/257, 10500 Bangkok, Thailand

(4) Institute of Mineralogy and Petrography, Clausiusstr. 25, ETH Zentrum, CH-8092 Zurich, Switzerland

(5) Laboratory of Inorganic Chemistry, ETH Hönggerberg, HCI, G113, CH-8093 Zurich, Switzerland

INTRODUCTION

Copper-bearing tourmalines (or “cuprian-elbaïtes”) with neon-blue colors are considered highly valuable gemstones matching prices that are normally only equaled by valuable rubies and sapphires. Part of the trade and some laboratories have introduced the new variety name “Paraíba” tourmalines for the “neon”-blue colored cuprian-elbaïte. (www.gemresearch.ch/news). Currently a large number of publications were released on copper-bearing tourmalines from various localities (see review Lit. Par11-44).

Copper-bearing tourmalines were discovered in the Paraíba State, Brazil, in the late 1980’s (Lit. Par22 and 23), in the neighboring Rio Grande do Norte State in Mulungu (Parelhas) and in Alto dos Quintos (Lit. Par20 and 28). On the African continent the tourmalines occurred in Idaban State and Ofiki in Ilorin State, Nigeria (Lit. Par17, 18, 31, 32, 40 and 44) as well as in the Mavuco area in the Alto Lingonha pegmatite district of Mozambique (Lit. Par41).

Historically, tourmalines from Paraíba were discovered first, followed by Rio Grande do Norte (both in Brazil), Nigeria and Mozambique. Cuprian-elbaïte occurs in different colors, such as purple, violet, blue and green. Heat-treatment of purple and violet colors can be transformed to neon-blue colors (See e.g. Lit. Par11 and 33). Cu-bearing tourmalines from Mozambique have become commercially important gems with colors such as purple, violet, blue. The copper-bearing, unheated tourmalines occur in extremely large size, fine clarity and vibrant colors (Fig. Par05). Some of the magnificent tourmalines of Paraíba-type neon-colors reached extremely large sizes exceeding 100ct (Fig. Par05). These magnificent pieces were mostly heat-treated (Fig. Par07). Large copper-bearing tourmalines of such excellent clarity are less commonly known from the Brazilian deposits. On the other hand, the color intensity of the “neon-blue” colors of Paraíba tourmalines from Brazil is almost unmatched (Fig. Par01, 09, 10 and 14d). A first

detailed chemical study aimed for origin determination using LA-ICP-MS has been published (Lit. Par11 and 33). Since it has been proposed that the separation of tourmalines of different origin using standard gemological testing is not possible, we acquired an extensive set of data using different analytical techniques.

In this study, we concentrate on the detailed chemical profile analyses of color-zoned copper-bearing tourmalines from Brazil and Mozambique using LA-ICP-MS spectroscopy and element concentration mapping by electron microprobe. New insights on the chemical evolution during growth of copper-bearing tourmalines were obtained with important consequences for origin determination and understanding of natural chemical zoning in these tourmalines. A test procedure is proposed that enables origin determination by the combination of ED-XRF and LIBS analyses in addition to LA-ICP-MS using matrix-matched calibration samples prior analyzed by EMPA and LA-ICP-MS.



Fig. Par01 Example of a pair of “neon-blue” copper-bearing tourmaline (or “Cuprian-elbaïte”) from Brazil in the mounting. This type of tourmaline is also known as Paraíba tourmaline in the trade. The tourmalines are the most valuable members of the tourmaline group. The two stones are total 15ct (7ct and 8ct). Photo courtesy P. Wild (Idar-Oberstein, Germany).

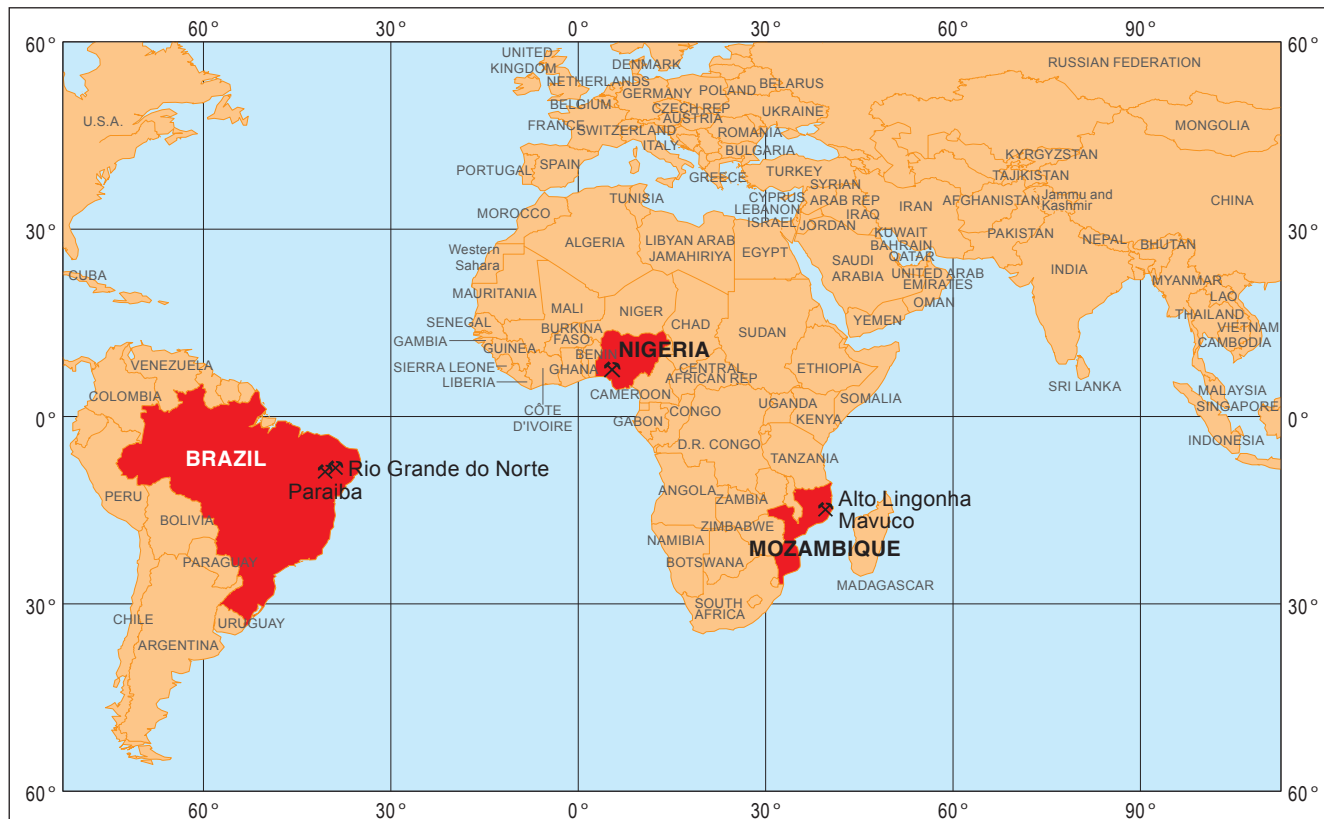


Fig. Par02 Geographic map shows the occurrence of copper-bearing tourmalines with commercial importance. The classical “Paraíba” tourmaline occurs in Brazil and new occurrences are found in Africa (Nigeria and Mozambique). The Brazilian occurrences are found in the state of Paraíba and Rio Grande do Norte (See Fig Par03).

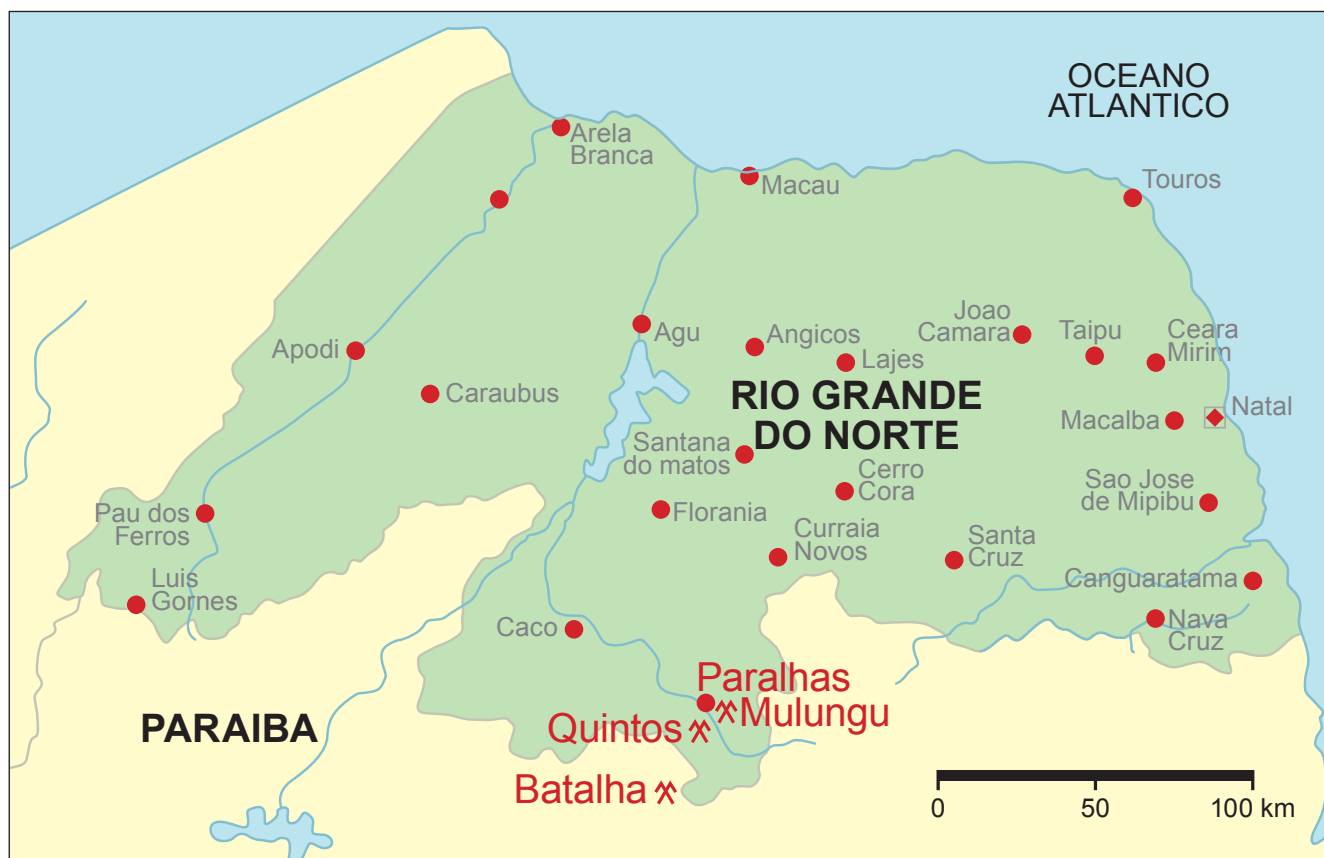


Fig. Par03 Map shows the occurrence of copper-bearing tourmalines in Brazil in the State of Paraíba and Rio Grande do Norte. Although not all the tourmalines occur in the state of Paraíba, all copper-bearing tourmalines from Brazil are called “Paraíba” tourmalines, particularly if they possess so-called “Neon”-colors.



Fig. Par04 Example of high valuable jewelry sets with "Paraiba"-type tourmalines as center stones. These copper-bearing tourmalines are of mixed origins, either from Brazil or Mozambique. Left: Stone in necklace is 72ct, in the ring is 32ct and in the ear clips of a total of 12ct. Jewelry set is of similar size but different design. Courtesy Hatta New World. Picture Among Imaging and Hatta New World. Presentation Miriam Peretti.

Different Types of Faceted Copper-Bearing Tourmalines from Mozambique



10 ct



11 ct

"Neon"-Greenish-Blue



31 ct



Violet 22ct



Pastel Blue 38ct



Vivid Violet 24ct



Purple-Pink 23ct



Vivid Purple 41ct



Vivid Green 16ct



Vivid Yellowish-Green 9ct

Fig. Par05 Examples of gem-quality faceted copper-bearing tourmalines (cuprian-elbaïtes) from the origin of Mozambique. The faceted bluish-green tourmaline over 140ct is one of the largest example of "Paraiba"-type color so far tested by GRS. Copper-bearing tourmalines of different other vivid colors are also found. Copper-bearing tourmaline from Mozambique with "neon"-blue colors are most similar in appearance to counterparts from "Paraiba" (Brazil).

MATERIALS

Copper-bearing tourmalines from Brazil were obtained at the Tucson show in 2005 from 3 different sources specialized in “Paraiba”-tourmaline from the Batalha mine (Van Wagoner, R.C. Gemmas, Bryan Pavlik). These materials were partially from old inventories from the production year 1988 (Lit Par16). Photographs of the materials see Fig. Par10, 17, 29, 58 and 61. Brazilian samples from Rio Grande do Norte were obtained from P. Wild (IdarOberstein, Germany) that originated from their own mining operation (Fig.Par64 and 65).

Copper-bearing tourmalines from Mozambique were received from Gebr. Bank (Idar Oberstein) in 2006 (produced in 2005, samples 2939, 2942, 2942.2, 2943, Tab. Par05) and further materials were acquired from African suppliers in Bangkok in the years 2006 and 2007 (Fig. Par06, 67a-b, 72, 74, 75 and 77). Nigerian copper-bearing tourma-

lines were acquired from Arnold Silverberg, Steve Jaquith in Bangkok and from Paul Wild. A total number of 120 faceted or rough materials were available for this study. From these stones 90% are unheated materials. All multicolored copper-bearing tourmalines used for LA-ICP-MS analysis are unheated. No multicolored samples were available from the origin of Nigeria.

In addition, over 100 gem-quality faceted “Paraiba”-type tourmalines from Brazil and over 600 faceted counterparts from Mozambique, both heated and unheated have been tested and certified in the GRS laboratory between 2004 and 2008. These high-valued gemstones are considered representative to the size and color of copper-bearing tourmalines available in the worlds gem market and have been used for a statistical study (Fig. Par07, 08, 11 and 12).



Fig.Par06 Examples of rough copper-bearing tourmalines from Mozambique of various colors including green, bluish green, pink, purple and violet as seen in Bangkok between 2006 and 2007. These samples were acquired from large lots from African dealers in Bangkok. Less than 1 percent of the samples were multicolored (See Fig. Par72, 74 and 77).

Statistics on Heated and Unheated Gem-Quality Copper-Bearing Tourmalines from Mozambique Sorted by Different Color-Categories

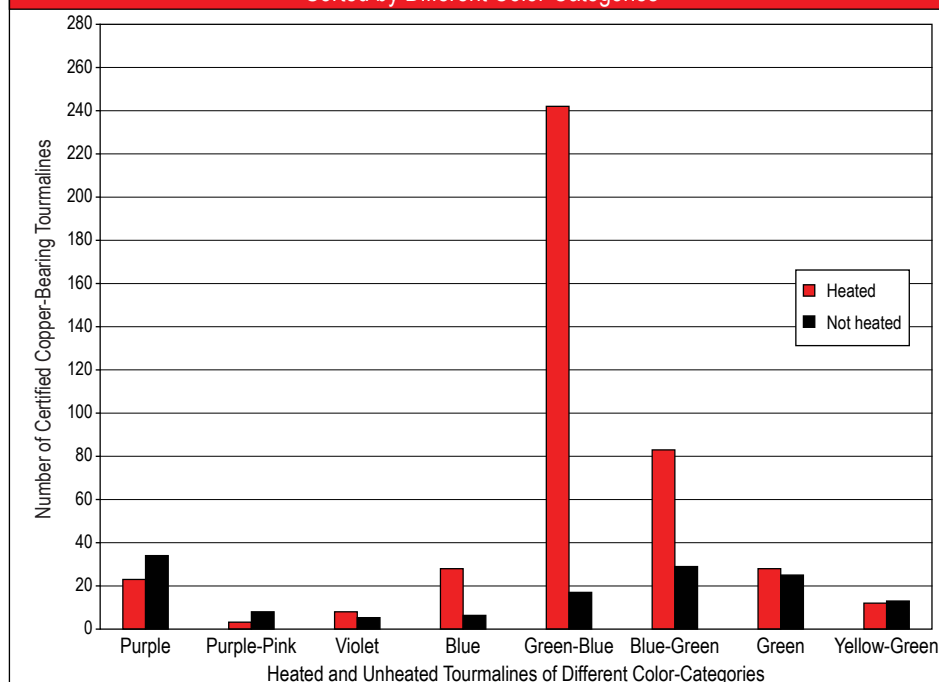


Fig. Par07 Statistics on the number of heated and unheated copper-bearing tourmalines from Mozambique in different color categories. Note that the so-called “Paraiba”-type colors (mixtures between green and blue) are dominantly heat-treated. Yellow-green and purple colors are mostly unheated but a surprising percentage of those tourmalines are heated as well. Due to the limited success of heat-treatment of this colors, they are expected to be mostly unheated (See heating experiments Lit. Par33).

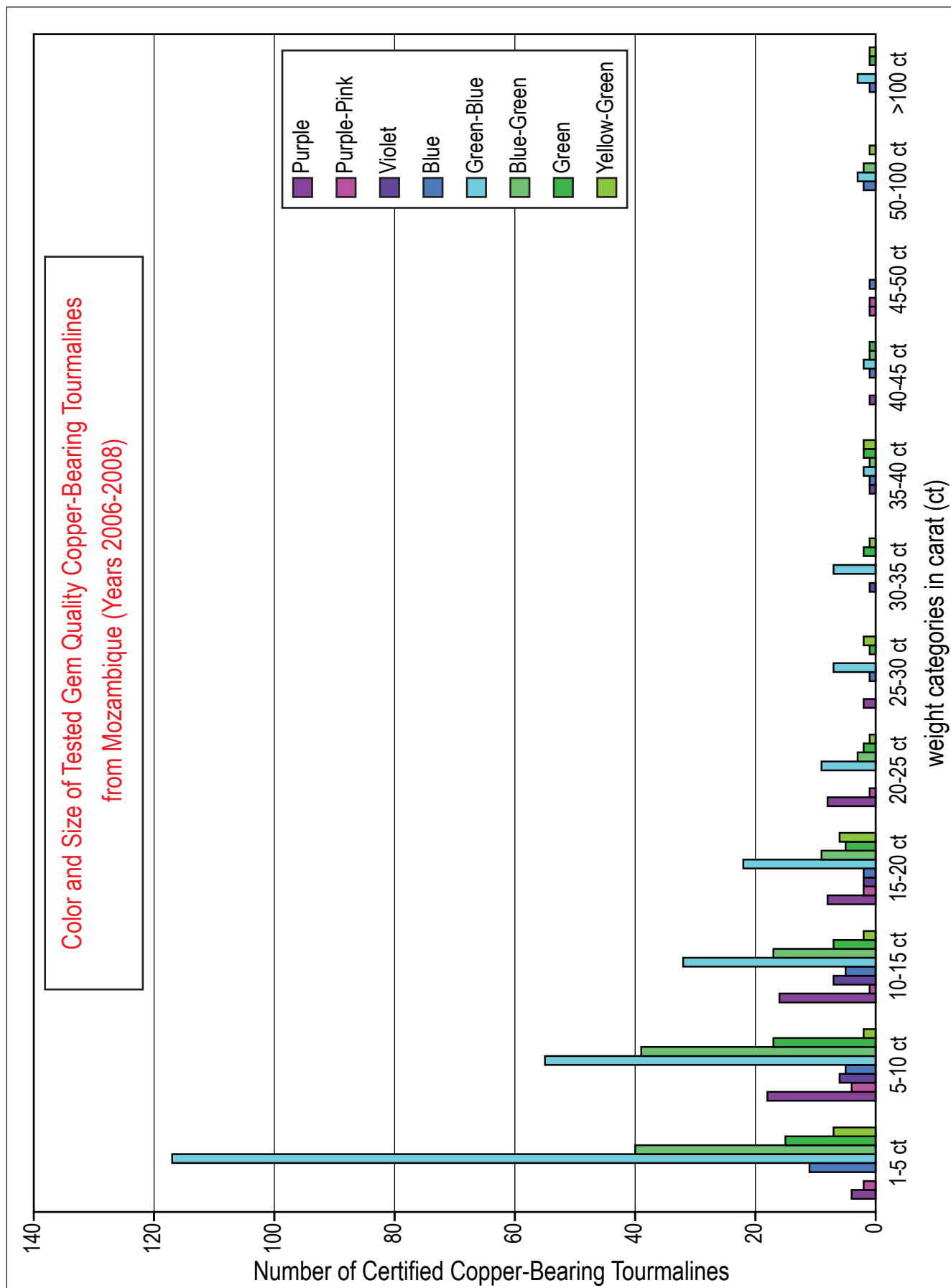


Fig. Par08 Statistics of number of certified copper-bearing tourmalines ("cuprian-elbaïtes") from Mozambique sorted by color and size, as tested in the years between 2006-2008. Only gem-quality faceted stones are included, both heated and unheated respectively (See Fig. Par07). The majority of these gems are below 20 cts in size. Larger sizes of all different colors are extremely rare. Sizes of over 100ct exist but they are generally heat-treated. The largest unheated violet and purple colors are in the category of 45-50 ct.

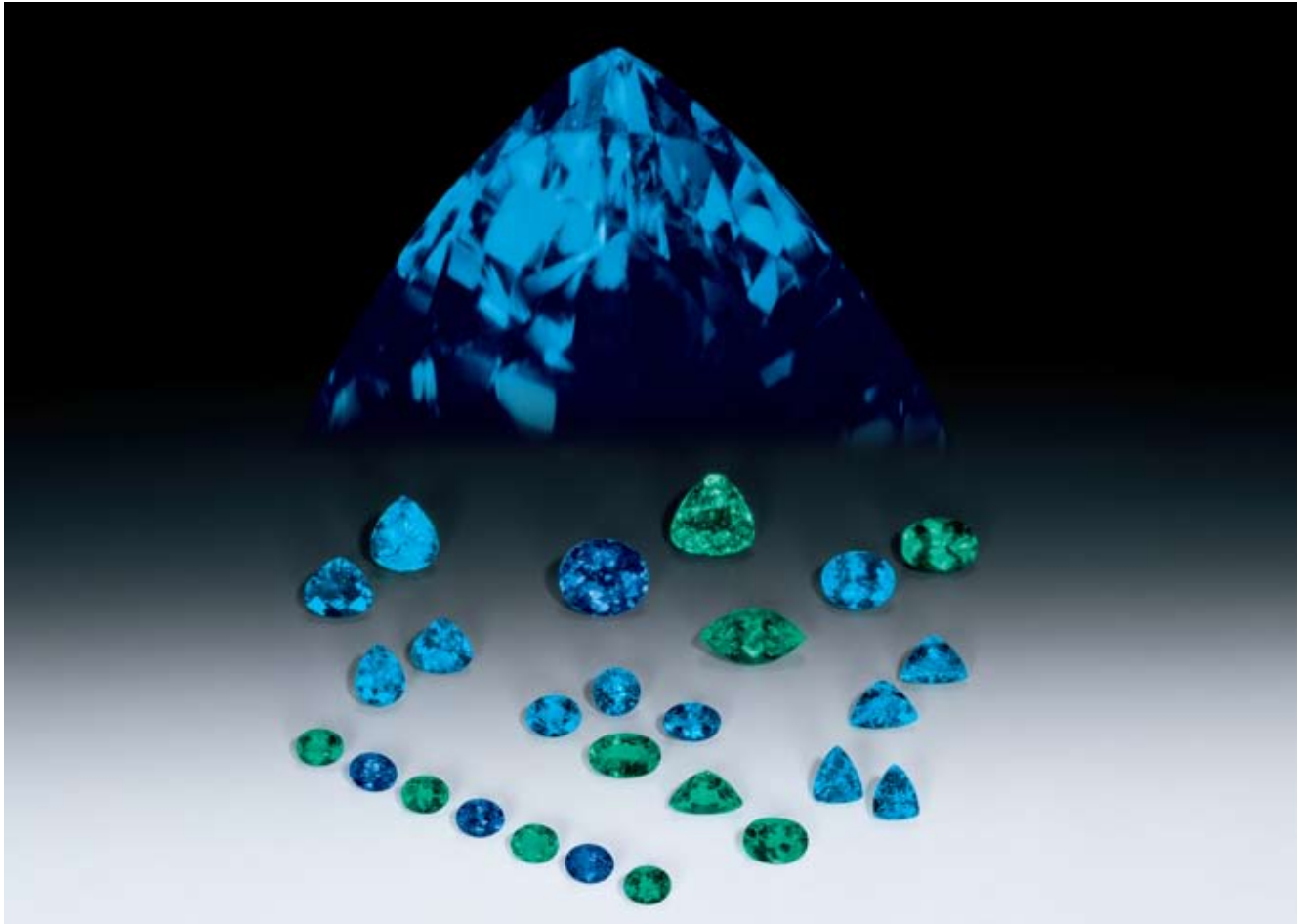


Fig. Par09 Examples of faceted “Paraiba”-tourmalines from the Batalha mine (State of Paraiba, Brazil) are shown. The colors of valuable “Paraiba”-tourmalines are vibrant greenish-blue colors that are described as “neon”-blue colors in the trade. All shades of transition of from green to blue can be found. Largest sizes are 11-12ct. Picture P. Wild Archive, Idar-Oberstein (Germany).



Fig. Par10 Example of a large-sized “Paraiba”-tourmaline rough with typical “neon”-blue color (from the Quintos mine, Rio Grande do Norte). The tourmaline section has been cut perpendicular to the c-axis and polished on both sides.

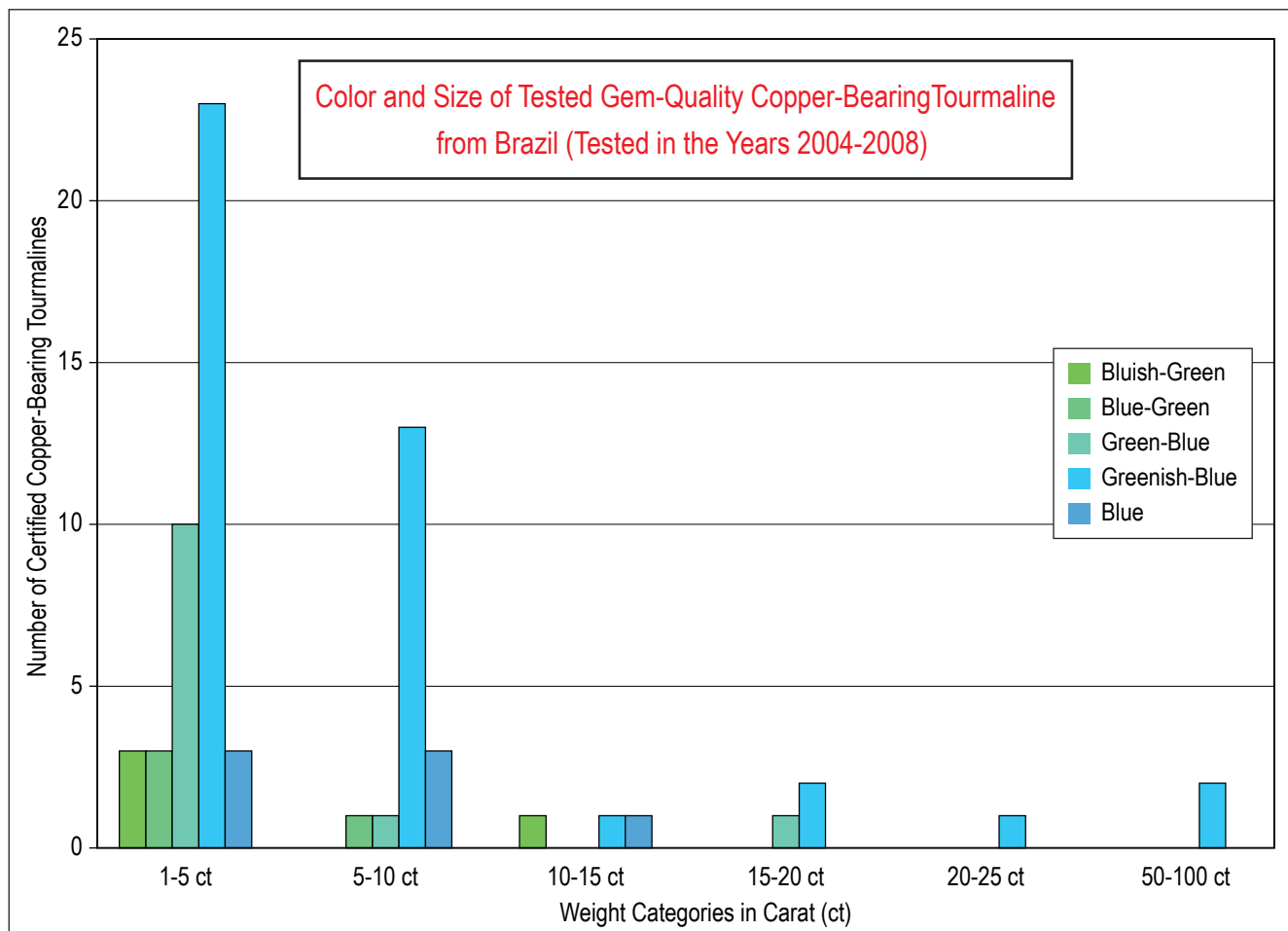


Fig. Par11 Statistics on certified copper-bearing tourmalines from Brazil, sorted according to color and size. They were tested and certified in the GRS laboratory in the years between 2004 and 2008. The stones listed are gem-quality faceted stones; both heated and unheated (see Fig. Par12). The majority of these gems are below 10 ct in size. Larger gem-quality Paraiba tourmalines over 10 ct are extremely rare and purple colors such as found in Mozambique in this size category did not appear in our laboratory (compare Fig. Par08).

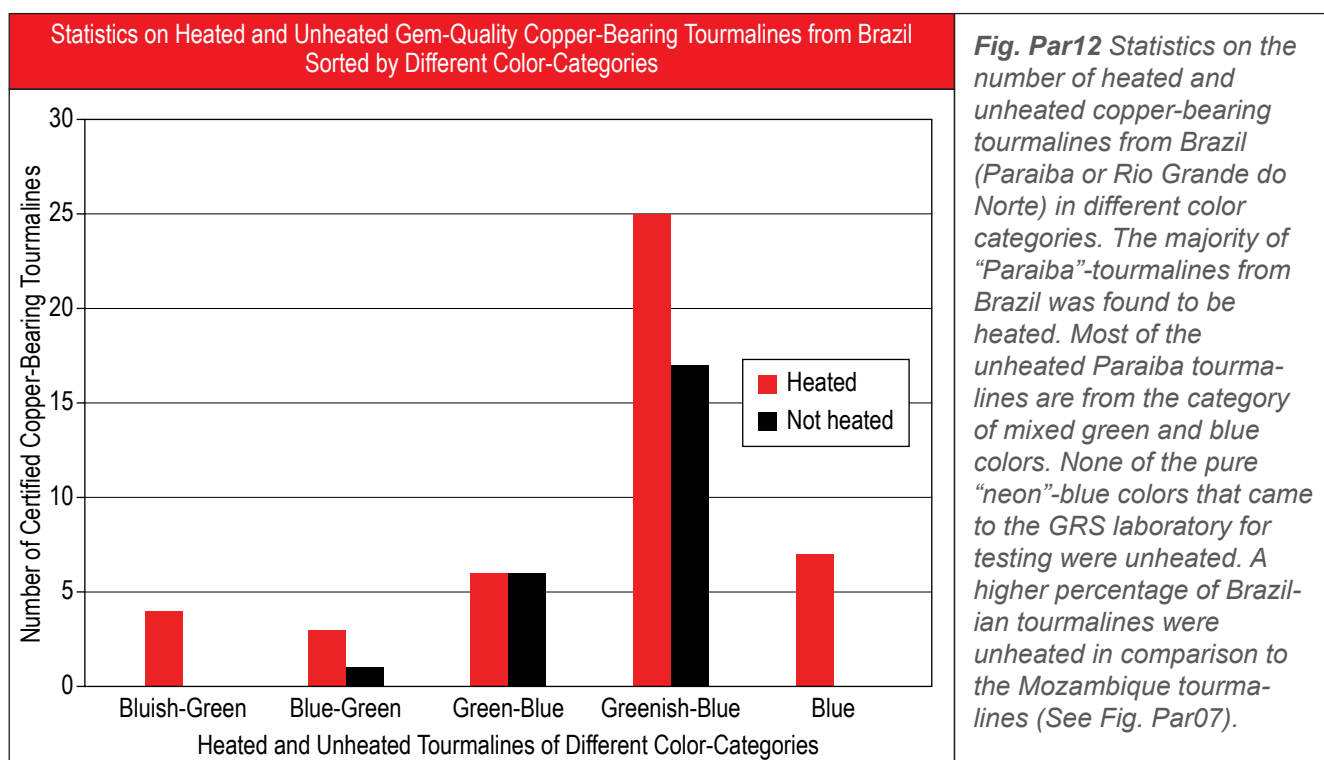


Fig. Par12 Statistics on the number of heated and unheated copper-bearing tourmalines from Brazil (Paraiba or Rio Grande do Norte) in different color categories. The majority of “Paraiba”-tourmalines from Brazil was found to be heated. Most of the unheated Paraiba tourmalines are from the category of mixed green and blue colors. None of the pure “neon”-blue colors that came to the GRS laboratory for testing were unheated. A higher percentage of Brazilian tourmalines were unheated in comparison to the Mozambique tourmalines (See Fig. Par07).



Fig. Par13a Overlook on the classical Batalha tourmaline mine in the State of Paraiba (Brazil). View from the top of the "Heitor"-hill towards the direction of Sao Jose da Batalha village. Picture by Markus Paul Wild in 2006. P. Wild Archive.

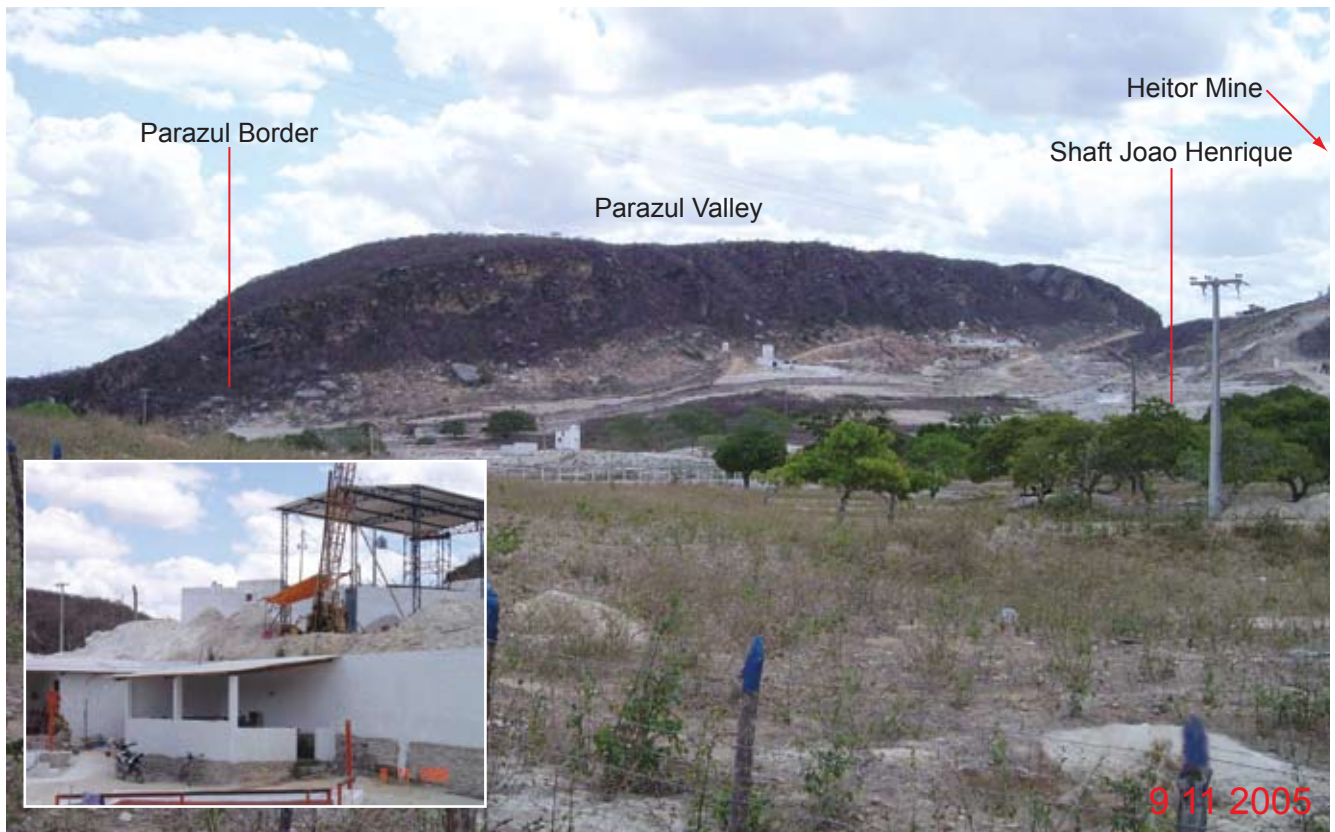


Fig. Par13b A large number of claims and shafts cover the area of many different mine owners. Mining shafts are labeled according to the owner of the mines. Heitor mine see Fig. Par13d. Picture P. Wild Archive.



Fig. Par13c



Fig. Par13d



Fig. Par13e



Fig. Par13f

Fig. Par13c-f A view into the underground mining of "Paraiba"-tourmalines in the Heitor shaft (Batalha mining area, Paraiba, Brazil). The vertical shafts are driven to a depth of 40m in soft "kaolinized" pegmatites (Fig. Par13e-f). Underground tunnels are partially collapsed (Fig. Par13d). Picture Markus Paul Wild. P. Wild Archive.

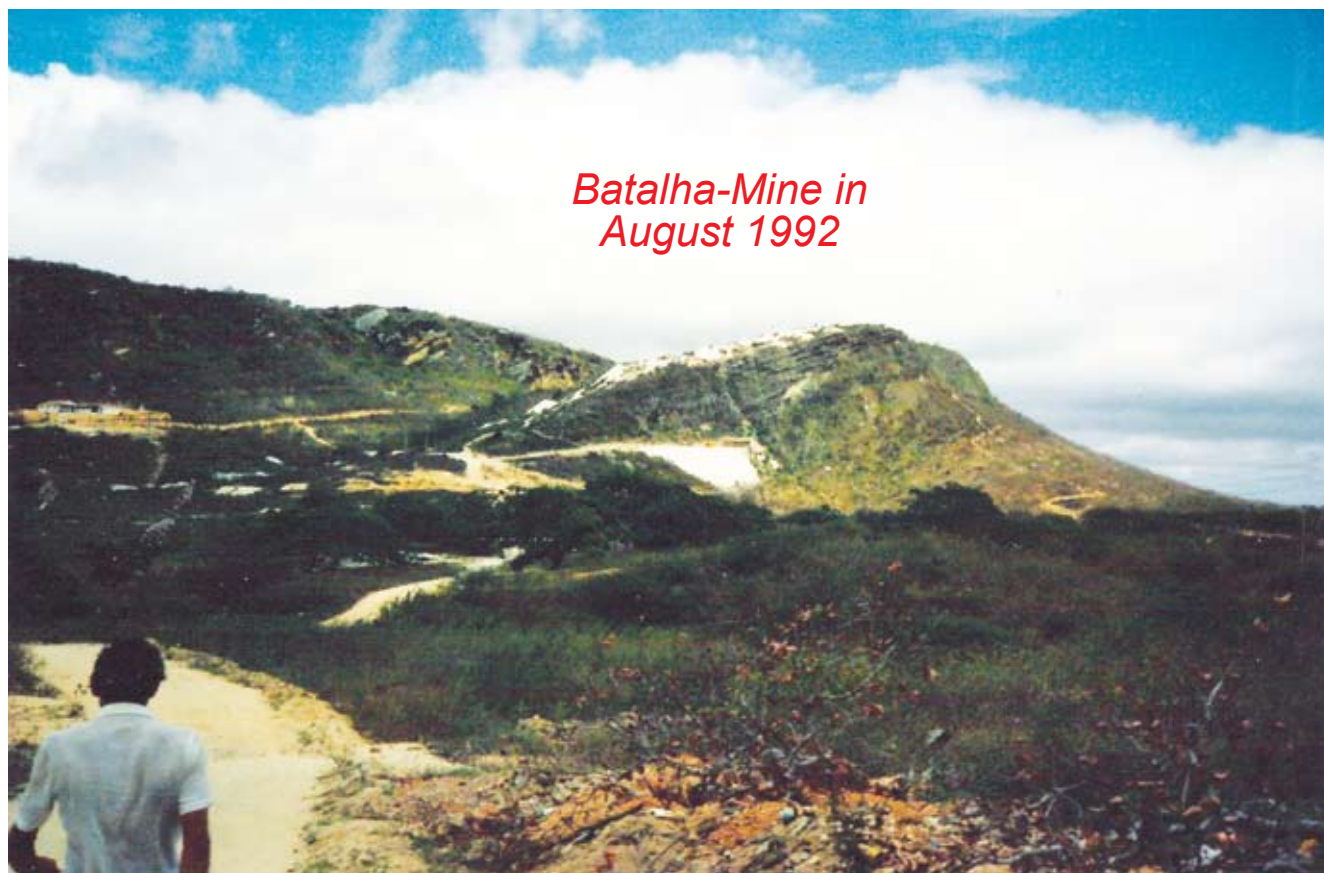


Fig. Par14a-b The original "Paraiba" tourmaline mine from Sao Jose da Batalha in August 1992 (Heitor mine). The whitish dumped material consists of kaolinized pegmatite materials and quartzite. Compare with the mining operation a decade later (See Fig. Par15a). Picture Bryan Pavlik.

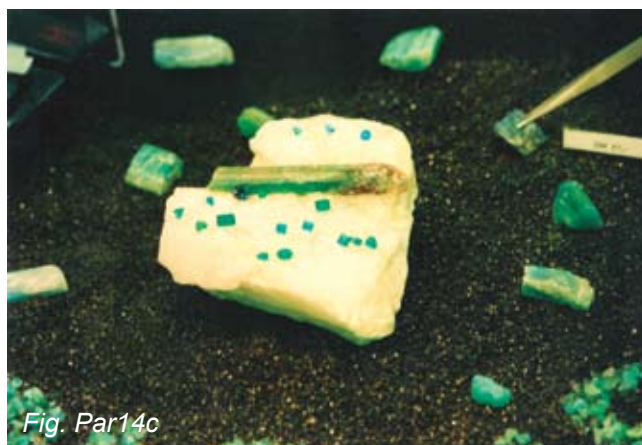


Fig. Par14c "Paraiba" tourmaline crystal in quartz matrix from the first mining period at the Batalha mine (Paraiba, Brazil). Length of tourmaline in matrix is 10 cm. Additional display of rough and faceted gemstones as shown at the Inhorgenta (Pavlik booth, Munich, 1993).

Fig. Par14d Faceted "Paraiba" tourmaline from the Batalha mine in a weight range of 1 to 5ct. These archived gemstones were pictured more than 10 years before the mines in Africa were discovered.

Picture (14a-d) are copyrighted by Bryan Pavlik and reproduced with permission of the "Pavlik Gem History Archive", Vienna, Austria.



Fig. Par15a View into a mining landscape with many claims and shafts. Same view as in Fig. Par14a-b but 13 years later. Note extensive mining activities have created a deepened valley with numerous fences and walls between the claims in the decade since the mine was opened. Picture by Markus Paul Wild in 2005. P. Wild Archive.



Fig. Par15b shows the so-called "Heitor-wall" at the top of a hill for the purpose of protecting the "Heitor"-mine claim. P. Wild Archive.



Fig. Par16a

Fig. Par16a-b Examples of color zoned "Paraiba"-tourmalines from the Batalha mine, which were used for detailed chemical analyses in this report. The core of the rough crystal fragments is purple, followed by "neon"-blue and green colors in the outer rim. (LA-ICP-MS analysis profiles see Fig. Par59, 60 and 62).



Fig. Par16b



Fig. Par17 A rare example of a perfect "Paraiba"-tourmaline crystal of intense "neon"-blue color. Such intensively unheated blue tourmaline crystals are exclusively found in Batalha (Paraiba, Brazil). Crystal length 4cm. These magnificent color varieties are named "Heitoritapura" and were typically found in the Heitor shaft (See Fig. Par15).



Fig. Par18a A view into the underground rock formations containing pegmatite materials with copper-bearing tourmalines, albite (white) and quartz (grey) in the "Heitor"-mine (Purple = tourmaline and lepidolite). Picture P. Wild Archive.



Fig. Par18b A spectacular hand specimen with a color-zoned "Paraiba"-tourmaline from the Batalha mine (Heitor shaft). Note: Only very small portion of the tourmaline show the desired blue "neon"-color. Tourmaline on rock matrix with citrine and quartz. Picture P. Wild Archive.



Fig. Par19 The Washing place at the P. Wild's Quintos mine in the State of Rio Grande do Norte (Brazil). P. Wild Archive.

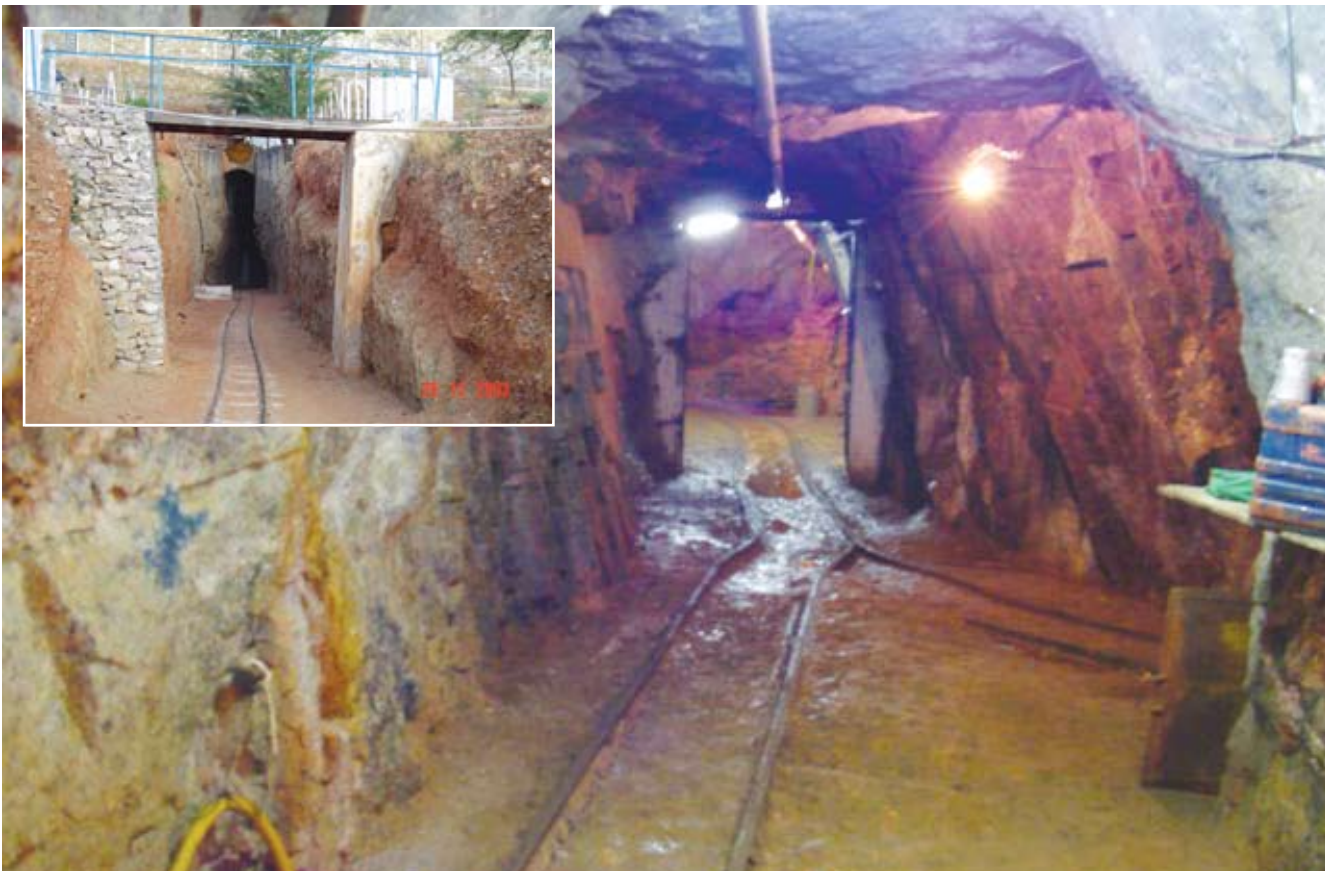


Fig. Par20 Underground mining tunnel at the Quintos tourmaline mine in Rio Grande do Norte State (Brazil) and view to the entrance tunnel (inserted). P. Wild Archive.

*Underground Mining and Occurrence of Copper-Bearing Tourmalines
in the Host Rock at the Quintos Mine in Brazil*

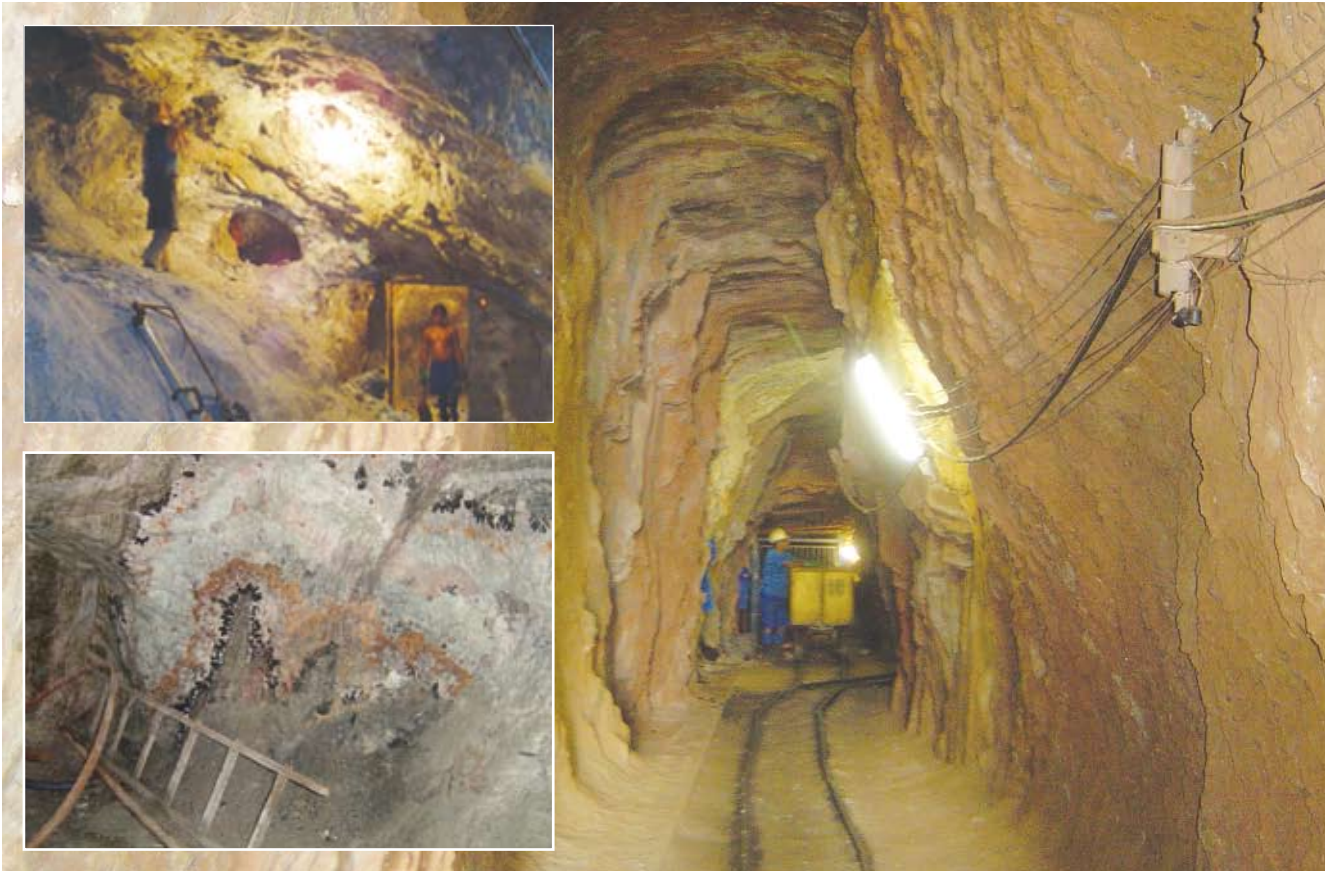


Fig. Par21 Underground tunnel in the Quintos tourmaline mine that was driven into the hard quartzite rock. Only at certain positions can the gem-bearing pegmatites be found (See inserted pictures). P. Wild Archive.

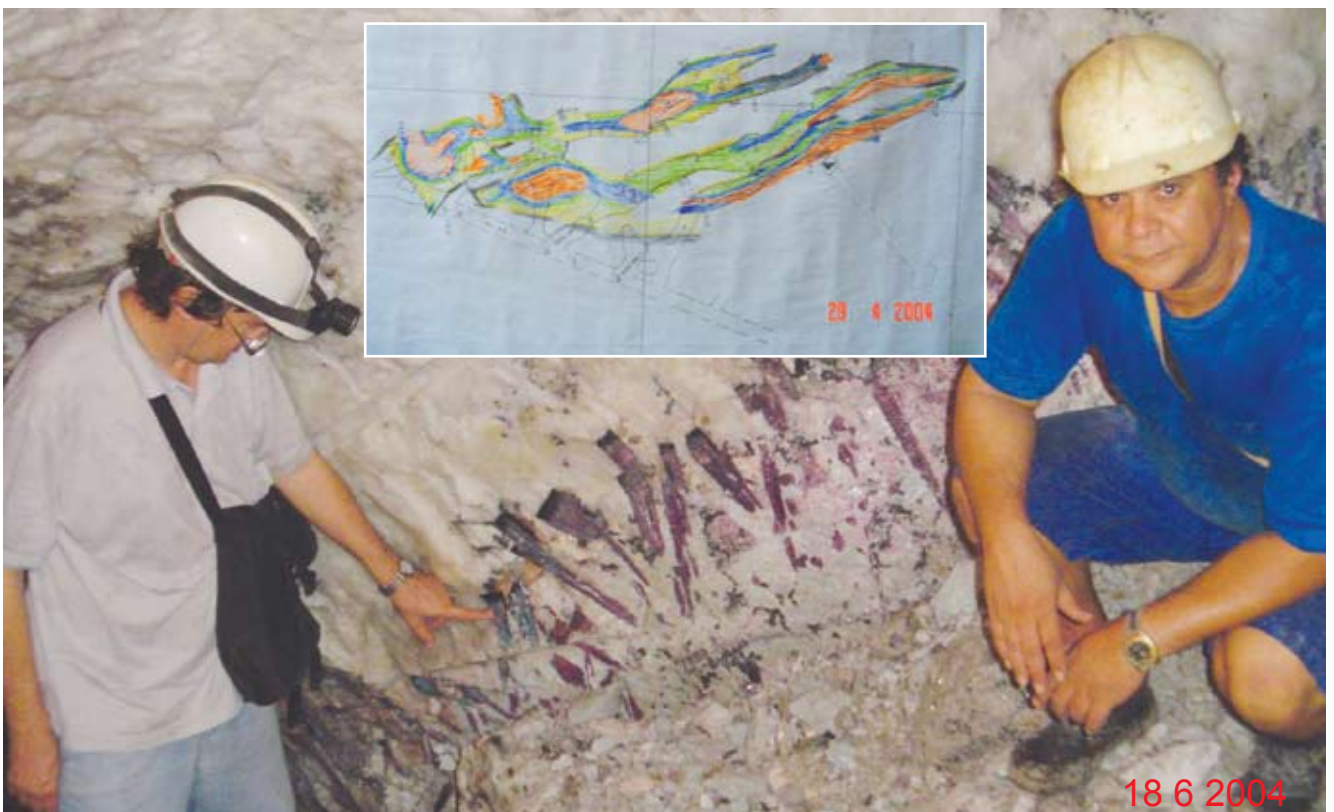


Fig. Par22 Occurrence of highly valuable copper-bearing tourmalines at the P. Wild's Quintos mine. A quartz-feldspar pegmatite has intruded a quartzite host rock. In some zones the desired "neon-blue" colored copper-bearing tourmaline was formed. In the picture on the left the mining geologist and on the right the mining engineer. The Geological map (inserted) helped to find the gem-bearing layers. P. Wild Archive.



Fig. Par23

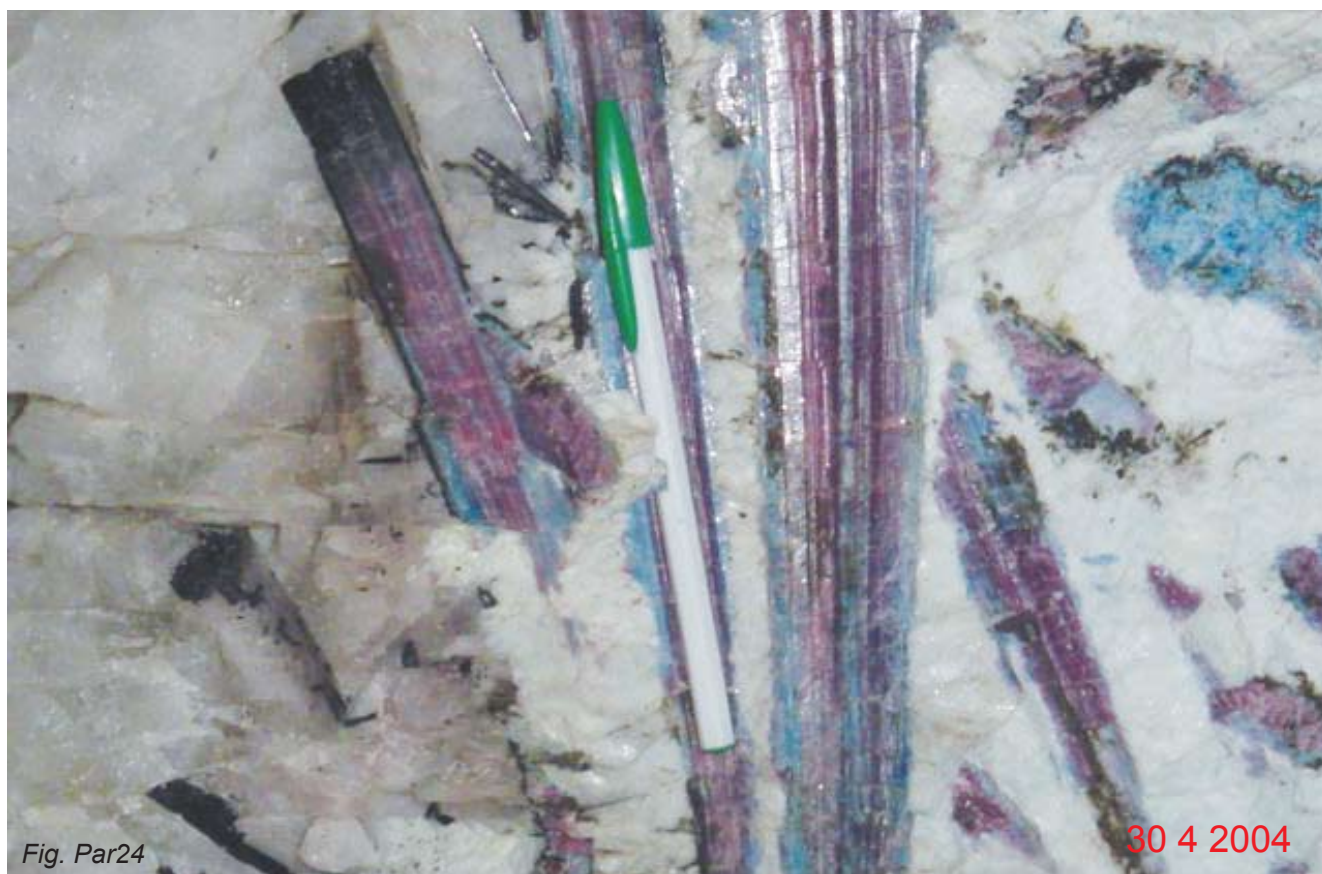


Fig. Par24

Fig. Par23, 24, 25, 26 A detailed view of the primary occurrence of copper-bearing tourmalines in the host rocks at the Quintos mine (Rio Grande do Norte, Brazil). Photo taken in the underground tunnel. The tourmaline crystals are growing in sizes larger than pencils. The multicolored tourmalines show a purple core and blue rim. The grey and white minerals of the matrix are quartz and feldspar respectively. P. Wild Archive.

*Multicolored Copper-Bearing Tourmaline in the Host Rock at the Quintos Mine
(Rio Grande Do Norte, Brazil)*



Fig. Par26

Fig. Par27 Spectacular example of a large sized “neon”-blue “Paraiba” tourmaline in a matrix of quartz (grey) and feldspar (white). These large tourmalines are heavily fractured and with numerous nontransparent areas. Only very small transparent areas are present in the large tourmalines that are suitable for faceting. P. Wild Archive.

ELECTRON MICROPROBE ANALYSIS

The electron probe microanalysis (EMPA) was performed on a JEOL JXA 8200 instrument equipped with 5 wavelength dispersive x-ray spectrometers (WDS) and an energy dispersive spectrometer (EDS). All samples were coated with a 20 nm layer of carbon. The

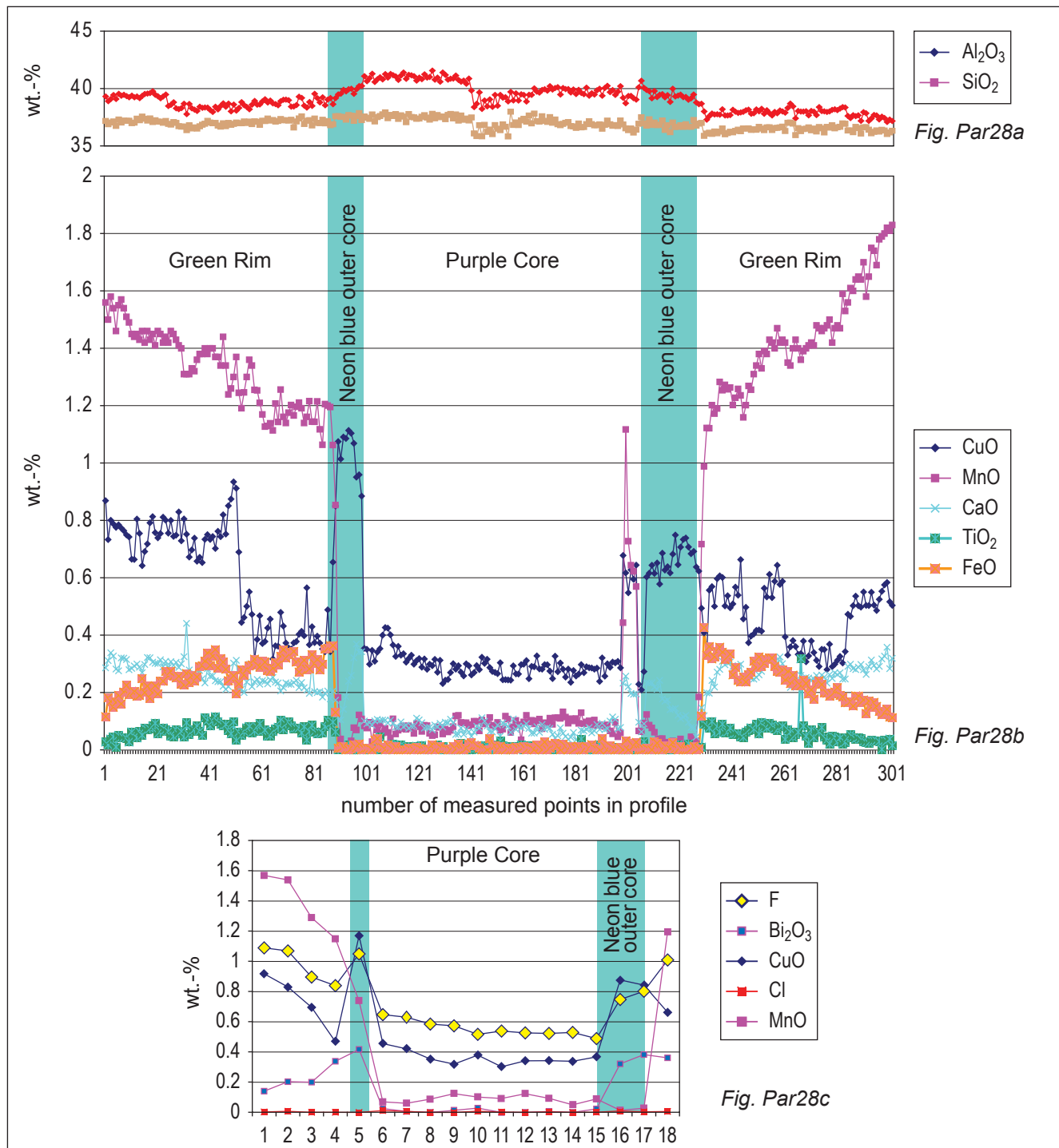


Fig. Par28a-c Electron microprobe profile analysis across a zoned “Paraíba”-tourmaline perpendicular to the c-axis. (See Fig. Par29). Fig. Par28a-b is from the same run and corresponds to the LA-ICP-MS analyses of Fig. Par36a. Lowest MnO-concentrations and highest CuO-concentrations are found in the “neon”-blue colored part of the tourmaline crystal. Fig. Par28c is from a second measuring session with less measuring points and was focussed on the measurement of some additional elements such as Fluor (F), Chlorine (Cl) and Bismuth (Bi). Both methods, EMPA and LA-ICP-MS-analyses respectively, produced exactly the same distribution pattern of the trace elements in the tourmaline crystal (compare Fig. Par28b with Fig. Par36a). Note that the increase of the F-concentrations is correlated with the increase in Cu-concentrations in point 5 (Fig. Par28c). For Zn-concentrations See Fig. Par31h and Tab. Par03.

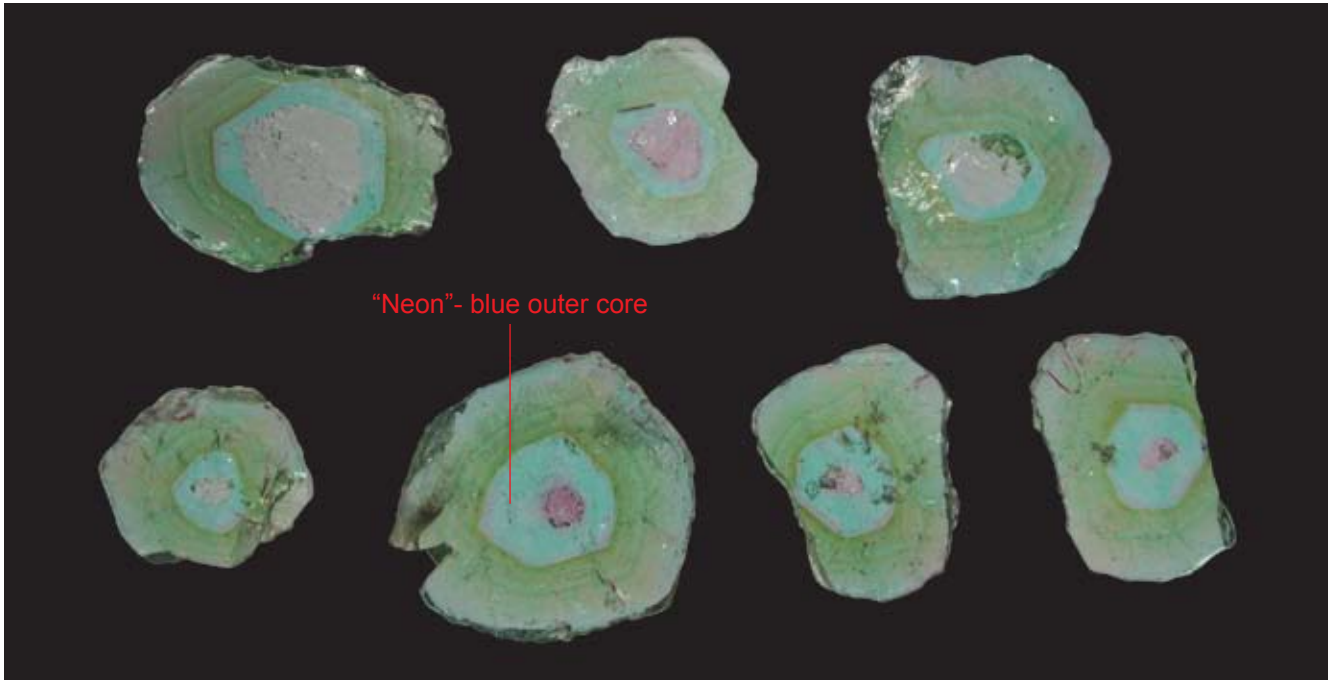


Fig. Par29 “Paraiba”-tourmaline cross sections cut perpendicular to the c-axis. Note the pronounced color zoning in these copper-bearing tourmalines with a purple inner core, a “neon”-blue outer core and a green rim. (Batalha mine, Brazil, R.C. Gemmas Co.). Sizes approx. 6-8 mm.

electron beam conditions for quantitative analysis were an acceleration voltage of 15kV, a beam current of 20 nA and a beam diameter of 10 μ m. The monochromator crystals used were LIF for the analysis of Zn, Cu, Fe and Mn, PET for Ca, K, Ti and Bi, TAP for Si, Al, Mg and Na and a multi-layer crystal (LDE1) for F. For all elements except Bi the K α lines were selected, whereas for Bi the M α line was used. The counting time on any element was 40 s on the peak and 40 s on background positions. The standards used were natural and synthetic silicate and oxide minerals. All measurements were corrected for detector dead time, instrumental drift and x-ray background. For the correction of the inter element effects (i.e. excitation, absorption, fluorescence) the CITZAF code (Lit. Par02) was applied. Because the quantification of B is not easily achieved a fixed amount of 11 wt-% of B₂O₃ was added to improve the inter element correction. The detection limit for Fluor was 0.1 wt-%.

For the elemental distribution maps an acceleration voltage of 15 kV, a beam current of 40 nA and a beam diameter < 1 μ m were applied. The dwell time was 1 s per image element.

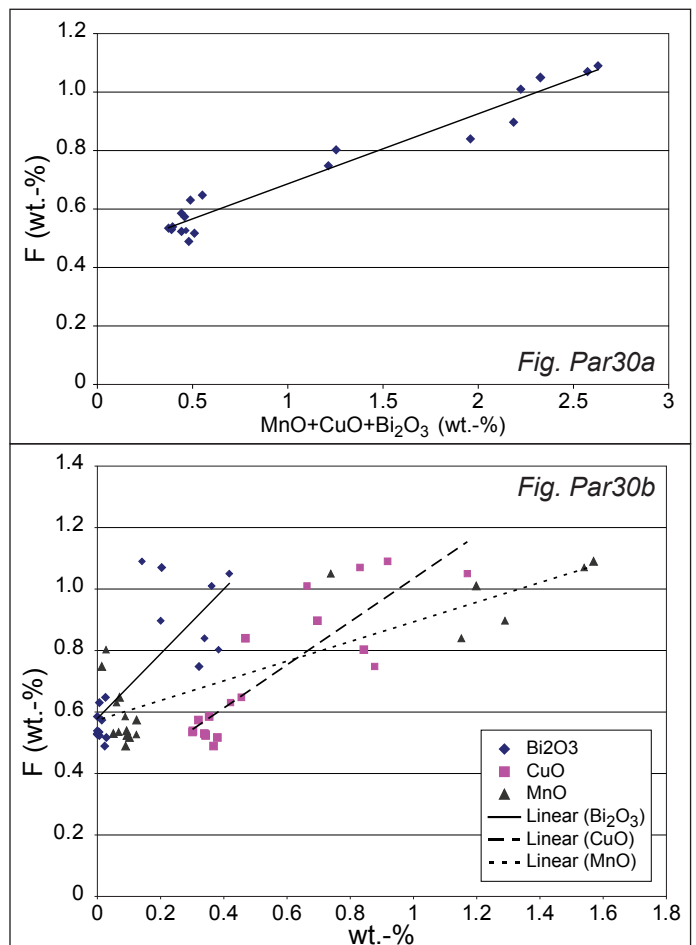
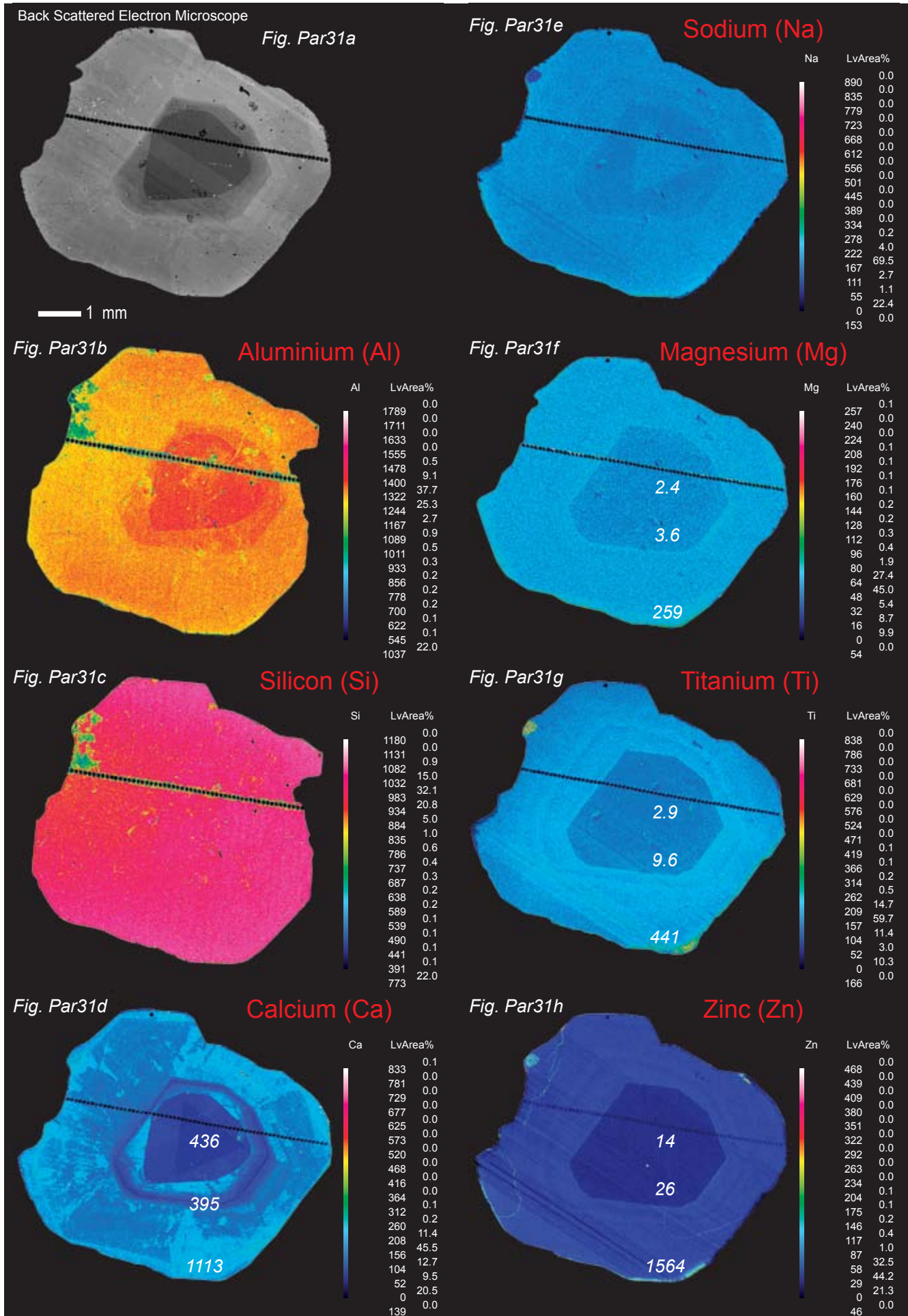
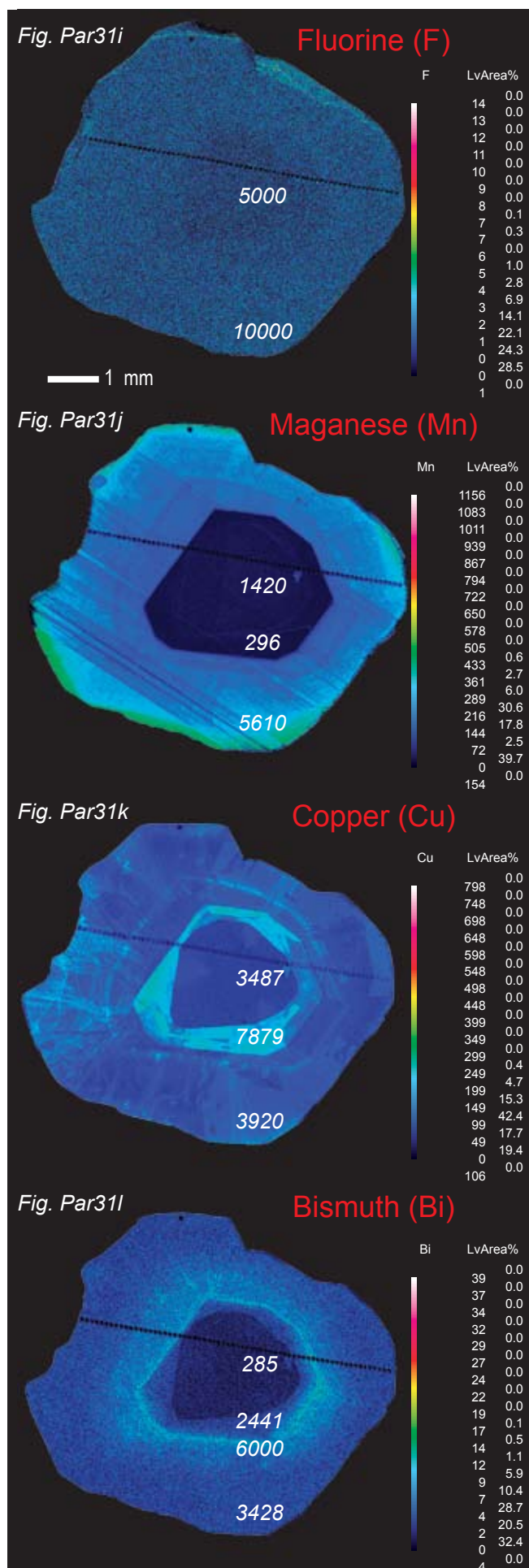


Fig. Par30a-b Regression plot of concentrations of minor elements against Fluorine (F). Increase in these minor elements is correlated with increase in F-concentrations in the tourmaline. Details on variations in F-concentrations, see Fig. Par28.





ELECTRON MICROPROBE ELEMENT DISTRIBUTION MAPPING

Fig. Par31 Elemental distribution maps were produced by electron microprobe analysis of important elements. The analyzed sample is a "Paraiba" tourmaline from the Batalha mine. The tourmaline has been cut perpendicular to the c-axis (compare Fig. Par28-29). The trail of the craters are from LA-ICP-MS analysis (Compare Fig. Par32-39). The picture of the tourmaline is shown in Fig. Par31 for comparison of the visual and the electron microprobe electron concentration mappings. The colors of the pictures shown in Fig. Par31a-l are artificial and arbitrary chosen to achieve maximum contrast to show the differences in element concentrations. To calibrate the chemical concentrations, average chemical analyses by LA-ICP-MS (Tab. Par02) are projected into the picture ($\mu\text{g/g}$).

Fig. Par31a Back scattered electron image (BSE)

The BSE-image provides different grey tones that are produced by the different atoms present. Higher total number of heavy atoms result in brighter grey tones. Fig. Par31a shows a dark core and lighter rim. This can be explained by the increase of heavy elements from the core to the rim of the crystal. Lighter grey tones can be correlated with increase in Mn, Cu and Bi (Fig. Par31k). The dark-grey core can be correlated with low concentrations of Mn and Cu (Fig. Par31j). The outer core is dominated by elevated copper- (Cu) and low Mn-concentrations in the BSE image (Fig. Par31k) correlates well with the visual color zoning (Fig. Par32). "Neon"-blue colors are found in the areas of the crystal at these elevated Cu and depleted Mn-concentrations. Elemental distribution of other elements such Si, Al, Ca, Na Mg, Zn, F and Bi may not be directly correlated with the visible color zoning as they are not the cause of blue color in the tourmaline (e.g. Lit Par10, 11, 33).

Fig. Par 31b-l Element distribution mapping of various elements

The element distribution mapping shows that Al-concentrations are slightly higher in the core than in the rim of the tourmaline (Fig. Par28a, 31b) whereas Si does not show any variation (Fig. Par31c). Ca- and Na-concentration revealed an "inner triangle" which was not evident in the microscope (Fig. Par31d-e). In this "inner triangle", the Ca-concentrations are depleted and Na-concentrations are enriched (Fig. Par31d-e). Higher Ca- and lower Na-concentrations are found in the zone of highest Cu-concentrations (compare Fig. Par31d and Par31k).

Bi-concentrations are highest at border of the Cu-rich outer core towards the inner rim of the crystal. The Bi distribution resembles an intense impact at the latest stage of the “neon”-blue growth phase that gradually faded away during further crystal growth (Fig. Par31a). F-concentrations are lowest in the core of the crystal and increase gradually to the mantle of the crystal (Fig. Par31i). They are well correlated with the backscattered image. Darker parts in the BSE-image match with low F-concentrations. Higher F-concentrations correlate with higher concentrations of Mn, Cu and Bi (See Fig. Par28c). Mg, Ti and Zn show a similar distribution like those observed for Mn. They increase towards the mantle of the crystal with very distinct oscillations at certain positions (compare Fig. Par31f, Par31g, Par31h and Par31j). A similar element concentration pattern was measured by LA-ICP-MS. However, the detection capabilities of LA-ICP-MS allowed to expand the analysis of the elemental distribution in “Paraiba”-tourmalines by focusing into other elements at µg/g concentrations that are below the limits of detection of electron microprobe analysis.

LA-ICP-MS ANALYSIS

Laser Ablation-Inductively Coupled Plasma Mass Spectrometry analysis were carried out using a 193 nm ArF Excimer laser ablation system (GeoLasM, Lambda Physik, Göttingen, Germany)

coupled to a DRCII + ICP-MS (Perkin Elmer, Norwalk, USA). A 20 cm³ ablation cell and a 1.5 m tube were used as transport system for the laser-generated aerosols. Helium was used as carrier gas and merged with argon in front of the ICP-MS torch to provide optimum excitation conditions within the ICP. The calibration was carried out using the NIST 610 glass. The element concentrations of NIST 610 were taken from Lit. Par03. The acquisition protocol included always 2 NIST 610 analyses at the beginning and the end of each run and allowed to analyze 16 sample positions in-between. Since tourmaline are heterogeneous systems and consist of a large number of major elements, the normalization procedures for metallic samples (Lit. Par06) and oxides (Lit. Par04) were applied. The analysis and data reduction were carried out following an acquisition, data reduction and quantification protocol (Lit. Par07).

427 individual LA-ICP-MS analysis were carried out on 6 Paraiba tourmalines (Samples 2079*, 2965*, 2972*, 2976.2*, 2976*, 3111-a*) and 260 individual analyses were acquired from 8 Mozambique samples (Samples 2939, 2942, 2942.2, 2943, 3134*, 3138, 3143, 7782* (*traverse)). The samples were surface polished prior to the LA-ICP-MS analysis. On each sample, 60 µm craters were place next to each other to provide spatial resolution across different growth zones of the tourmalines.

Tab. Par01 EMPA-Analysis

	Minimum	Maximum	Average	Sigma
SiO ₂	36.88	38.46	37.74	0.44
TiO ₂	bd	0.08	0.02	0.03
Al ₂ O ₃	40.05	42.75	41.77	1.07
FeO	bd	0.37	0.08	0.12
MnO	0.01	1.57	0.45	0.58
MgO	bd	0.04	0.01	0.01
CaO	0.03	0.31	0.13	0.10
Na ₂ O	1.71	1.95	1.83	0.07
K ₂ O	bd	0.17	0.02	0.04
CuO	0.30	1.17	0.55	0.27
ZnO	bd	0.26	0.07	0.09
Bi ₂ O ₃	bd	0.41	0.13	0.16
F	0.49	1.09	0.72	0.22
Cl	bd	0.012	0.003	0.004
B ₂ O ₃	11	11	11	
Total	93.4	95.0	95.0	

Tab Par01 Electron microprobe analysis of sample 2976 (in wt.-%). B₂O₃ assumed as 11 for correction purposes. Lowest and highest value for each element and average are given. More details see Fig. Par28. Same sample is analyzed by LA-ICP-MS (See Fig. Par35). Difference to total of 100% due to non-measured element concentrations of Li₂O and H₂O (bd = below detection).

CHEMICAL COMPOSITION

The major, minor and trace elements of tourmalines from Paraiba and Mozambique were analyzed and sorted accordingly to the color of the individual growth zones. The most pronounced changes in color representative for the chemical evolution of the tourmalines are accompanied by a significant change of the minor element concentrations of Cu, Mn, Bi (See Fig. Par36a, 46a-b, 55a-b, 59a, 62a, 66a, 75a-b, 78a-b, 90a-b and 91c-d). This chemical transition can also be extracted from the Pb-Zn-Mg correlation (Fig. Par34, 59b, 62b, 66b-c, 76b and 91b). These trends can further be supported by the elements such as Be, and Fe and Ti (Fig. Par33b, 41a, 43a-b, 49b, 59c,e, 62b,f, 66b,d, 76a, 78f, 84, 85, 86 and 87). In addition to the major and minor elements, 1-5 µg/g concentrations were determined for Sr, Nb, U, Th, La, Ce, Pr, V and Ta. Concentrations between 0.01 and 1 µg/g were determined for Sn, Cr, Co, Rb, Zr, Mo, Ag, Cs, Ba, Nd, Sm, Eu, Gd, Tb, Er, Ho, Tm, Yb and Lu, whereas 0.01 represents the lowest limits of detection determined throughout this study (See table Par02-05 and corresponding figures on pages 25-40 and pages 48-53).

ACCURACY

Testing of the accuracy was carried out using EPMA concentration and LA-ICPMS concentration profiles across the Paraiba Tourmaline sample 2976 (compare Fig. Par28b with Fig. Par36a-b). The accuracy of the quantification approach using NIST 610 for calibration applied for LA-ICP-MS was carried out using different spatial resolution for the two independent, but complementary techniques (EPMA approx. 10 µm and LA-ICP-MS approx. 60 µm). Based on the difference in the spatial resolution, 65 data points (LA-ICP-MS) and 306 data points (EPMA) were acquired on the same traverse shown in Fig. Par28b-c and 36a. It can be seen that the concentration profiles (Na, Ca, Ti, Fe, Cu, Bi and Mn) are in very good agreement between the two independently calibrated techniques. For example, the profile of Mn starts for both methods at very similar concentrations (EPMA 12000 mg/kg, LA-ICP-MS 11500 mg/kg). For further comparison, the average concentrations of the most homogeneously distributed elements (n=306 and n=65, RSD < 5 % for both techniques) were calculated (Data from Tab. Par01 and Tab. Par03). Using this approach, Na concentration of 13500 + 570 mg/kg and Si concentration of 196800 + 2460 mg/kg (EPMA) were closely matched to Na 13800 + 740 mg/kg and Si 181100 + 8140 mg/kg. Even the copper concentration was determined to be approx within 8 % when comparing LA-ICP-MS and EPMA.

LIBS ANALYSIS

Laser induced breakdown spectroscopy (LIBS) was used for direct analysis of the tourmalines. Therefore, a 30 mJ frequency double 266 nm Nd:YAG (Continuum, USA) with a pulse width of 6 ns was coupled to an in-house built ICCD/Echelle spectrometer with a working range of 190-900 nm. The ICCD detector works in a wavelength range between 180-800 nm. The crater ablated on the sample and every element was acquired using 20 spectra (single pulse). Single element spectra were acquired for Cu (324.754 nm), Be (313.042 nm) and Mn (403.076 nm). Ablation crater were generated closely matched to the position of LA-ICP-MS analysis. The concentrations were correlated using the LA-ICP-MS data. Crater diameters using LIBS were selected in the same order of magnitude as applied for LA-ICP-MS to ensure similar destruction of the sample. The results on the LIBS-measurement in comparison to the LA-ICP-MS of same samples are shown in Fig. Par85 and 86.

ED-XRF ANALYSIS

ED-XRF analysis are carried with a Fischer Instrument (XAN-DP) using a 50kV acceleration voltage, a 1000micron Al-Filter, using different beam collimators (0.2mm-2mm, smaller collimators with longer measuring time) and a drift correction mode. The measurement was carried out for minimum of 50-100 seconds. A standard-less element calculation procedure provided by the manufacturer was used to obtain element concentrations of Al, Cu, Mn, Bi, Fe, Zn and Ga. For validation purpose, we measured 12 LA-ICP-MS standards with ED-XRF analyses. The sampling volume of the LA-ICP-MS and ED-XRF are different and the number of measured points by LA-ICP-MS had to be averaged (Tab. Par02-05), before they could be compared to ED-XRF analyses. A linear regression was made for each element measured by 2 different methods (LA-ICP-MS versus ED-XRF) on the basis of 12 standards. A consistent difference between ED-XRF and LA-ICP-MS was detected for the different elements of approx. 30%. This is not surprising because lighter elements (atomic weight below Al) are not measured with this relatively in-expensive ED-XRF instrument. A correction of the ED-XRF data was carried out based on the linear regression coefficient to lower values (See Fig. Par82d). We plotted the corrected ED-XRF results of 112 tourmalines of known origin and compared the results derived by the different methods (See Fig. Par82a-c, Par90a-b and Lit. Par01).

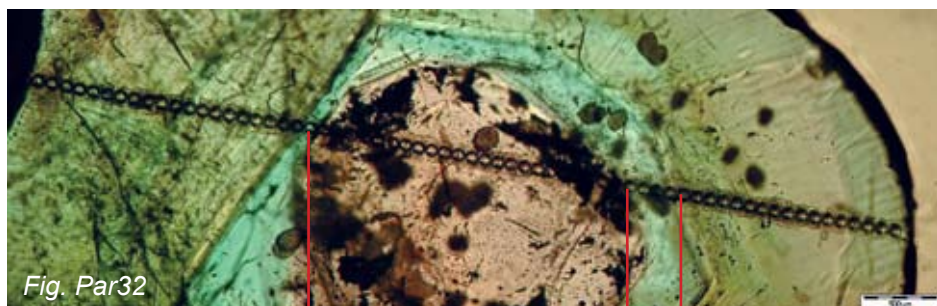
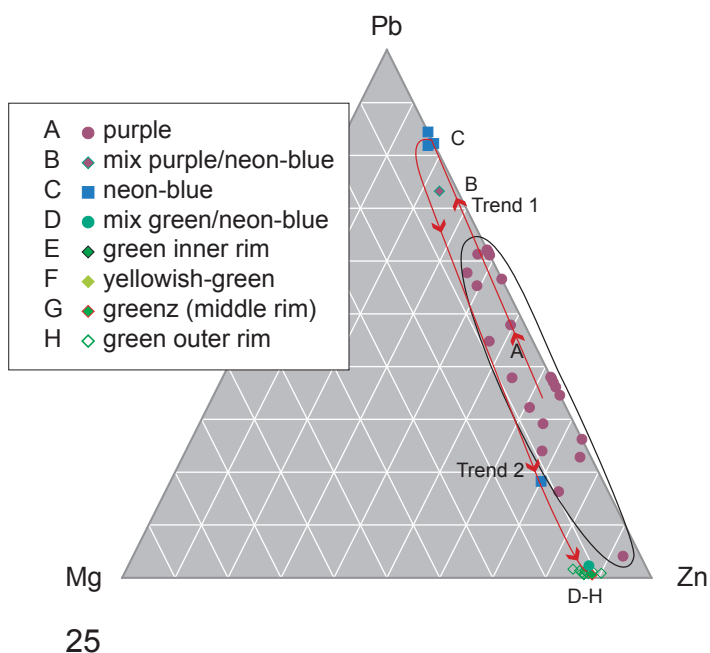
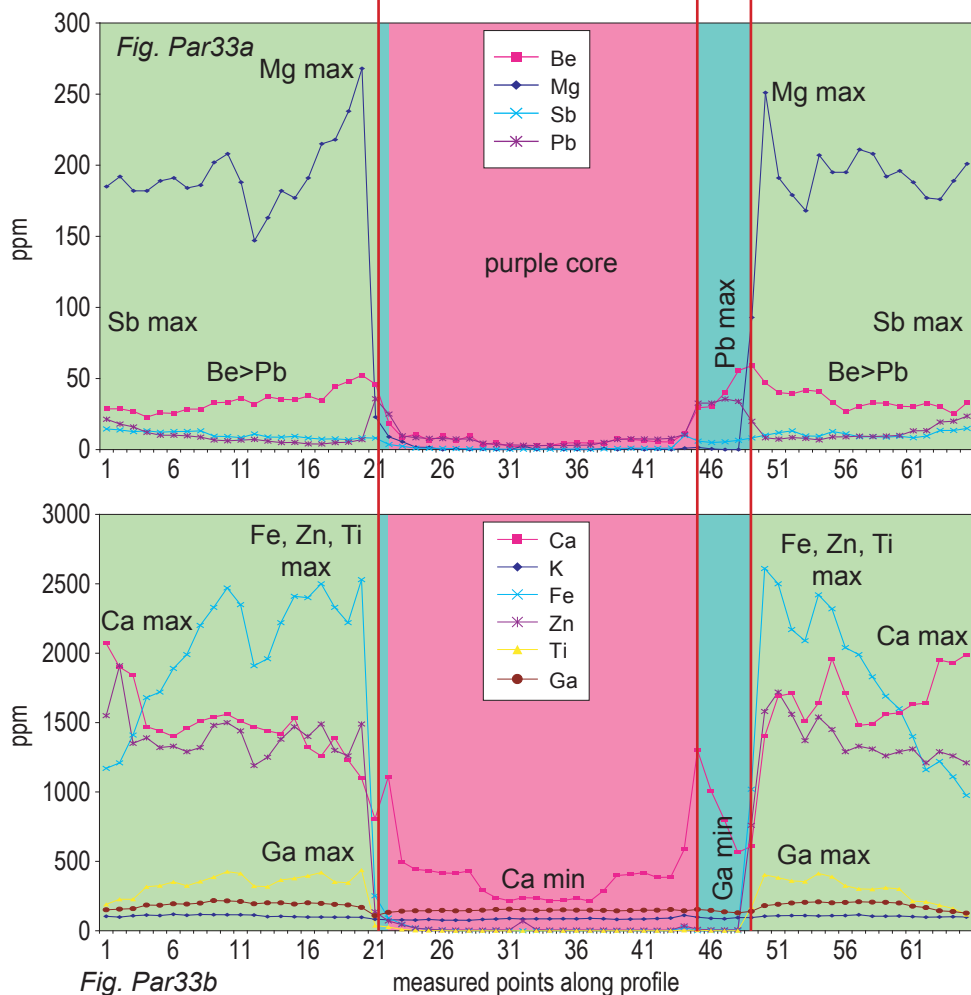


Fig. Par32 Photograph of a multicolored tourmaline from Brazil (Paraíba mine Source RC Gemmas). The tourmaline has been cut perpendicular to the c-axis (thin parallel plate, both sides polished). The sample is from the lot shown in Fig. Par29. The string of craters visible in the picture is induced by LA-ICP-MS analysis. Different color zones are visible.



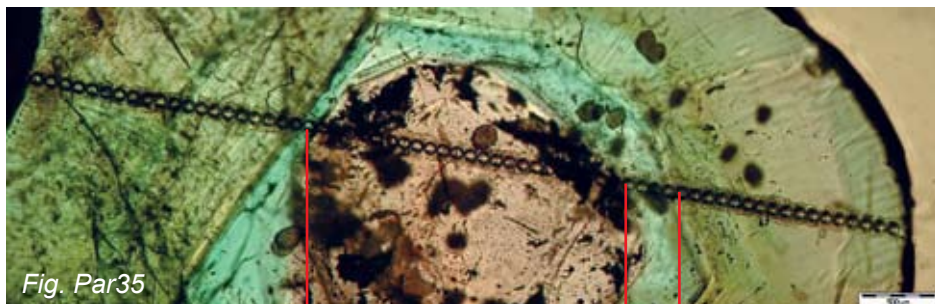


Fig. Par35 Photograph of a Paraíba tourmaline analyzed with LA-ICP-MS perpendicular to the color zoning. Correlation with profile analysis aims at reconstructing the chemical variations of the tourmaline in different growth stadiums (details see Fig. Par32).

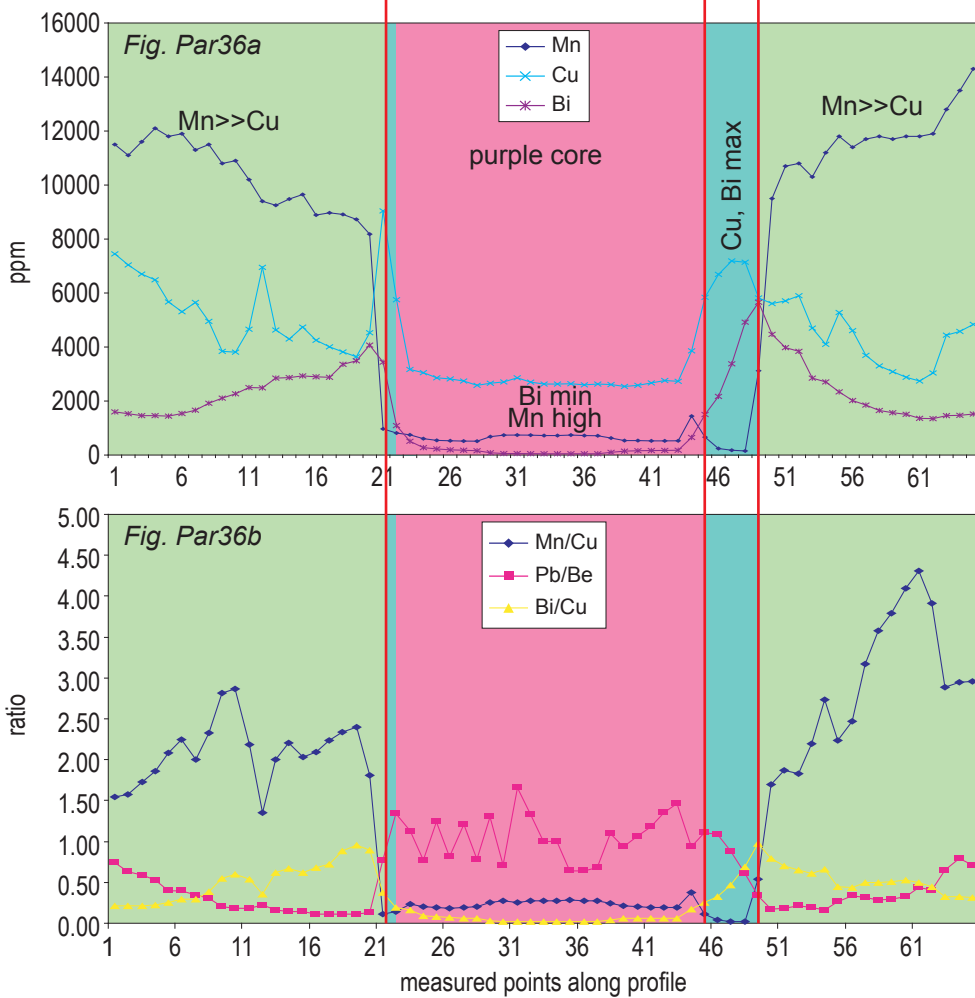


Fig. Par 36a Variation in Mn-, Cu- and Bi-concentrations.

Purple growth zone: Mn-concentrations are higher than Cu-concentrations and Cu-concentrations are higher than the Bi-concentrations. "Neon"-blue growth zone: Cu-concentrations are higher than Mn-concentrations, Bi-increases to equal those of the Cu-concentrations. Compare with EMPA analyses Fig. Par28b.

Fig. Par36b Variation of Mn/Cu-, Bi/- and Pb/Be-concentration ratios

Pb/Be-ratios are highest in the purple core of the tourmaline and decrease with increase in Mn/Cu-ratios. Higher Mn/Cu-ratios are found in the purple core and the green rim. Mn/Cu-ratios constantly increase towards the rim but decrease at the outer green rim. The highest Bi/Cu-ratios are found at the beginning of the trend of higher Mn/Cu-ratios at the transition to the green rim.

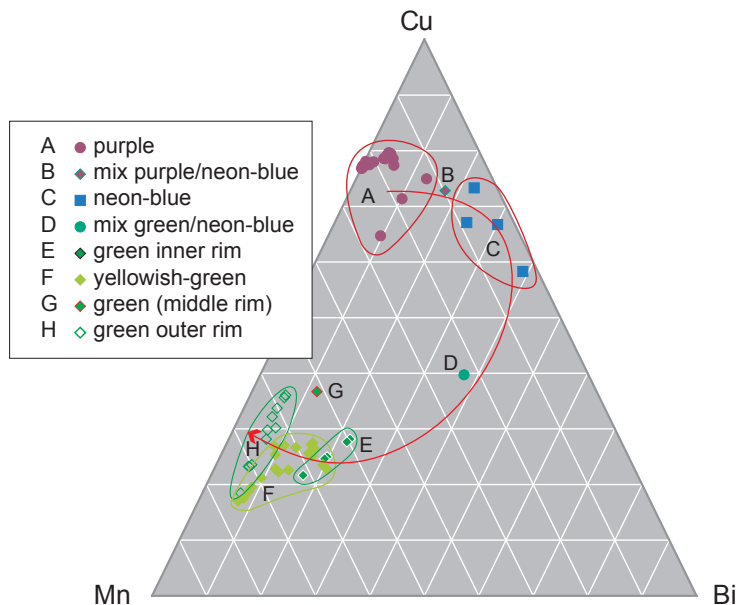


Fig. Par37 Ternary Cu-Mn-Bi diagram showing the variation of Cu-, Mn, and Bi-concentrations from the core (A) to the rim (H) (LA-ICP-MS analysis, in $\mu\text{g/g}$)

A: High Cu-concentrations and Mn-concentrations, low Bi-concentrations (Cu-Mn-dominated growth phase)
A to C: Mn-concentrations depleted, Cu-concentrations enriched, and Bi-concentrations increase (Cu-dominated-growth phase")
C to H: Increase of Mn-concentrations, decrease in Cu- and Bi-concentrations (Mn-dominated growth phase)

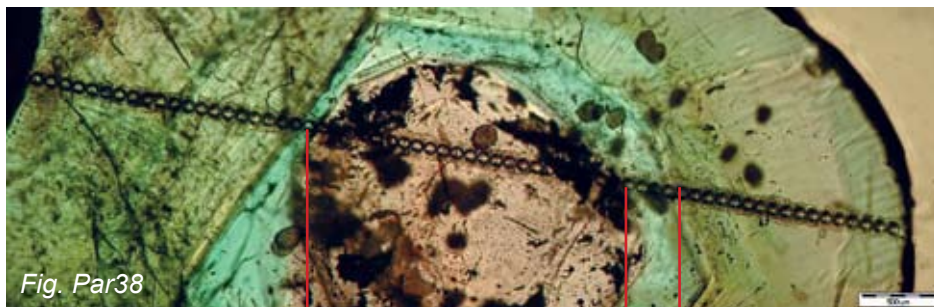


Fig. Par38 Photograph of a Paraíba tourmaline with color zoning is correlated with LA-ICP-MS analyses (in ppm) of rare earth elements (REE), strontium (Sr) and calcium (Ca) (See Fig. Par39a, b and Par41a-d)

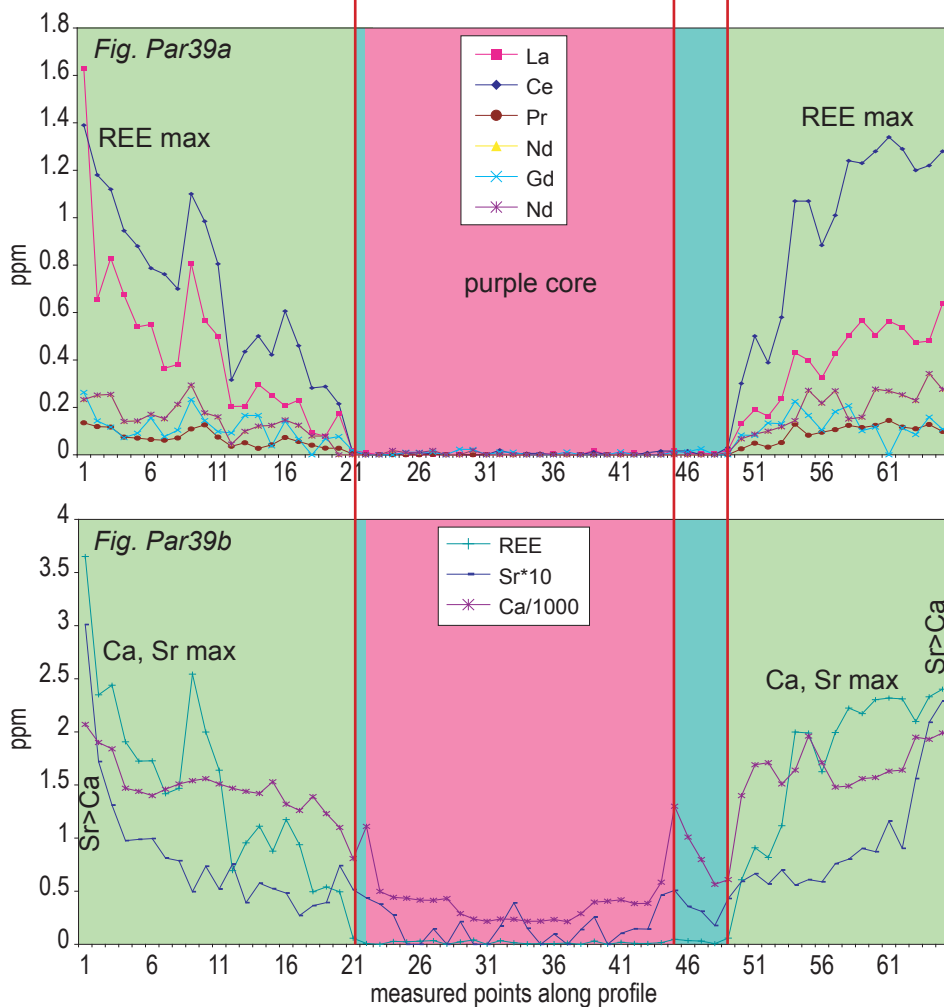


Fig. Par39a-b Concentrations of the REE elements La, Ce, Pr, Nd, Gd and Nd were detected in the green rim of the Paraíba tourmalines. These REE-elements were not detected in the “neon-blue” growth phase (Fig. Par39a). Ce and La dominate the concentrations of REE. The sum of all REE concentrations (Fig. Par39b) correlate well with increasing Sr- and Ca-concentrations along the measured profile. They are found in the rim of crystal.

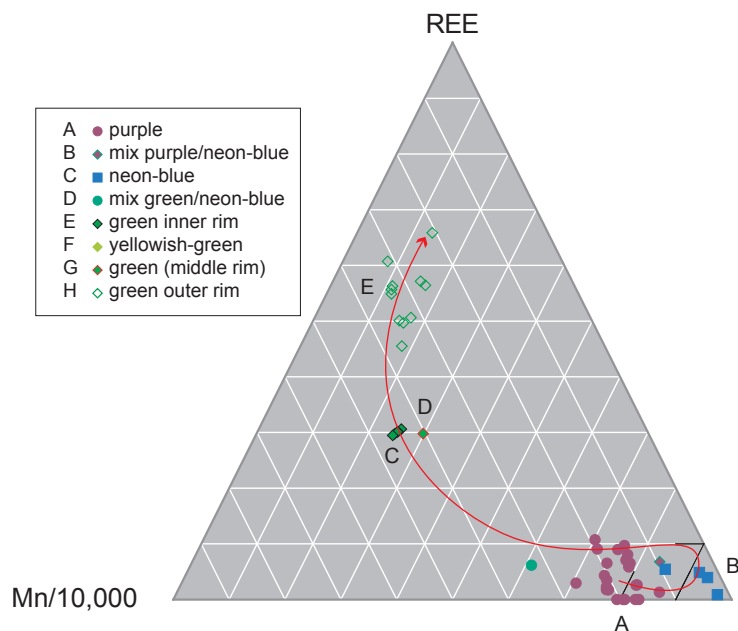


Fig. Par40 Ternary Mn-Cu-REE diagram showing the trend of total REE-concentrations in the tourmaline from the core (A) to the rim (H) in relation to variations in Cu- and Mn-concentrations (LA-ICP-MS analyses, in $\mu\text{g/g}$).

The changes in chemical compositions from core to rim of the tourmaline define a trend that is indicated by the arrow. REE-concentrations increase sharply at the end of the Cu-dominated (“neon”-blue) growth phase. REE-concentrations increase along with Mn-concentrations in the green rim of the tourmaline.

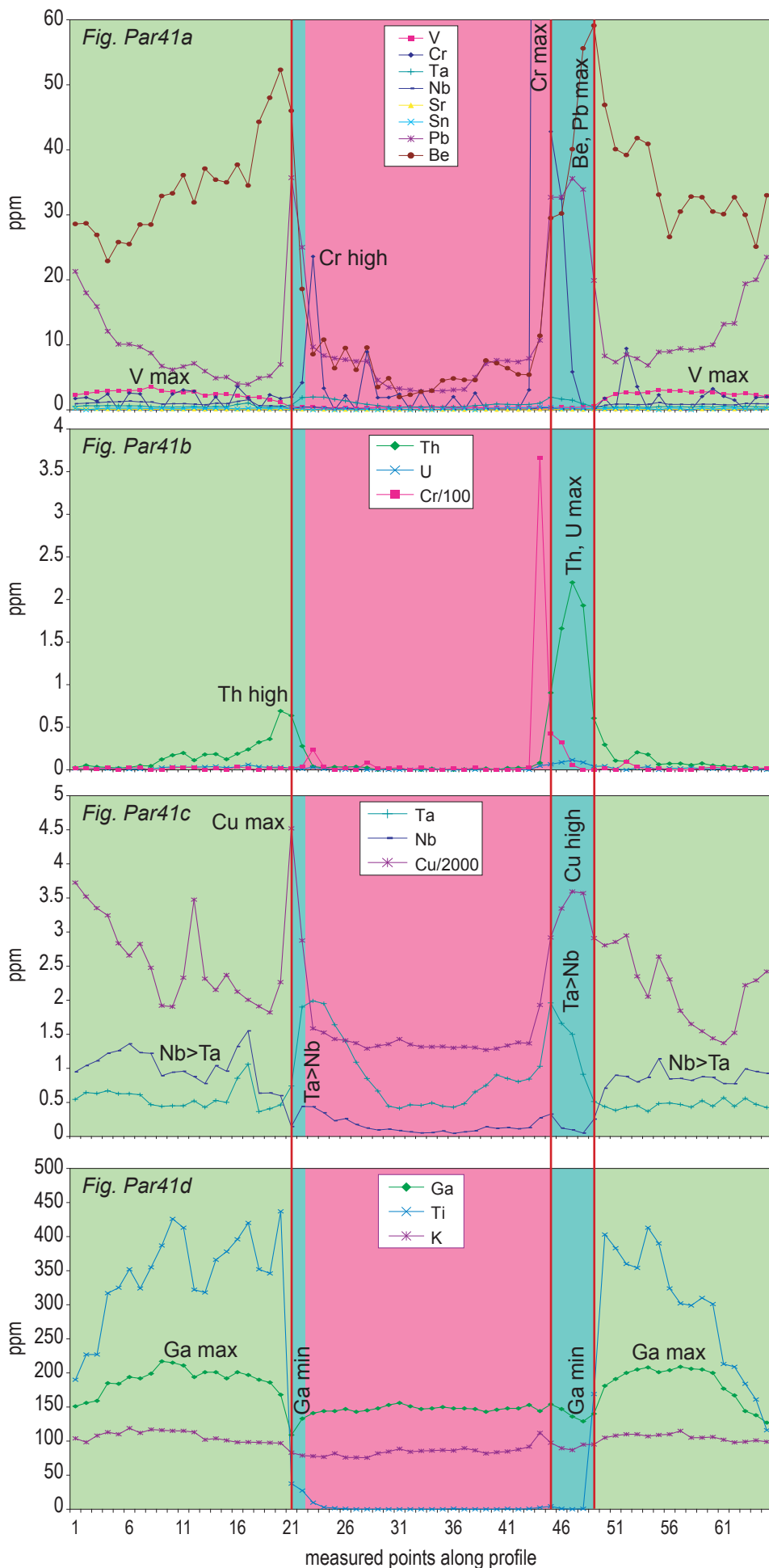


Fig. Par41a Variation in V- and Cr-concentrations

A very distinctly localized growth zone with Cr-concentrations is found at the onset of the "neon-blue" growth phase (see also Fig. Par 41b). V-concentrations are not correlated with the occurrence of the Cr-concentrations in the tourmaline. V-concentrations can only be found in the green rim. These Cr-concentrations are found symmetrically along the chemical profile at the same position at the border of the purple core to the neon-blue zone. They are therefore not the product of a contamination.

Fig. Par41b Variation in Th- and U-concentrations

Distinct Th- and U-concentrations occur in certain growth zones of the tourmaline. The elevated Th-U-concentrations are not correlated with those of the isolated Cr-concentrations. The Th- and U anomaly is localized at the final stage of the "neon"-blue (Cu-dominated) growth phase and at the beginning of the dramatic increase in Mn-concentrations at the border to the green rim. During the growth phase of the green rim, however, Th- and U-concentrations decrease sharply.

Fig. Par41c Variation in Ta- and Nb-concentrations

Ta-concentrations were detected in the "neon"-blue growth zone of the tourmalines. High Ta/Nb-ratios (>1) are found in the same position of first appearance of high Cu-concentrations from the core to the rim in the crystal. Ta and Nb show opposite concentration trends in the measured profile. Ta-concentrations are higher than Nb-concentrations in the purple and "neon"-blue growth zone; Nb-concentrations are higher than those of Ta in the green rim.

Par41d Variation in K-, Ti- and Ga-concentrations

An increase in K-, Ti- and Ga-concentrations occur at the transition to the green rim. It can be correlated with the increase of REE-, Ca- and Sr-concentrations (Fig. Par39b) and Ti-, Fe- and Zn-concentrations (Fig. Par33b). Towards the end of the crystal growth, in the outer dark green rim, the concentration of Ti, Fe and Zn are slightly decreasing. This trend is opposite to the general increase in Nb-, Ca-, REE- and Sr-concentrations. These elements continuously increase towards the outer rim.

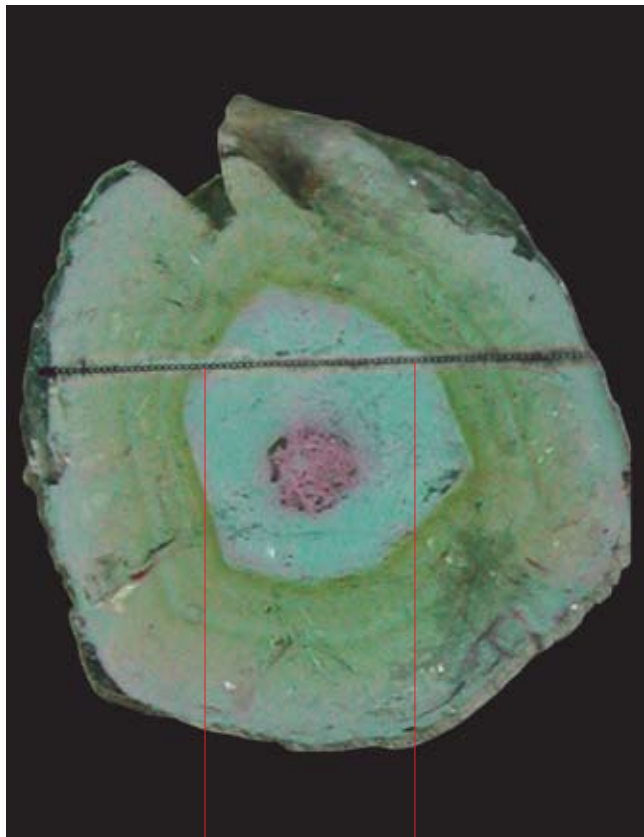


Fig. Par42 Photograph of a multicolored tourmaline from the series of similar sections of same lot and same origin (Fig. Par29). The tourmaline has been cut perpendicular to the c-axis (thin parallel plate, both sides polished). The string of craters visible in the picture represent LA-ICP-MS analysis. The profile has been positioned across the “neon”-blue growth zone and green rim without targeting the purple core of the sample. It is aimed to verify the trends found in another sample from the same lot, which had only narrow zones of “neon”-blue colors (Fig. Par32). It can be shown below that the trends can be reproduced. Chemical analysis profiles see Fig. Par43a-b, 46a-b, 49a-b and 51b-d. A second profile through the purple core of the same sample is shown in Fig. Par 52. It is aimed to also verify the chemical trends in the purple core in a second sample.

Fig. 43a-b, Variation in Fe-, Ti-, Zn-, Pb-, Mg-, Be- and Sb-concentrations

The maximum of the Mg-concentrations are found at the end of the “neon”-blue growth phase. During the “neon”-blue growth phase, Zn- and Mg-concentrations are depleted. High Mg-values are found at the position of high Bi-concentrations in the profile (compare Fig. Par46b). The increase of Mg-concentrations coincides with the first major increase in Mn-concentrations and higher Mn/Cu-ratios in the green rim (Fig. 46b). The concentrations of other elements Pb, Be, Zn, Ca, K, Fe and Ti show major changes as well:
1.) Pb and Be is high along with high Cu in the “neon”-blue growth zone (Fig. Par43b)
2.) Zn increases in the green rim along with Ca, K, Fe and Ti (Fig. Par43a).

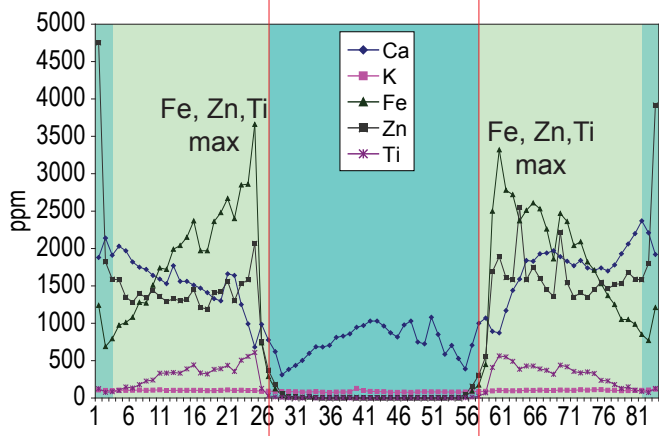


Fig. Par43a

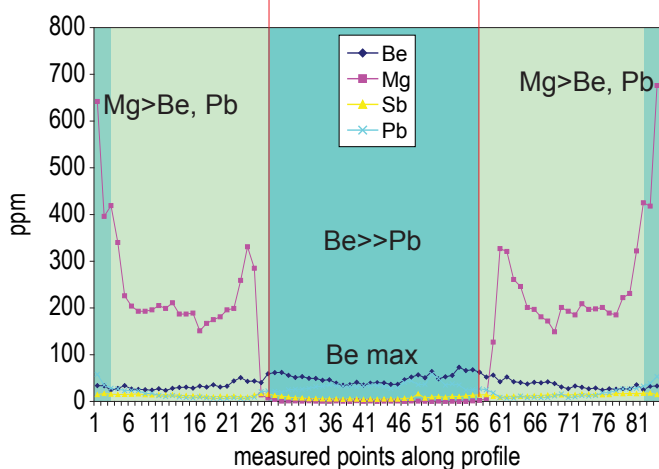


Fig. Par43b

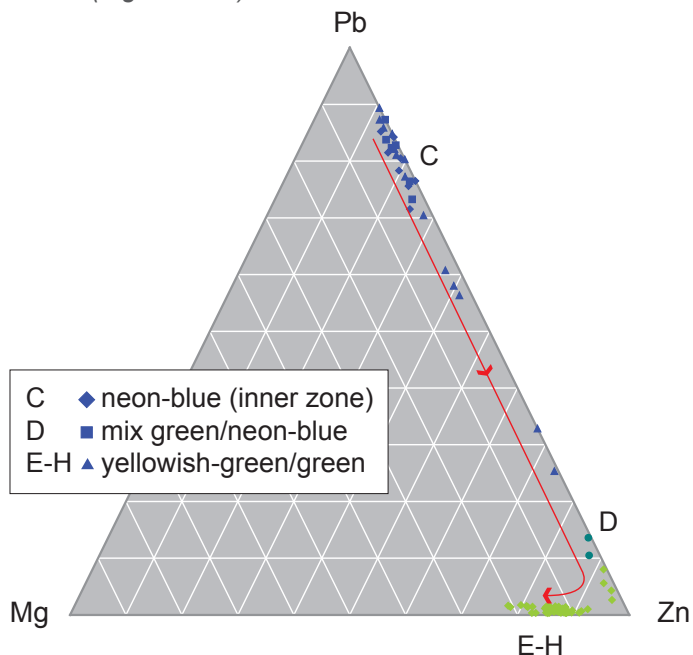


Fig. Par44 Mg-Pb-Zn Triangle (LA-ICP-MS analysis in $\mu\text{g/g}$)
The chemical variations in the relative amount of Mg-, Pb- and Zn-concentrations can be correlated with transition of the “neon”-blue to green growth zones in the tourmaline. The trend (red line) from the “neon”-blue zone to the rim is marked by an increase in Zn and Mg in the outer rim.

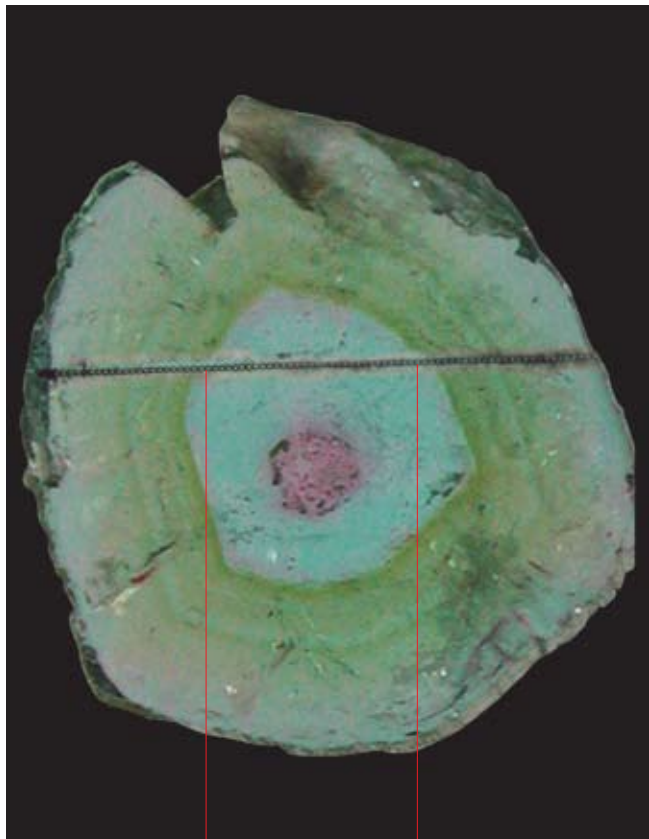


Fig. Par45 Photograph of a multicolored copper-bearing tourmaline in cross section and the trail of craters induced by LA-ICP-MS (detailed description see Fig. Par42).

Fig. Par 46a. Variation in Cu-, Mn- and Bi-concentrations.

In the "neo-blue growth zone, the Cu dominates Mn and Bi. A sharp increase in Bi occurs towards the end of the "neon-blue" growth phase. This confirms the earlier findings in a section of the same lot (Fig. Par36a).

Fig. Par46b Variation of Mn/Cu-, Pb/Be- and Bi/Cu-ratios

Pb/Be ratios are approximately 1 in the neon-blue growth phase of the Paraíba tourmaline and decrease towards the inner rim and finally increase in the outer rim. The highest Bi/Cu-ratio is found at the transition of the "neon"-blue to the green rim. Higher Mn/Cu-ratios are present at the end of the crystal growth.

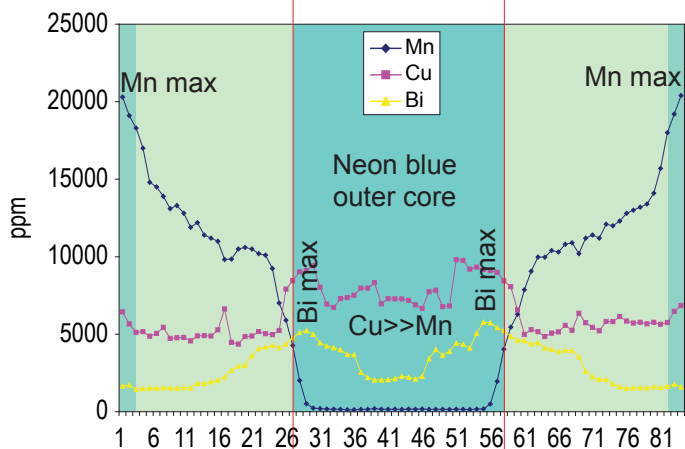


Fig. Par46a

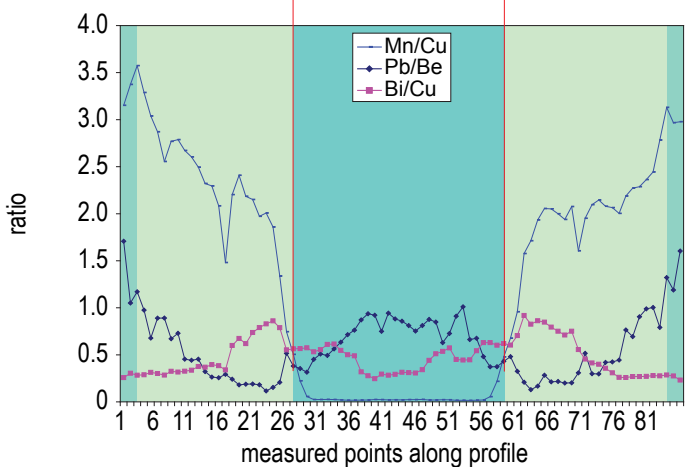


Fig. Par46b

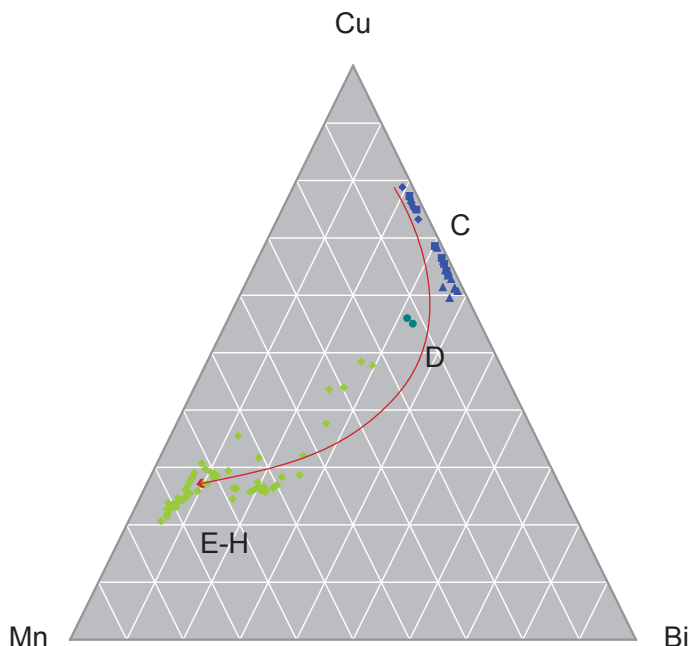
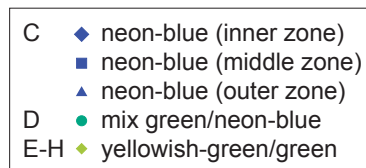


Fig. Par47 Ternary diagram showing the chemical variation of Cu-, Mn-, and Bi-concentrations from the "neon"-blue growth zone (C) to the rim (H) (LA-ICP-MS analysis, $\mu\text{g/g}$)

C to H: Increase of Mn-concentrations, decrease in Cu- and Bi-concentrations (Mn-dominated growth phase)

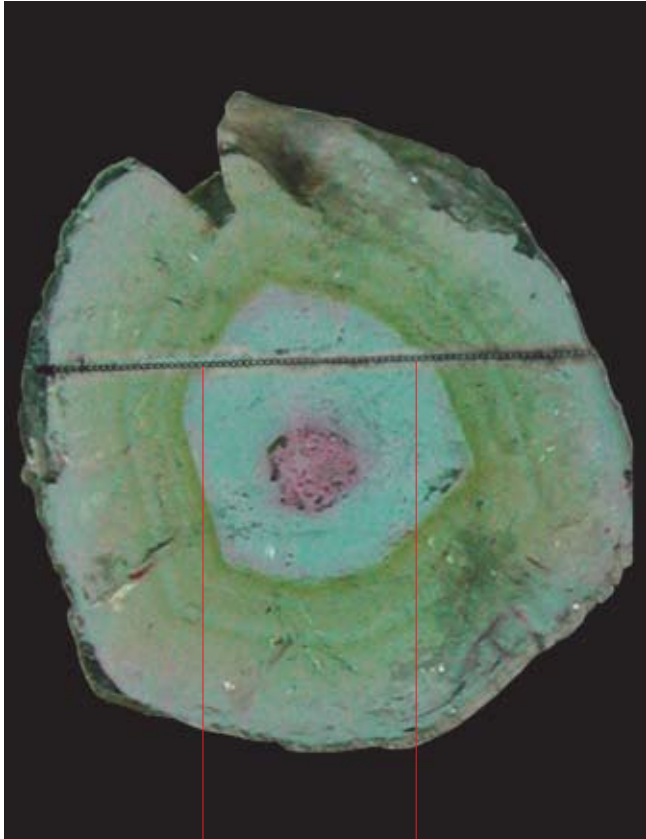


Fig. Par48 Photograph of a multicolored copper-bearing tourmaline in a cross-section and the trail of craters induced by LA-ICP-MS (detailed description see Fig. Par42). Growth and color zones are correlated with chemical profile analyses (LA-ICP-MS) focusing on the concentrations of REE (Fig. Par 49a), Pb- and Be-concentrations (Fig. Par49b).

Fig. Par49a REE are mainly found in the second half of the Paraíba tourmaline growth phase (green sector) with a slight increase in the center of the “neon-blue” growth phase. Ce and La dominate the concentrations of REE.

Fig. Par49b Pb- and Be-concentrations are highly variable over the “neon”-blue growth sector and with a high Pb/Be-ratio (highest Pb/Be-ratio is found in the rim).

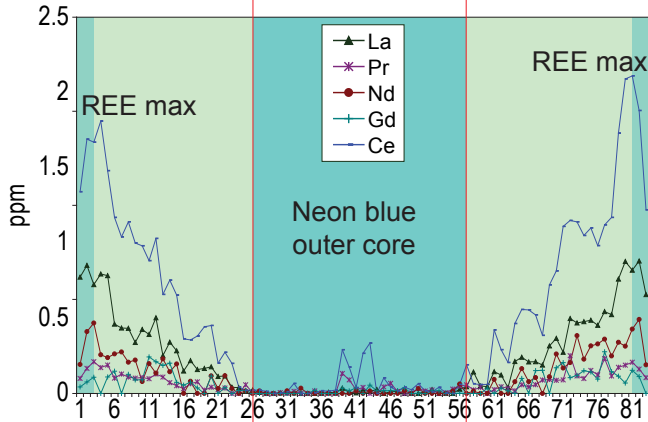


Fig. Par49a

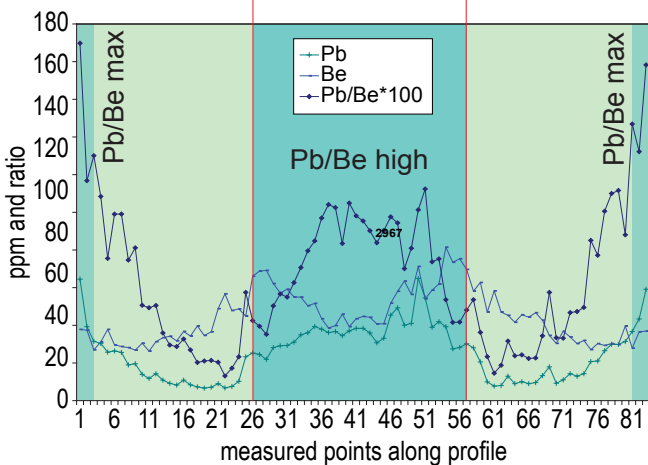


Fig. Par49b

- C ◆ neon-blue (inner zone)
- neon-blue (middle zone)
- ▲ neon-blue (outer zone)
- D ● mix green/neon-blue
- E-H ◆ yellowish-green/green

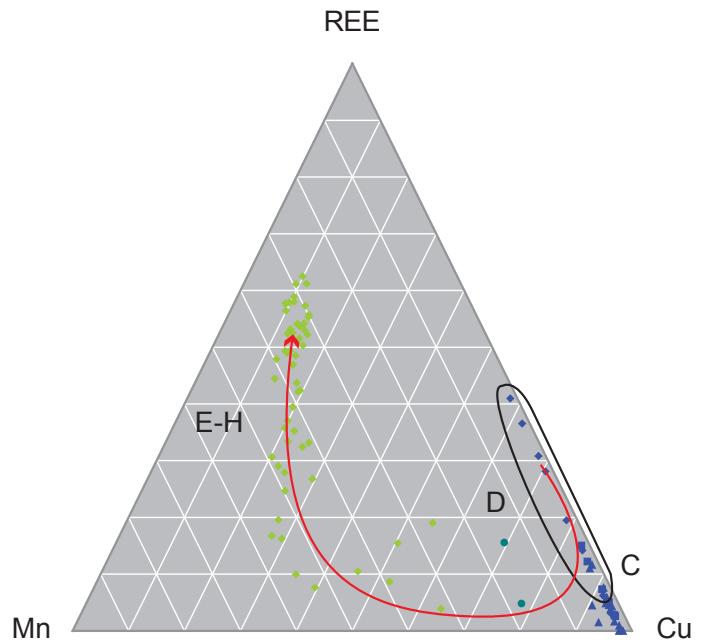


Fig. Par50 Ternary Mn-Cu-REE diagram showing the trend of total REE-concentrations in the tourmaline from the “neon”-blue growth zone (C) to the rim (H) in relation to variations in Cu- and Mn-concentrations (LA-ICP-MS analyses, in $\mu\text{g/g}$) The triangle shows that the REE do occur within and after the termination of the “neon”-blue growth phase. Increase in REE-concentrations is correlated with increasing Mn-and decreasing Cu-concentrations.

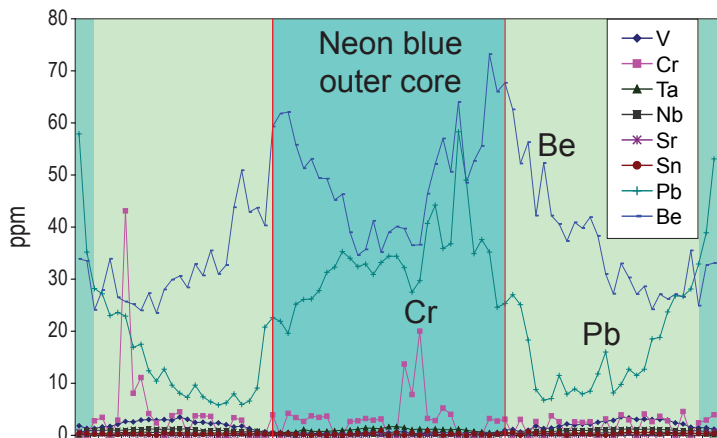


Fig. Par51a Variation in V- and Cr-concentrations

A very distinctly localized Cr-concentration is found only within the “neon”-blue growth phase. V is not correlated with Cr and can only be found in the rim.

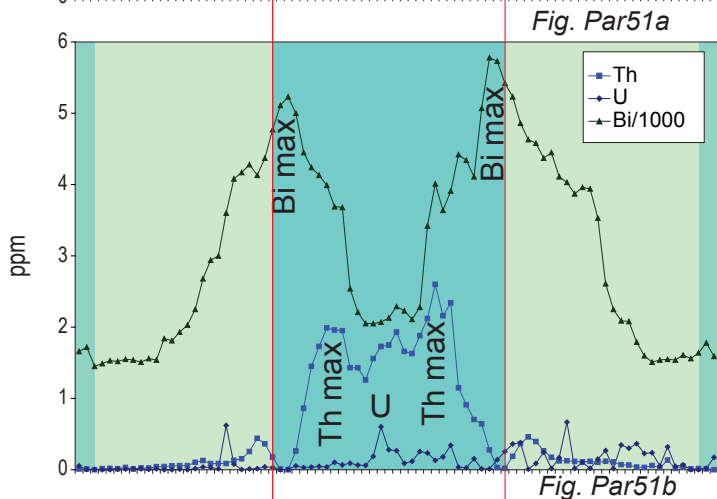


Fig. Par51b Variation in Th- and U-concentrations

Th- and U- concentrations are symmetrically detected in the profile and the positions are not identical. They can be correlated with the maximum of the Bi-concentrations. The Th-concentrations were formed first, before the high Bi-concentrations occurred.

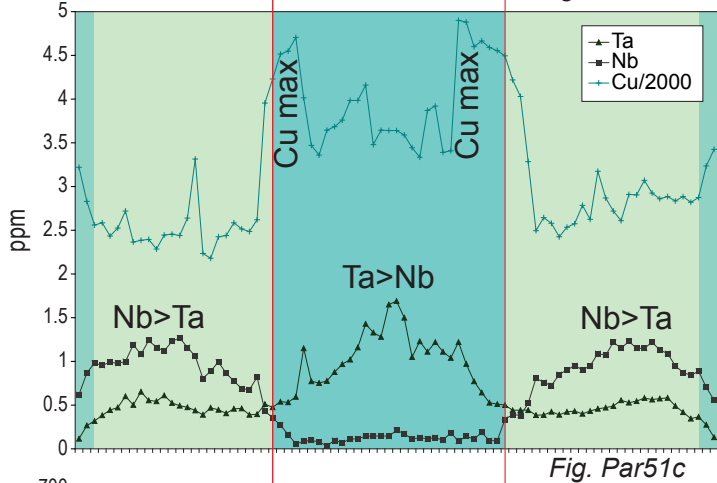


Fig. Par51c Variation in Ta- and Nb-concentrations

Ta- and Nb-concentrations show an opposite distribution in the crystal. Highest Ta- and lowest Nb-concentrations are found within the “neon”-blue growth phase of the tourmalines.

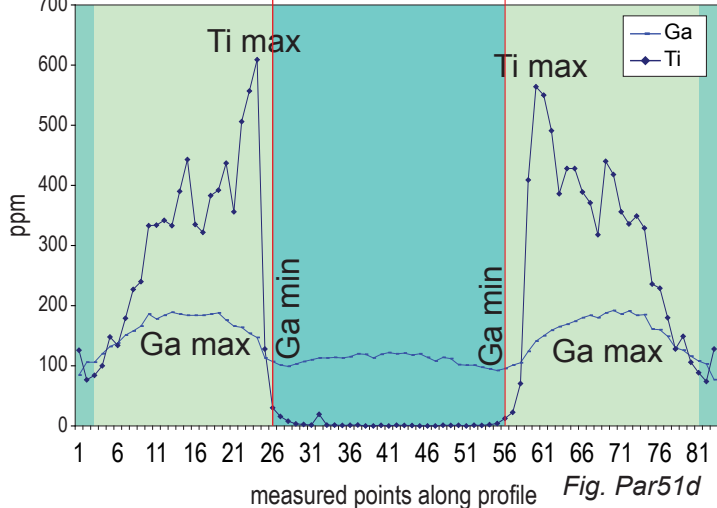


Fig. Par51d Variation in Zn-, Fe-, Ti- and Ga-concentrations

A sharp increase in Ti-, Zn- and Fe-concentrations occur at the beginning of the Mn-dominated growth phase. It can be correlated with the increase of REE, Ca and Sr. Ti-, Fe- and Zn-concentrations are highest at the contact to the green rim. Towards the end of the crystal growth, their concentrations are constantly decreasing. This trend is opposite to the general increase of Nb, Ca, REE and Sr, which increase towards the outer rim. Slightly elevated Ga-concentrations are found in the green rim of the tourmaline.

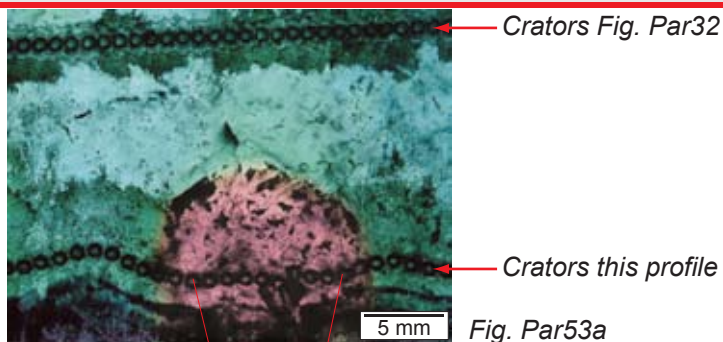
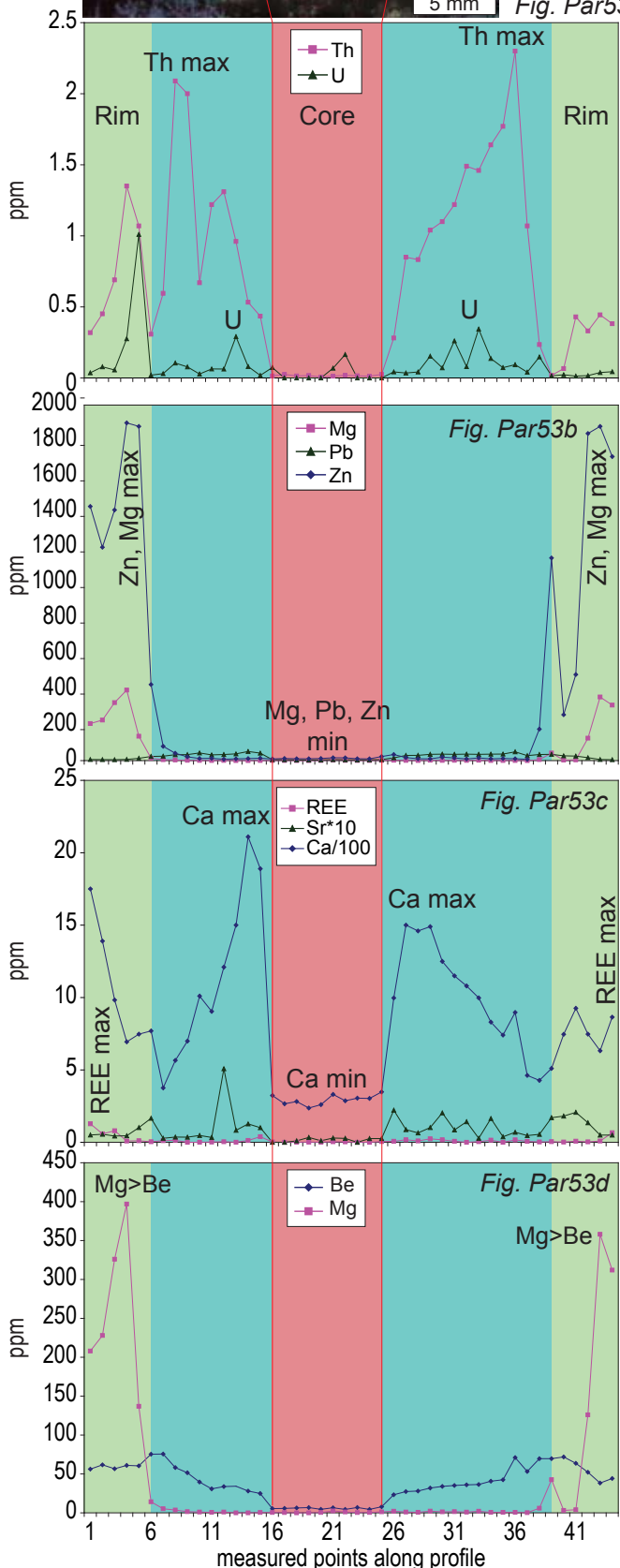


Fig. Par 52 Photograph of a multicolored tourmaline analyzed by LA-ICP-MS. Two profiles of craters are visible in the picture. One targeting the chemical composition in the "neon"-blue color zone (See Fig. Par42) and one through the purple core.

Fig. Par53a-d Variation of Pb-, Mg-, Be- and Sb-concentrations

The maximum of the Mg-concentrations are well correlated with the end of the "neon"-blue growth phase. During the "neon"-blue growth phase, Zn- and Mg-concentrations are depleted. The increase in Mg-concentrations is in coincidence with the first major increase in concentrations of Mn. This observation confirms the findings of another sample (Fig. Par33a). The following observations do also confirm the previous findings in the first sample:



- 1.) Pb and be are enriched in the "neon"-blue growth zone (Fig. Par53b, d)
- 2.) Zn increases in the green rim along with Mg (Fig. Par 53b)
- 3.) Th- and U-concentrations are slightly enriched in the "neon"-blue growth zone. Th-concentrations are higher than U-concentrations (Fig. Par53b). The highest U-concentrations appear before the Th-maximum in the profile from the core to the rim (See also Fig. Par51b).
- 4.) The Ca- and Sr-maximum is correlated with the REE-maximum (Fig. Par53c).

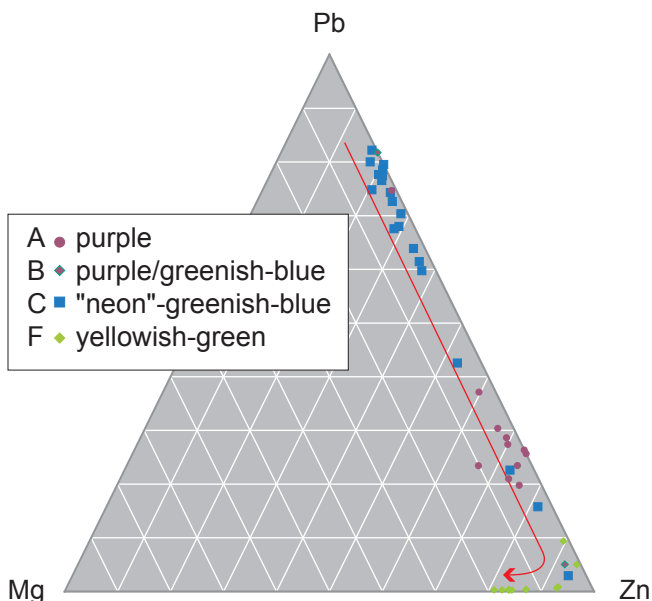


Fig. Par54 Ternary Mg-Pb-Zn Diagram

The same trend in the concentration variations of Mg, Pb and Zn was found as described in Fig. Par 34.

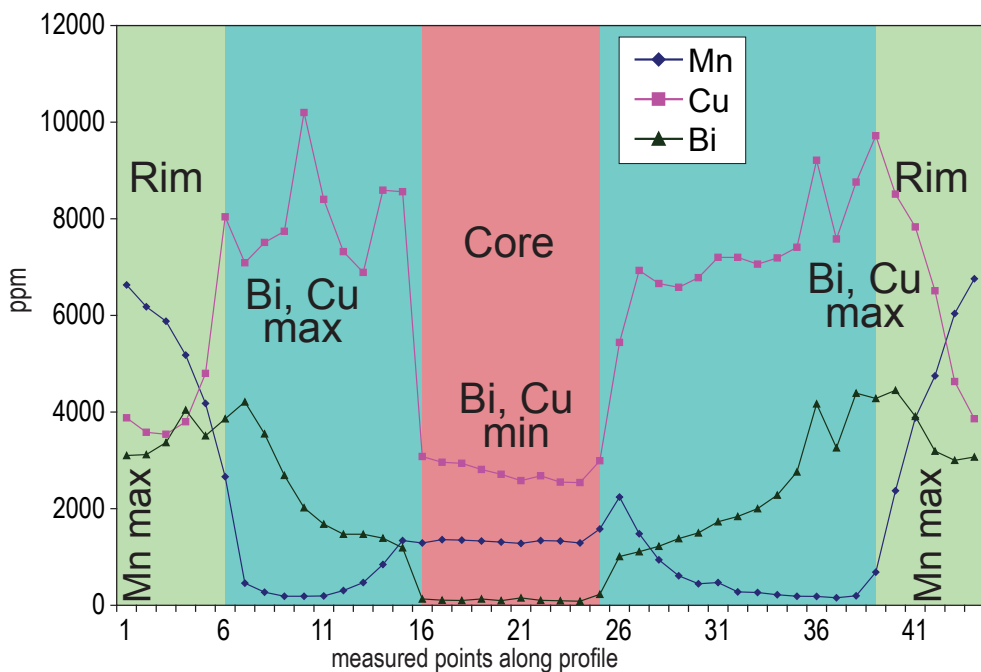


Fig. Par55 Variations in Cu-, Mn- and Bi-concentrations

Lowest Cu- and Bi-concentrations are found in the purple core and highest concentrations of these elements are found in the outer rim of the "neon"-blue colored growth zone. The highest Mn-concentrations are found in the rim.

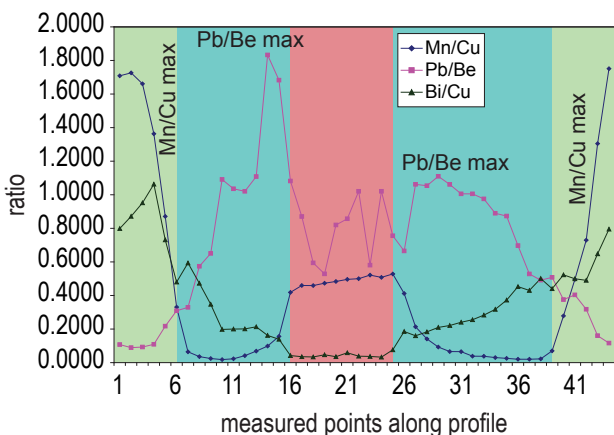


Fig. Par55b Variation in Mn/Cu-, Pb/Be- and Bi/Cu-ratios

Pb/Be ratios are approximately 1 in the neon-blue growth phase of the Paraíba tourmaline and decrease towards the inner rim. It finally increases in the outer rim. The highest Bi/Cu-ratio is found at the transition of the neon-blue to the green rim. Higher Mn/Cu ratios are present at the end of the crystal growth. This confirms earlier findings in another sample of the same lot (Compare Fig. Par36b).

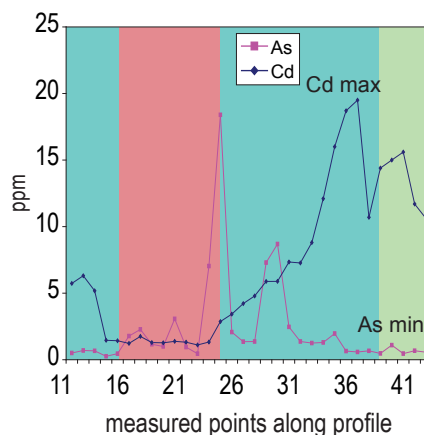


Fig. Par56 Variations in As- and Cd-concentrations

The highest Cd-concentrations and lowest As-concentrations are found at the same position as the maximum of the Cu- and Bi-concentrations (See Fig. Par55).

Fig. Par57 Ternary Cu-Mn-Bi diagram

The same trends were found in another sample from the same lot. See Fig. Par37 for explanations.

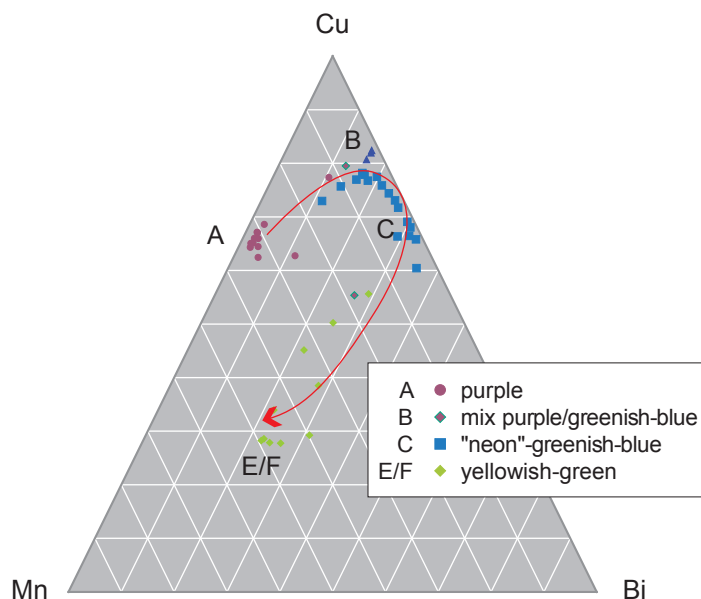




Fig. Par58 Photograph of a multi-colored tourmaline from Brazil from another source (Paraiba, Batalha mine, source: Wagoner)

Note: Intense purple-, blue- and green color zoning is visible from core to the rim. The trail of craters is from LA-ICP-MS analysis. Chemical analysis profiles see Fig. Par59a-d and Fig. Par60a-d.

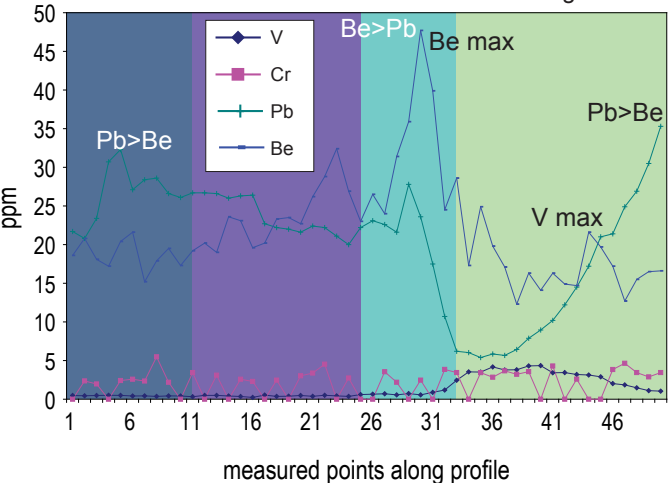
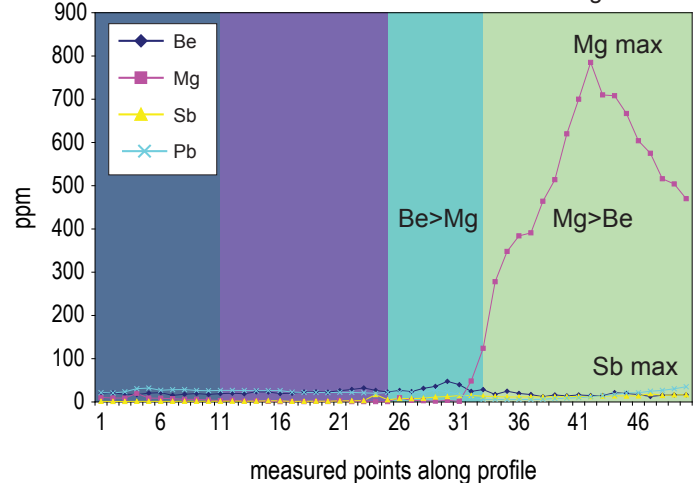
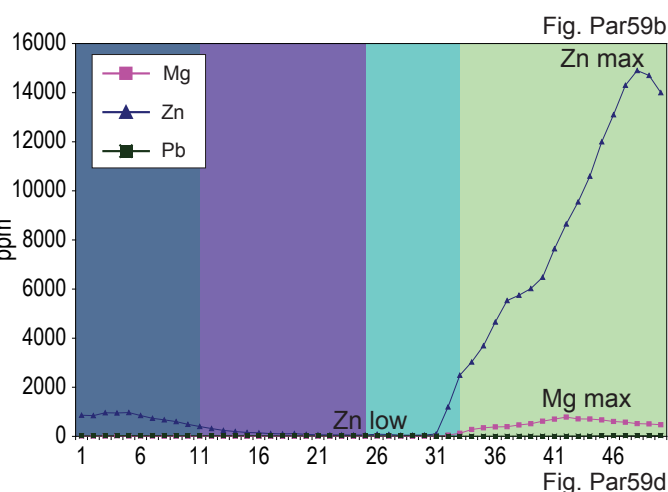
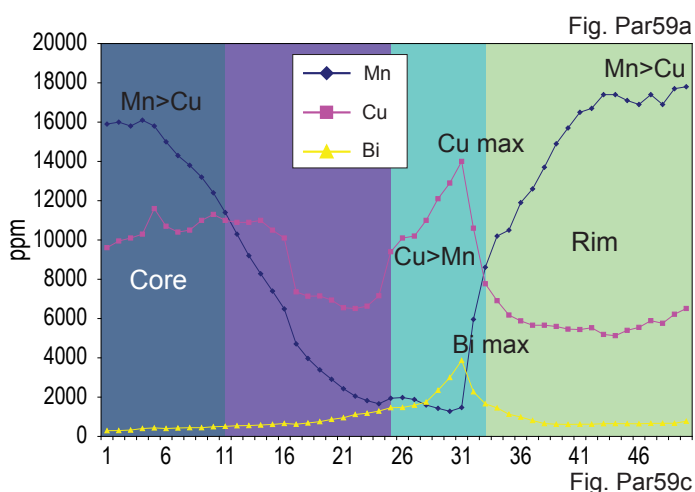


Fig. Par59a-d Chemical analysis profile by LA-ICP-MS. Chemical variations are correlated with color zoning. The “neon”-blue color zone is characterized by a decrease in Mn- and an increase in Cu- and Bi-concentrations (Fig. Par59a). The inner core of the crystal is characterized by high concentrations of Mn, followed by a sudden decrease in Mn-concentrations in the “neon”-blue growth zone. The Mn-concentrations resume their concentration level during crystal growth towards the rim. A very similar profile has been published in the literature from the same type locality (Lit. Par16) with almost identical results regarding the Mn- and Cu-trends. Other trace element concentrations can be correlated with these changes in the minor elements. Be is enriched in the “neon”-blue zone (Fig. Par59d) and Zn and Mg in the green rim (Fig. Par59b-c).

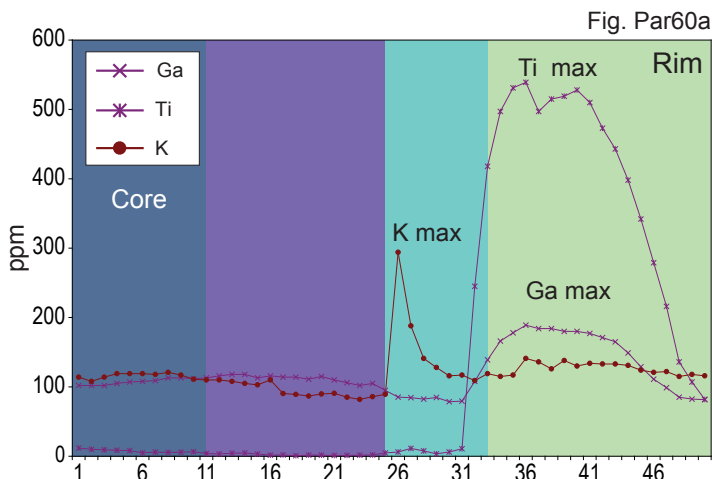


Fig. Par60a Variation in Ga- and Ti-concentrations

Ga and Ti are enriched at the same positions in the green rim.

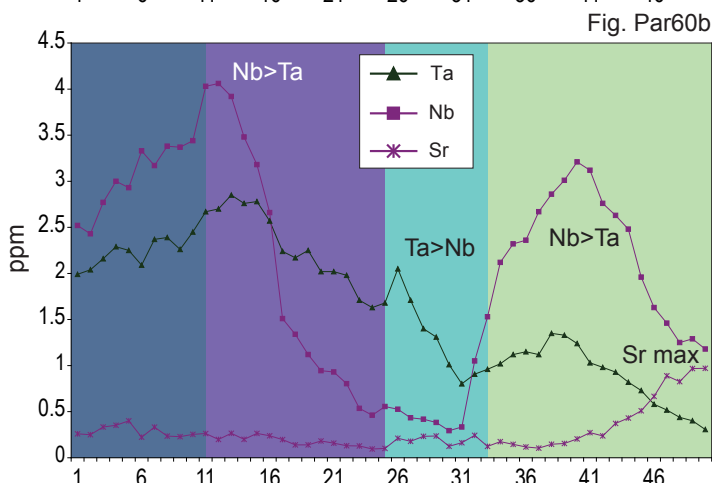


Fig. Par60b Variation in Ta- and Nb-concentrations

The variations of these elements can be correlated with the variations in concentrations of Cu and Mn:

Nb- and Ta-concentrations are enriched in the core and the rim of the tourmaline crystal and they are depleted in the Cu-rich growth zone. The Ta/Nb-ratio changes across the profile with highest Ta/Nb in the copper-rich growth zone of the tourmaline with "neon"-blue color. The ratio reverses in the green rim.

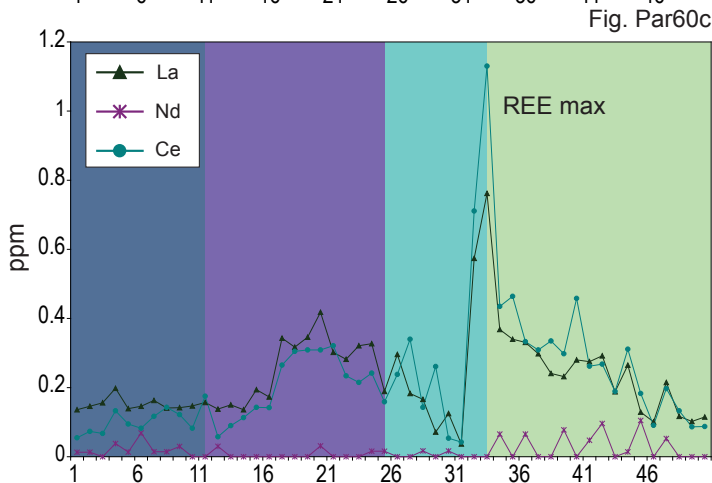


Fig. Par60c Variation in REE-concentrations

REE-concentrations (La, Nd and Ce) are enriched at the transition from the "neon"-blue color zone to the green rim.

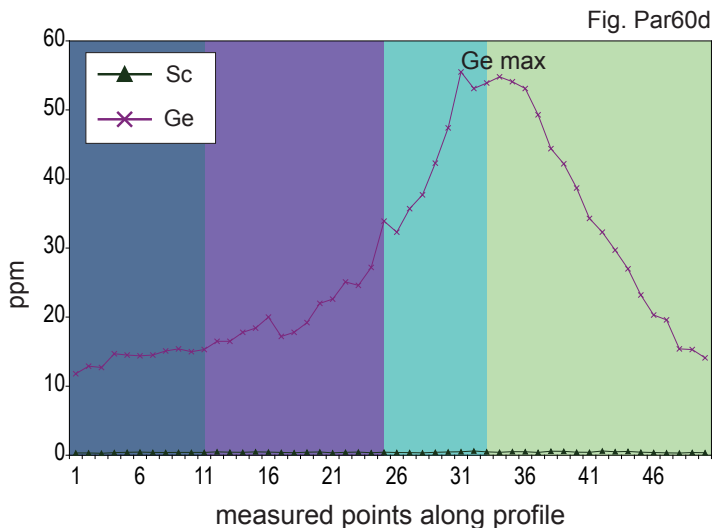


Fig. Par60d Variation in Ge- and Sc-concentrations

Ge-concentrations are highest in the transition zone from the "neon"-blue to the green color zoning.

In conclusions, the following typical chemical composition can be found in the "neon"-blue blue color zone in the tourmaline:

Cu-, Bi- and Be-concentrations are enriched and Nb, Ga-, Zn-, Pb- and Mg-concentrations are depleted.

Sr, Ti, Zn, Pb and Mg concentrations along with Fe (not plotted, concentrations see Tab. Par03) are enriched in the green part of the crystal.

The "green" rim is also characterized by an increase in the concentrations of Ti and Ga (Fig. Par60a), Pb (Fig.59d) and Sr (Fig. Par 60b).

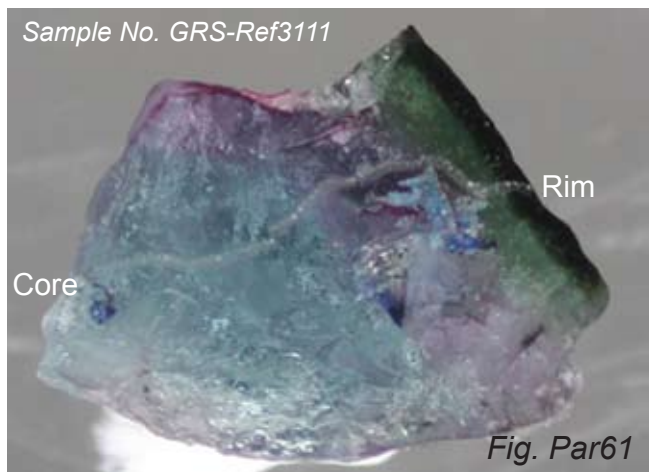
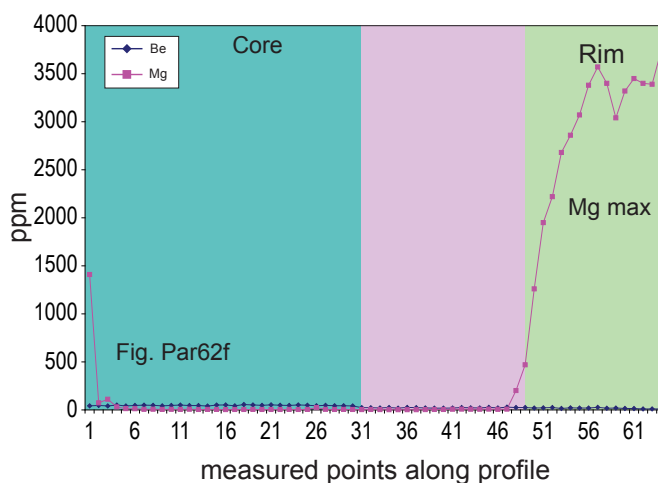
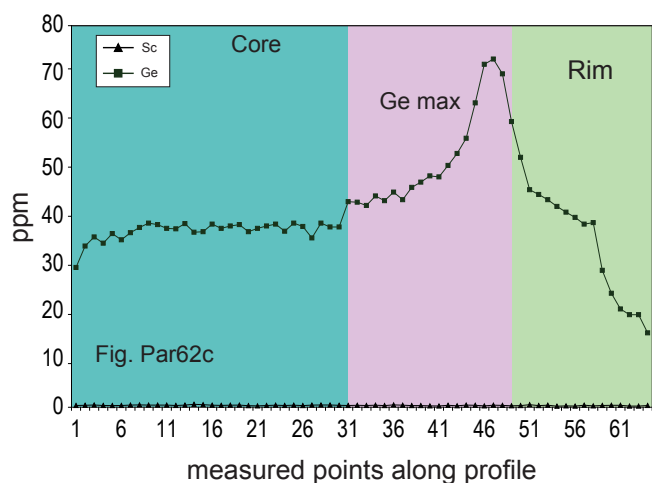
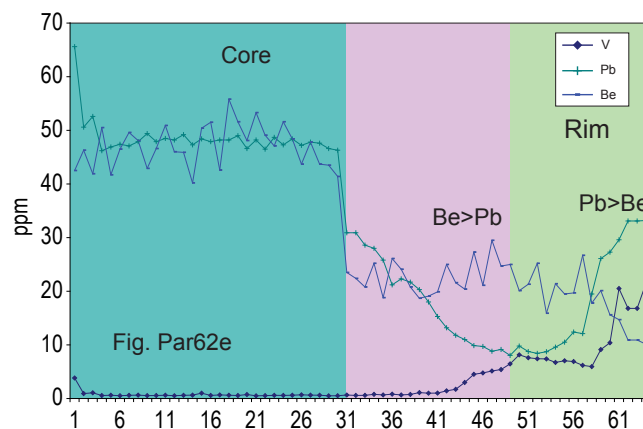
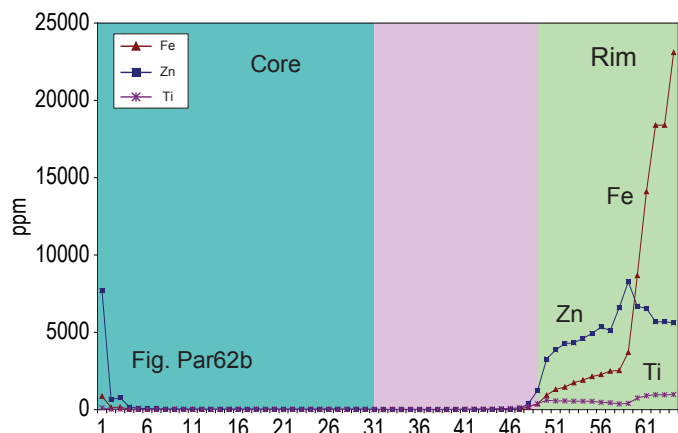
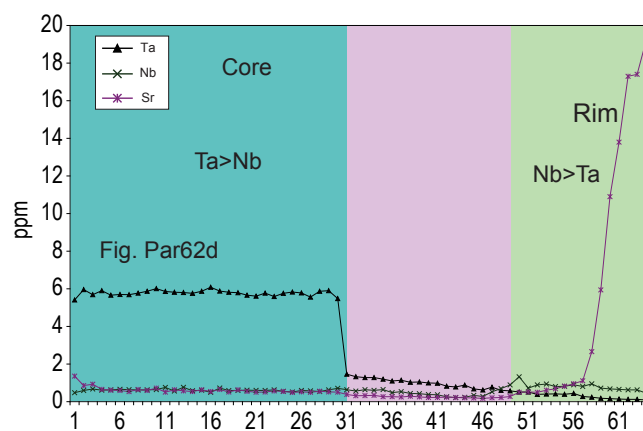
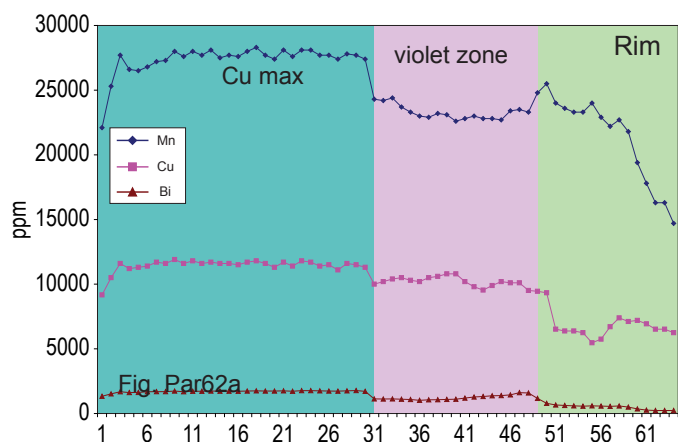


Fig. Par61 Photograph of multi-colored tourmaline from Brazil (Paraíba, Batalha mine, Heitor mine, 1988, source: Pavlik), Sample No. GRS-Ref3111. Note: blue, violet and green color-zoning (from core to rim). Laser ablation crater visible. Chemical analysis profiles see Fig. Par 62a-j

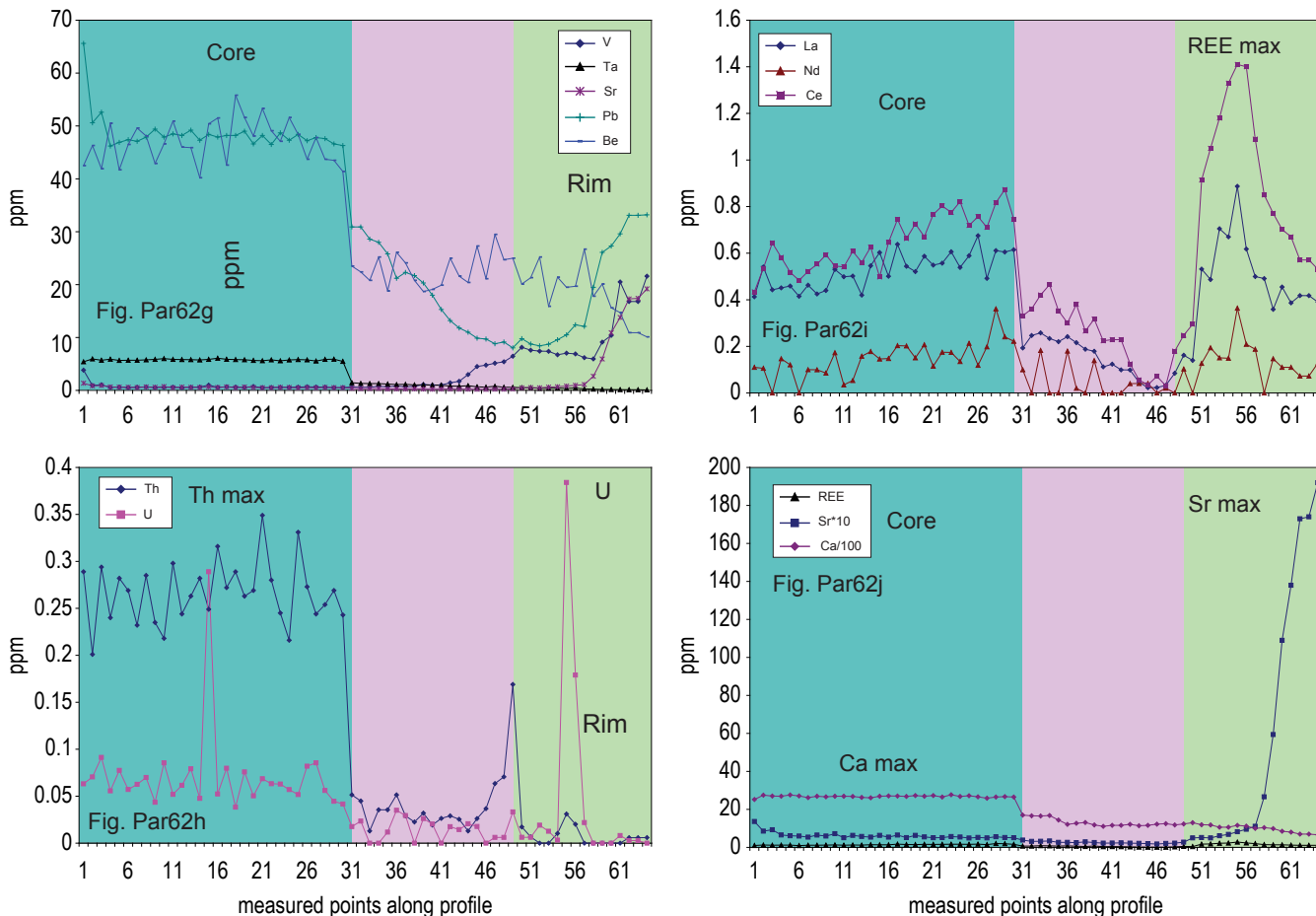
Fig. Par62a-j Variation in Th-, U-, Ta-, Cu-, Mn-, Bi-, Be- and Pb-concentrations.

Chemical variations are correlated with the color zoning. The following elements are enriched in the blue core of the crystal: Th, U (Fig. Par62h); Ta (Fig. Par62d); Cu, Mn and Bi (Fig. Par62a), Be and Pb (Fig. Par62e).

Elements enriched in the green rim: Mg (Fig. Par62f); Sr and V (Fig. Par62d, g);



LA-ICP-MS Chemical Analysis Profiles of Paraíba Tourmaline, Batalha Mine 1988, Pavlik Collection, Sample No. GRS-Ref3111



Rare Earth elements (Fig. Par62i, j and Fig. Par63) and Fe, Zn and Ti (Fig. Par62b). “Ge”-enrichment is found in the transition zone from the violet to the green rim of the crystal (Fig. Par62c). A similar situation was observed in another sample (See Fig. Par60d). Higher Pb/Be-ratios (Fig. Par 62e) and higher Nb/Ta-ratios (Fig. Par62d) are found in the green rim of the crystal.

REE (La, Ce, Nd)-Concentration Variations in Tourmalines from Brazil

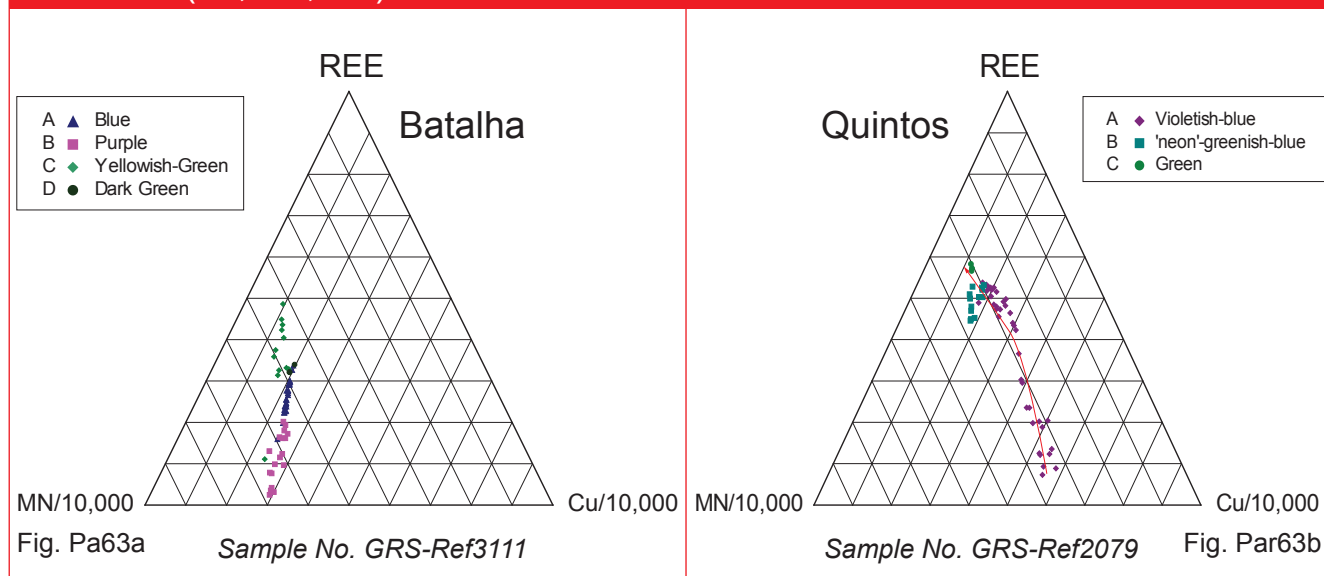


Fig. 63a-b Triangular plot of Mn, Cu (concentrations divided by 10000) and Rare Earth Elements (REE) in two multicolored copper-bearing tourmaline from two different mines in Brazil (Batalha, Paraíba State and Quintos, Rio Grande do Norte). Chemical compositions are measured in a profile from the core to the rim of the crystal (A-D). The chemical compositions show a trend towards higher REE along with higher Mn/Cu-ratios regardless of the origin. Towards the end of the crystal growth, REE-concentrations are highest (Details see cross section profiles Fig. Par60c and 62j).

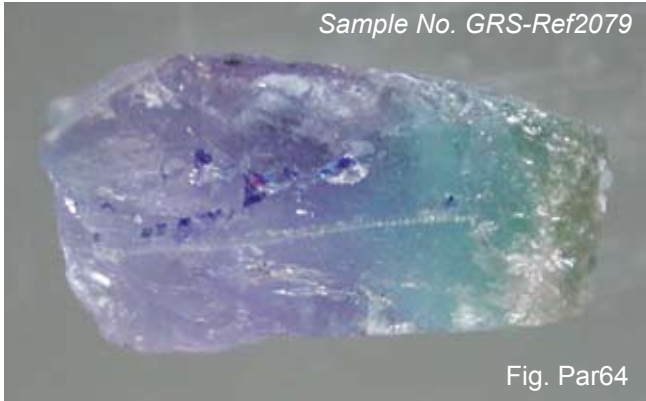


Fig. Par64 Photograph of multi-colored tourmaline from Brazil Rio Grande do Norte, Quintos mine (P. Wild), sample GRS- Ref 2079. Note: Violet, blue and green color zoning (from core to rim). Laser ablation craters are visible (size 60 micrometers). Chemical analysis profiles see Fig. Par66a-j.

Chemical analysis profile of "Paraiba"-tourmaline from Brazil (Sample No. GRS-Ref2079, GRS collection). Chemical variations are correlated with the color zoning (see Fig. Par66a-j).

Fig. Par66a. Variations of Cu-, Bi- and Mn-concentrations.

The concentrations of Cu and Mn gradually change over the measured profile (Fig. Par66a). Higher concentrations of Cu than Mn were found in the core of the crystal (Cu/Mn-ratio is greater than 1). In the rim of the crystal, the Cu/Mn-ratio is less than 1.

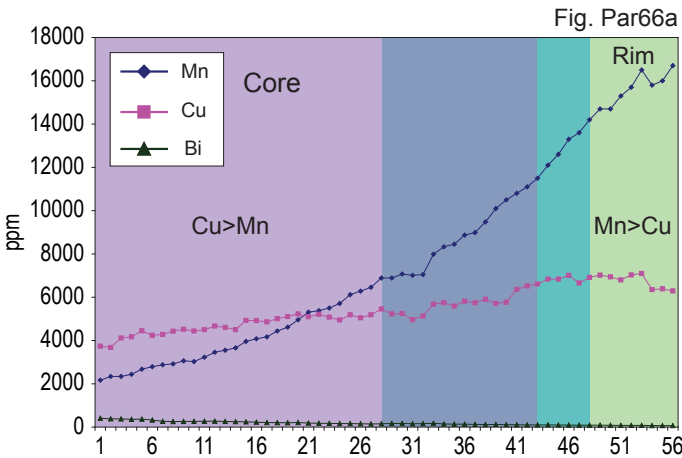


Fig. Par66b-j Variations in REE-, Ta-, Nb-, Ti-, Fe-, Zn-, U-, Th- and Mg-concentrations

From the core towards the rim, other element concentrations also increase, such as rare earth element La and Ce (Fig. Par66i and Fig.66j). A decrease in element concentrations over the same profile is observed for Ta and Nb (Fig. Par66e, g) and Ge (Fig. Par66h). Isolated increase of higher element

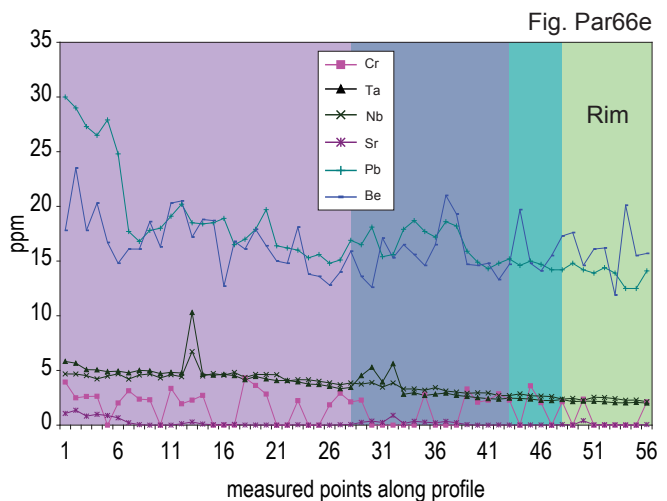
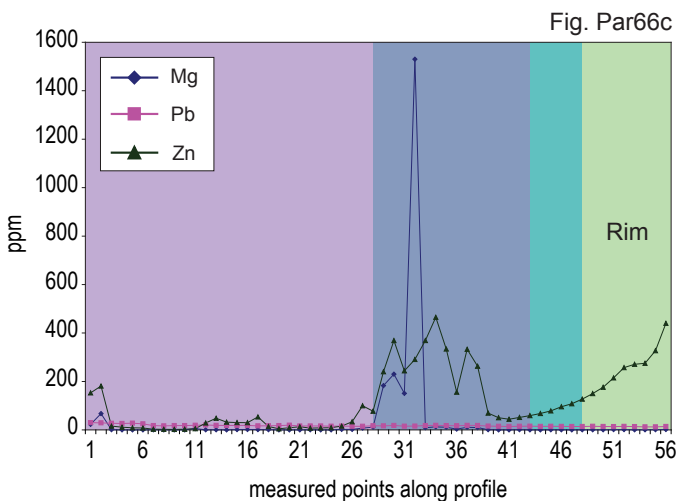
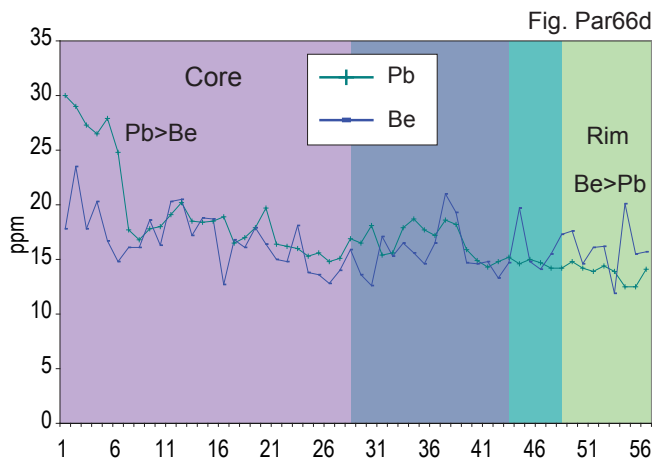
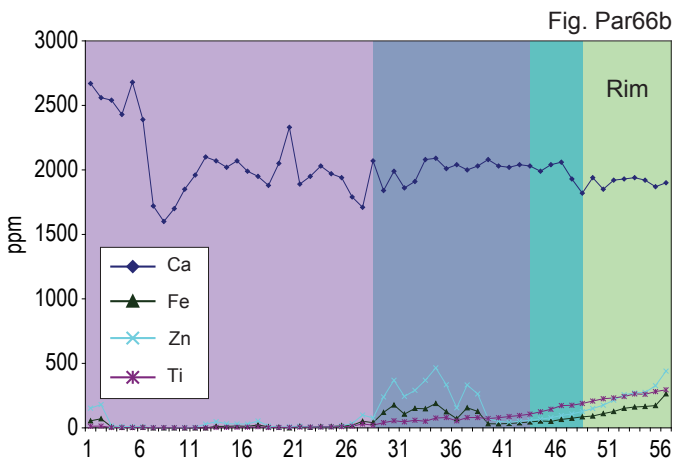




Fig. Par65

Fig. Par65 A spectacular unheated copper-bearing tourmaline from Brazil (P. Wild, Quintos mine, Rio Grande do Norte). Size: 378.65ct, length= 52mm and width= 36mm.

Note the violet-blue color in the center of the crystal, followed by a "neon"-blue color of the main part and a green rim.

The tourmaline fragment that has been measured by LA-ICP-MS is from another sample that showed a more distinct color zoning developed over a shorter distance (Fig. Par64).

concentrations of Ti, Fe and Zn (Fig. Par66b), Th, U (Fig. Par66f) and Mg (Fig. Par66c) were detected at particular growth stages of the crystal. Fe, Ti and Zn increase towards the rim of the crystal (Fig. Par66b). Pb- and Be-concentrations remain constant along the measured profile at low levels (Fig. Par66d).

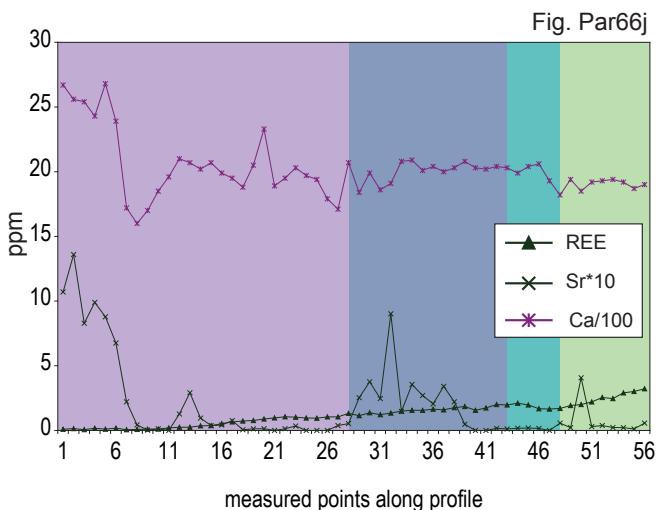
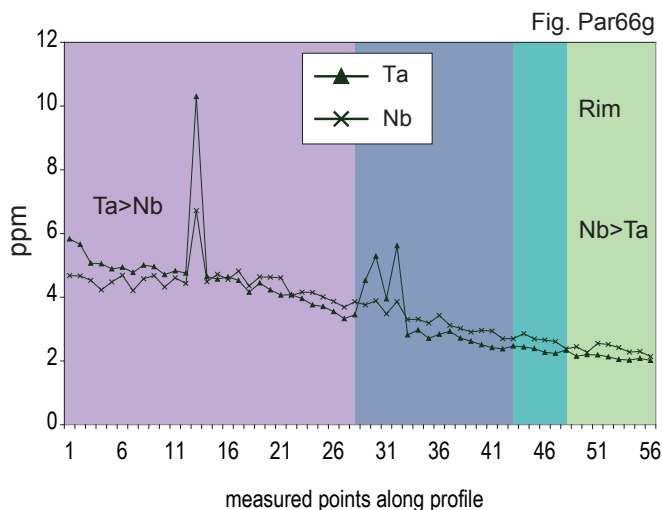
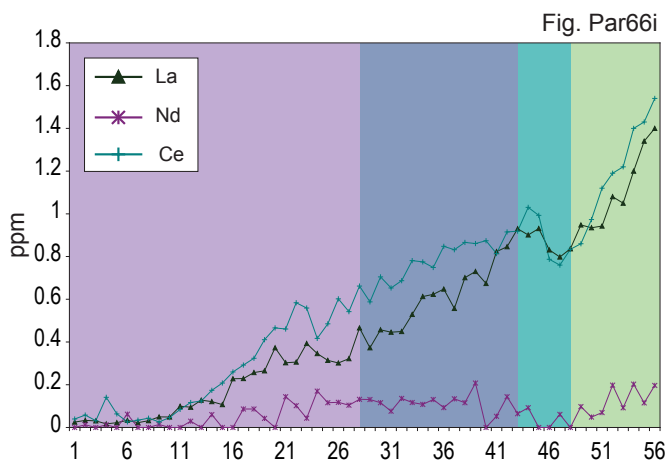
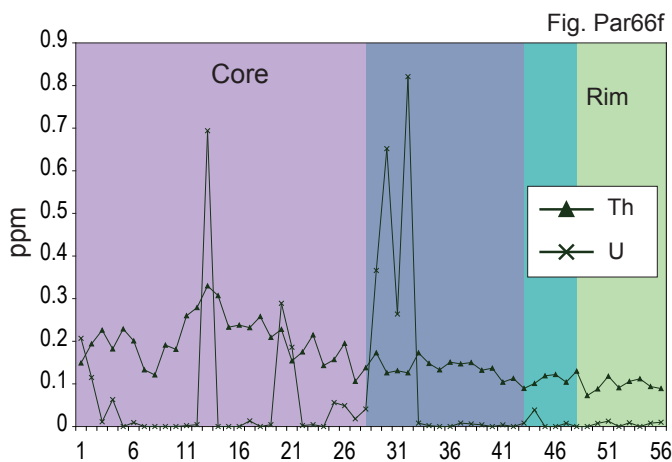
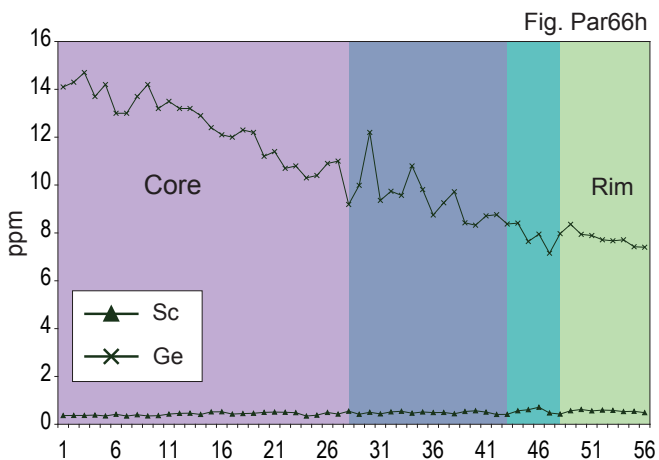




Fig. Par67a



Fig. Par67b

Fig. Par67a-b An example of a large copper-bearing tourmaline rough from Mozambique is shown. It has been experimentally faceted in our own GRS cutting studio into a set of 13 faceted gemstones for this report (Fig. Par68a). The rough of 983ct was acquired from an African supplier in 2007. The largest tourmaline obtained after faceting is over 103 ct and the smaller pear-shapes are between 3 to 7 ct. A small portion of the stones was of a “Paraiba”-type green-blue color. The remaining stones were bluish-green, green and yellowish-green. All faceted stones are in GRS collection. An inclusion case study was performed on these samples that all originated from the same rough (See Fig. Par68-71).

*Inclusion Research Case Study of a Copper-Bearing Tourmaline from Mozambique:
Orange Growth Tubes and purple "Halo"*

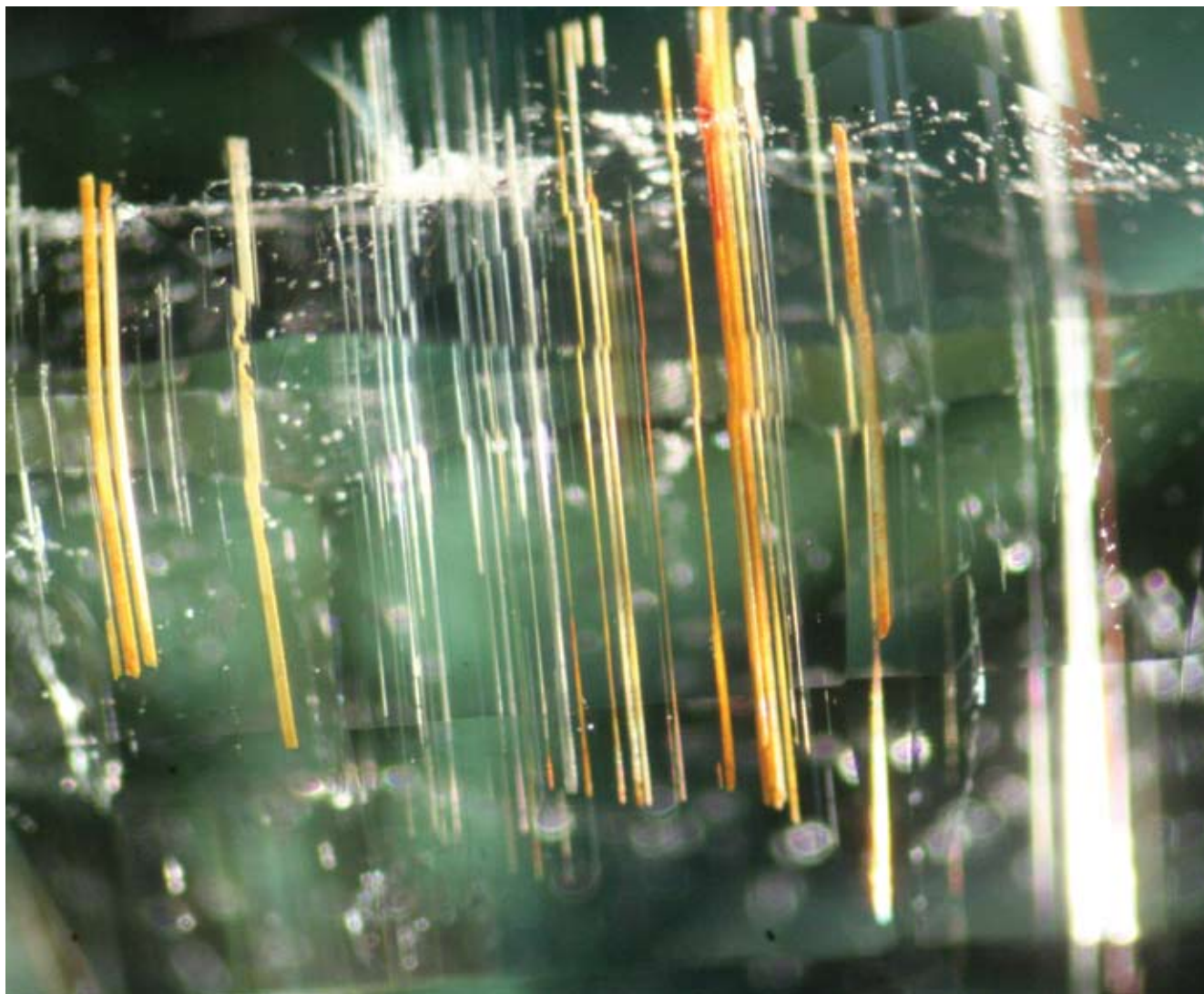


Fig. Par68a Yellow-orange colored growth tubes in a bluish-green copper-bearing tourmaline from Mozambique.



Fig. Par68b

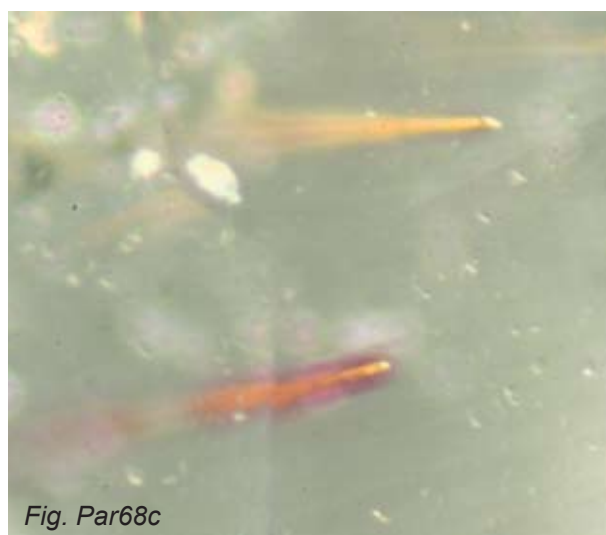


Fig. Par68b-c Same growth tubes such as shown in Fig. Par68a but observed in another faceted stone from the lot shown in Fig. Par67b (all faceted stones originally from the same rough, See Fig. Par67a). Narrow purple "halos" were present around these particular orange growth tubes.

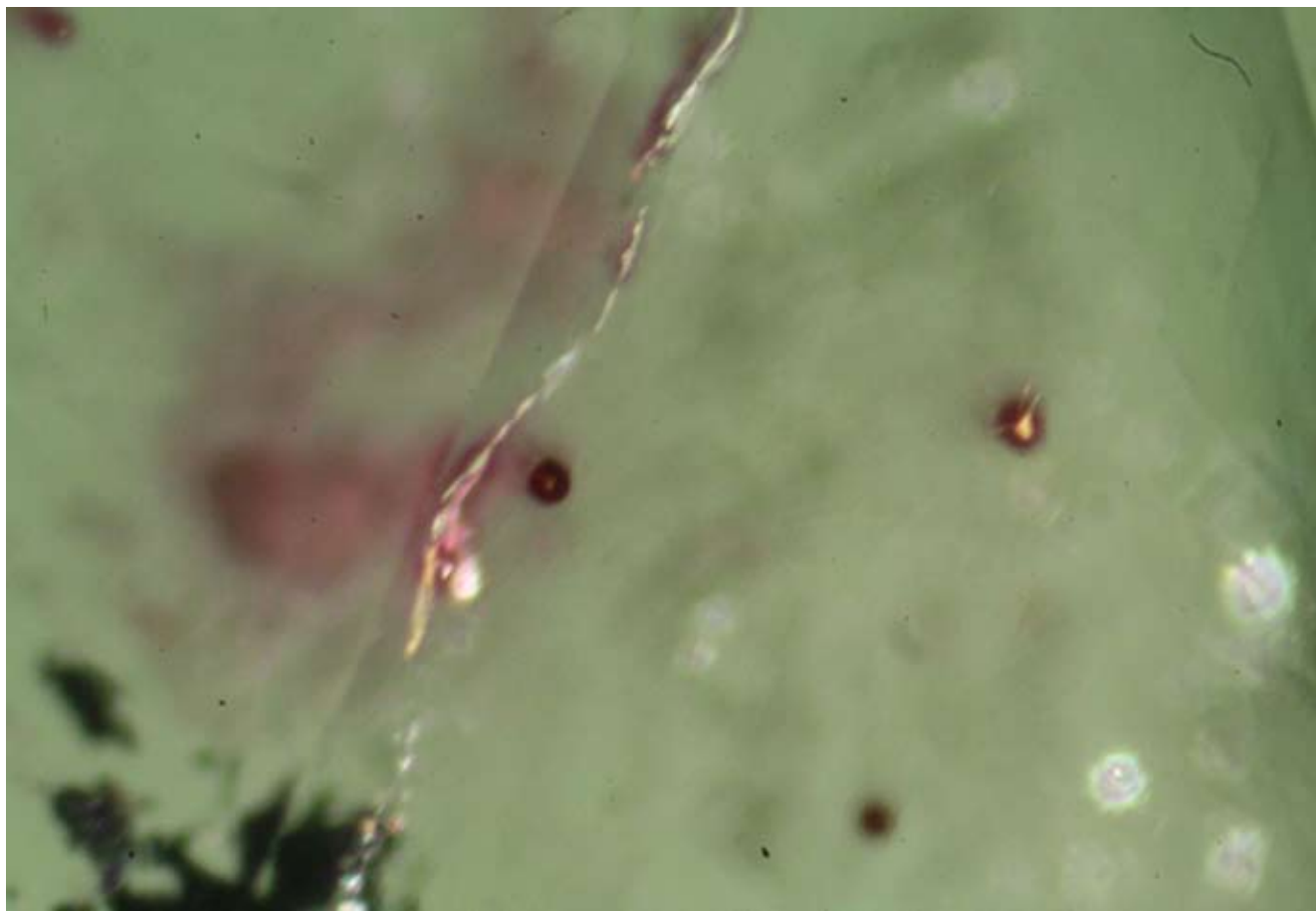


Fig. Par69a



Fig. Par69b

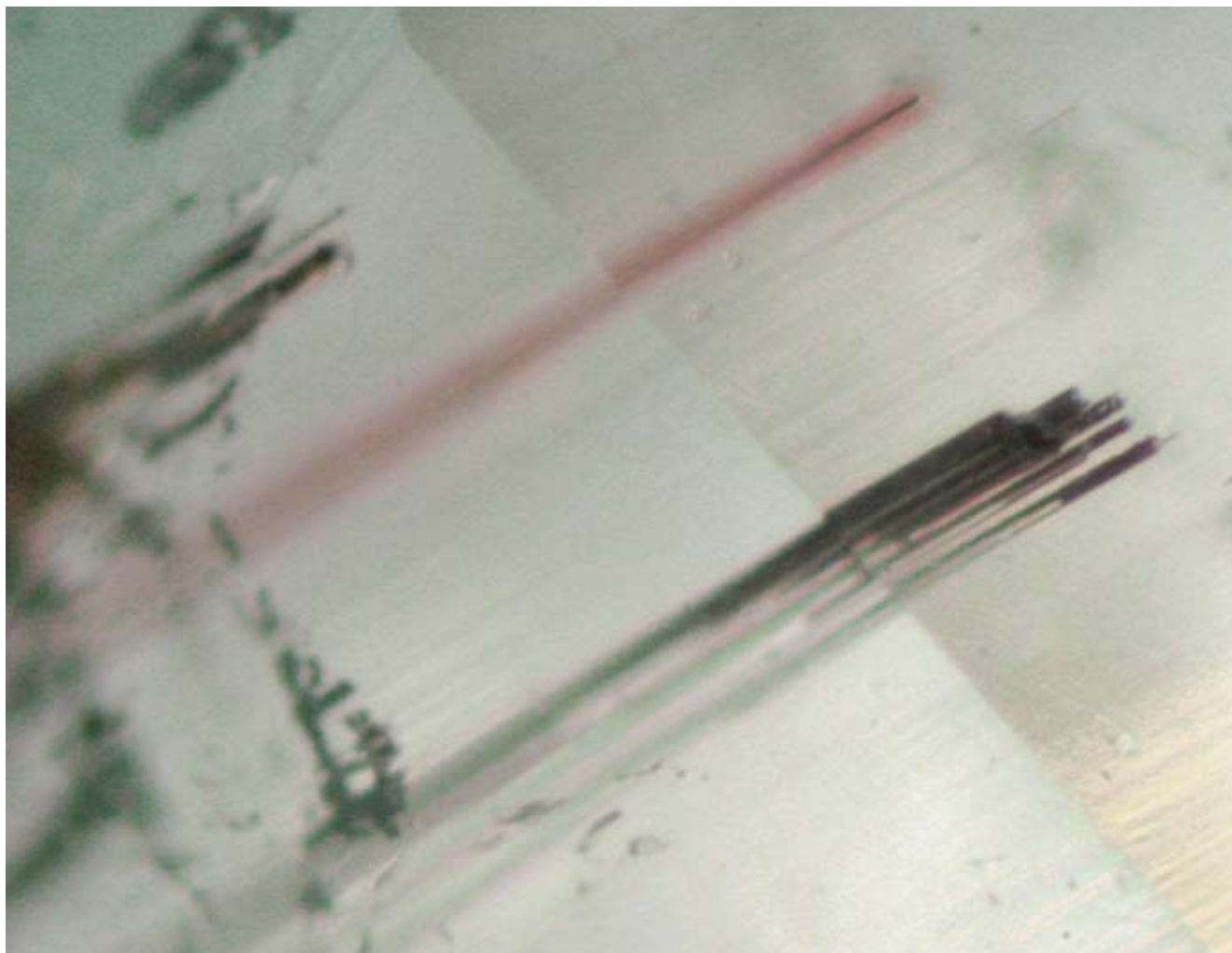


Fig. Par69d

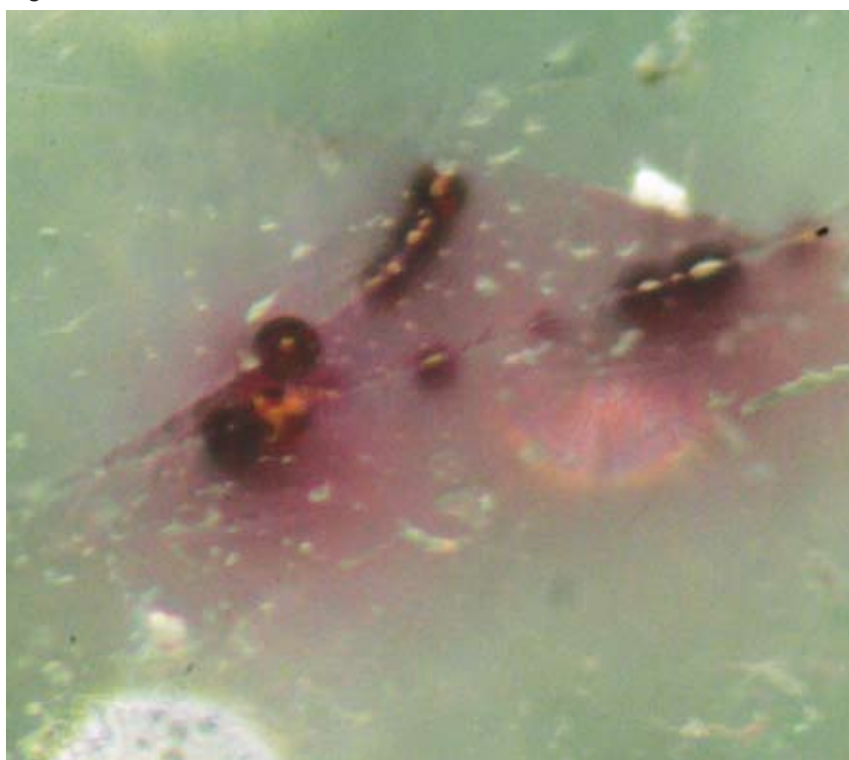


Fig. Par69c

Fig. Par69a-d Microphotographs showing growth tubes in copper-bearing tourmaline from Mozambique. View in direction perpendicular to the c-axis (Fig. Par69a-c). Note the presence of purple “halos” around the orange growth tubes. This purple “halos” was also found adjacent to fissures in the tourmaline that also contained the same orangey material fillings in extremely thin films. The purple “halos” are interpreted as the result of natural irradiation (See Box Par1 and Lit Par48).

Composition of orangy materials: The orange substance in the growth tubes has been measured by LA-ICP-MS in two other samples. Increased concentrations of Fe, REE (Dominated by Ce, see Fig. Par76e), Mg, Cr, V, Pb and Ba (See Fig. Par76a and 76d) occurred along with U (Fig. 76g and 78g). No Cu- or Mn-enrichments were detected in these zones (Fig. Par75b).

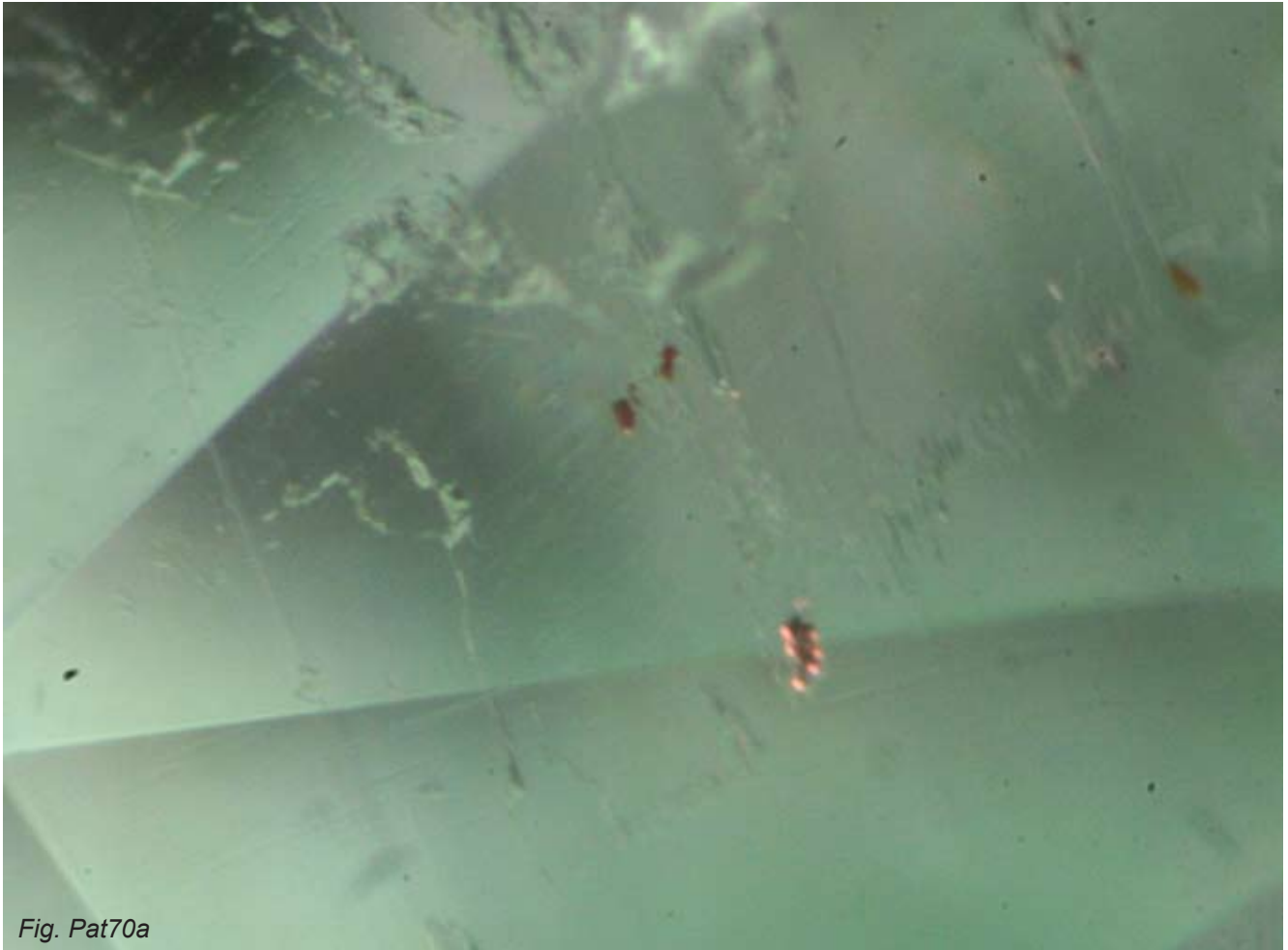


Fig. Pat70a

Fig. Par70a-b 3-phase inclusions are found in the copper-bearing tourmaline from Mozambique (Fig. 67a). The solid daughter minerals in the fluid inclusions are highly reflective and of a color typical for “native copper”. No further attempts have been made yet to identify them by more sophisticated methods (e.g. SEM-EDS or Raman).

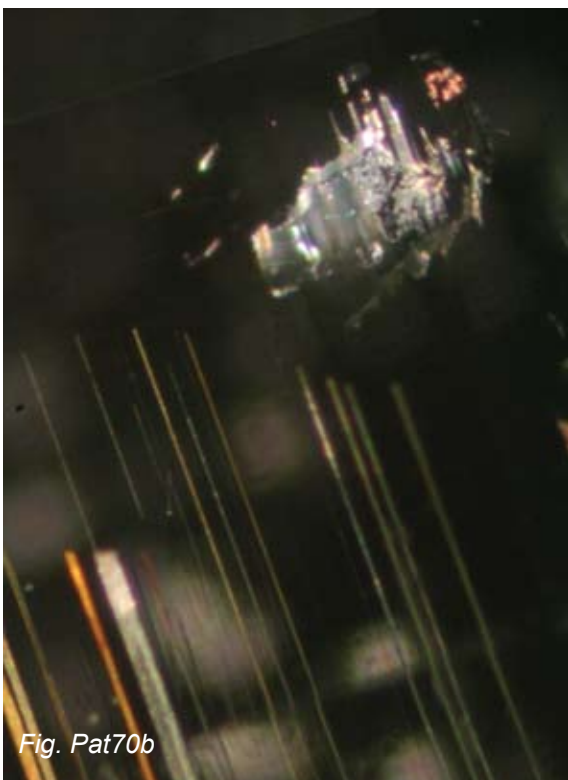


Fig. Pat70b



Fig. Pat70c

Fig. Par70c Microphotograph of a highly reflecting opaque inclusion in a bluish-green copper-bearing tourmaline from Mozambique (Type C). The opaque inclusion shows a narrow purple “halo” around it. This “halo” is interpreted as induced by irradiation (See also Lit. Par48). It is therefore most likely that the inclusion is radioactive.

**BOX PAR1: SUMMARY AND INTERPRETATION OF INCLUSIONS IN
BLUISH-GREEN TOURMALINES FROM MOZAMBIQUE (FIG. PAR69-71):**

The following inclusion features were found: Orangy filled growth tubes and cracks (Fig. Par68a-c and 69d) without or with purple halos (Fig. Par68b-c and 69a-d), opaque inclusions with purple halos (Fig. Par70c) and 2- and 3-phase fluid inclusions (solid, liquid and vapor) (Fig. Par71a-c). All observation was made in faceted samples (Fig. Par67b) originating from the same unheated tourmaline rough (Fig. Par67a-b). These tourmalines were classified as Type C (See Fig. Par90a-b). For the chemical compositions of minor elements

**Chemical Concentrations of Minor and Trace Elements of "Type C"- Tourmalines
(See Fig. Par67b)**

	bluish-green	pastel-green	green	yellowish-green
Mn (in %)	3.23 (6)	4.69 (2)	4.46 (4)	3.88 (1)
STDEV	1.09	0.17	0.33	
Cu (in %)	0.16 (6)	0.22 (2)	0.22 (4)	0.22 (1)
STDEV	0.07	0.04	0.05	
Fe (in %)	0.03 (6)	0.03 (2)	0.03 (4)	0.06 (1)
STDEV	0.03	0.01	0.04	
Bi (in %)	0.02 (6)	0.02 (2)	0.02 (4)	0.02 (1)
STDEV	0.01	0.00	0.00	

ED-XRF analysis in wt.-%, averaged from a number of measurements (in brackets) and divided into color groups (Definition Type C, see Fig. Par90)

of the tourmalines of this inclusion case study see the inlayed table. These tourmalines are characterized by high Mn-concentrations. A theory of the formation of the "purple" halos was published at the printing date of this report (Lit. Par48). It is believed that these halos were produced by irradiation. During LA-ICP-MS analysis of orangy contaminations in the tubes and cracks, we detected isolated uranium-concentrations that are 10x higher than the concentrations found in the tourmaline matrix and about 30-60x above the detection limit (0.01ppm) in two different samples (Fig. Par76g and 78g). The presence of this radioactive element in the orange materials is support for the theory of formation of the "halos" by irradiation (Lit. Par48). Furthermore, "halos" are also observed around isolated solid inclusions that are not associated to cracks and tubes (Fig. Par70c). This is further supporting the theory. The "halos" around these inclusions, however, occur from the radiation that are produced by the mineral inclusion itself and not from contaminated orange colored substances. Elevated Cu-concentrations were not found in the orange zones (Other elements present, see Fig. Par76a-f and 78c-g).

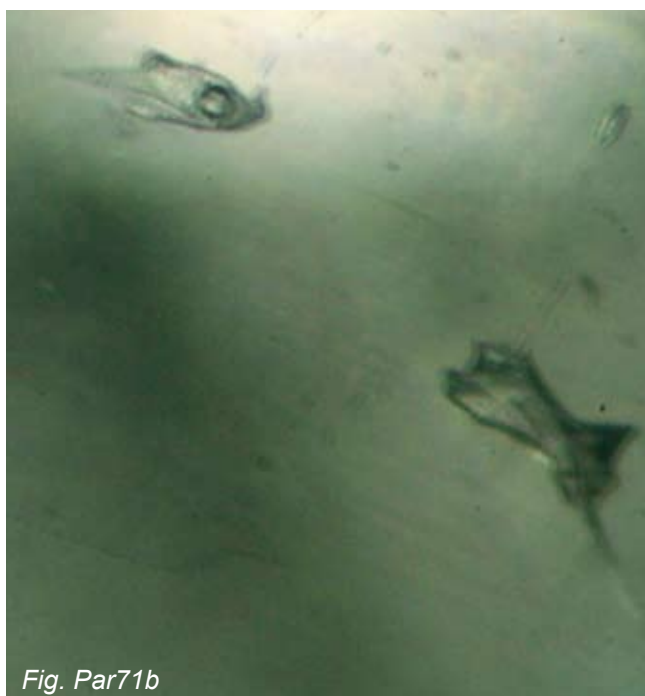


Fig. Par71a-b Fluid inclusions were frequently present in these Mozambique tourmalines. The picture shows 2-phase inclusions found in a sample originating from the same rough of Fig. Par67a. Note that the fluid inclusion tubes do not have any expansion cracks. Therefore, no indications are present that the tourmaline has been subjected to a heat-treatment.

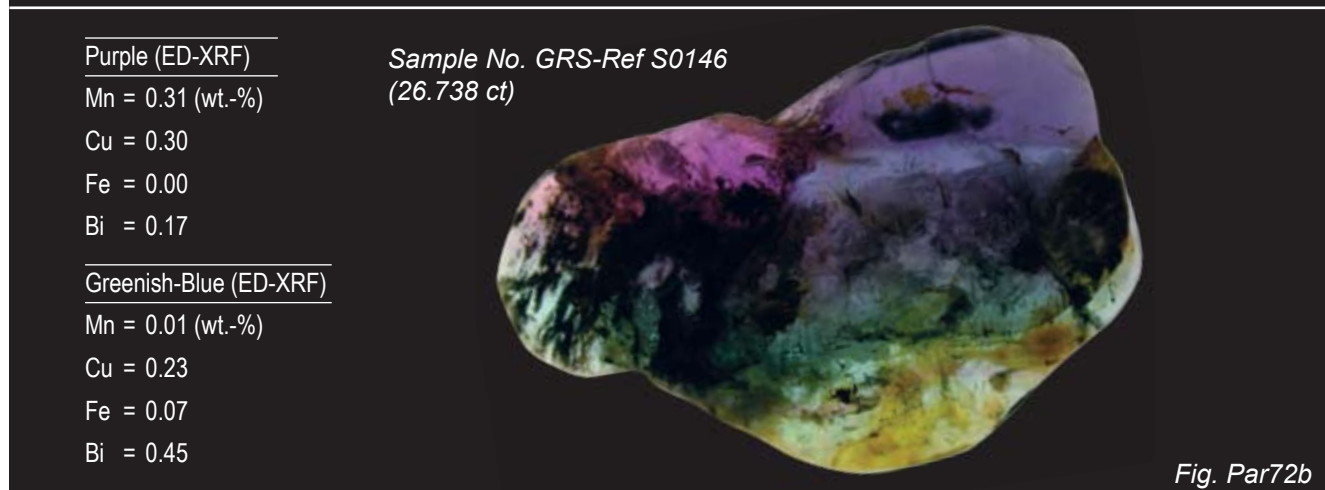


Fig. Par72a-b Color-zoned unheated copper-bearing tourmalines from Mozambique (GRS collection). Note the typical succession of colors from the core to the rim: Purple core, greenish-blue and blue intermediate growth zone and green rim. The outermost rim may be yellowish-green followed by a dark green outer layer. The same type of materials was also described in the literature (Lit. Par33). ED-XRF chemical analyses of the color zones are included. According to our classification (Fig. Par90a), the outer green rim in Fig. Par72a is a "Type C"-tourmaline.

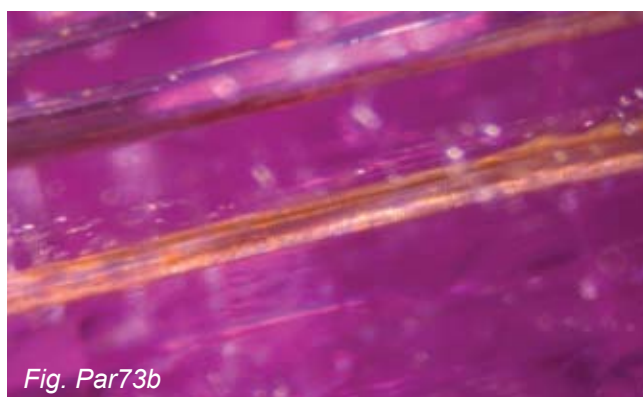
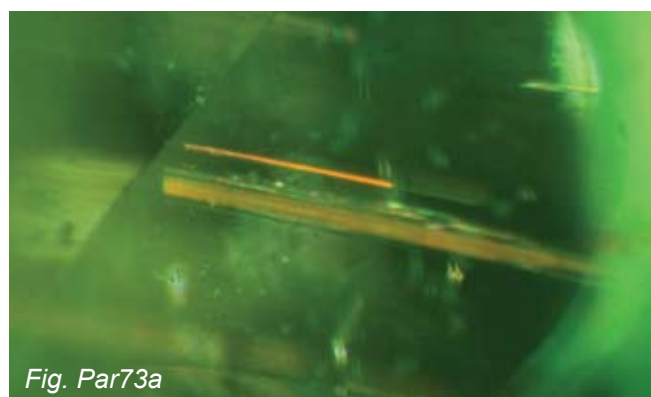


Fig. Par73a-b Microphotograph of two Mozambique tourmalines with vivid green and vivid purple color. Both faceted stones contained growth tubes with orange colors. Purple "halos" were absent.

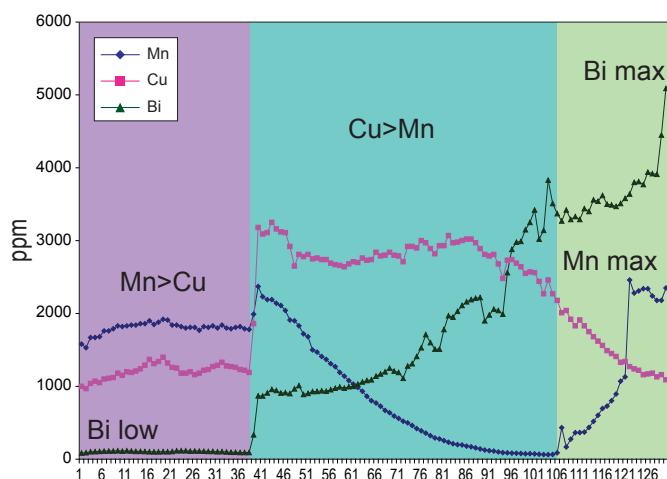
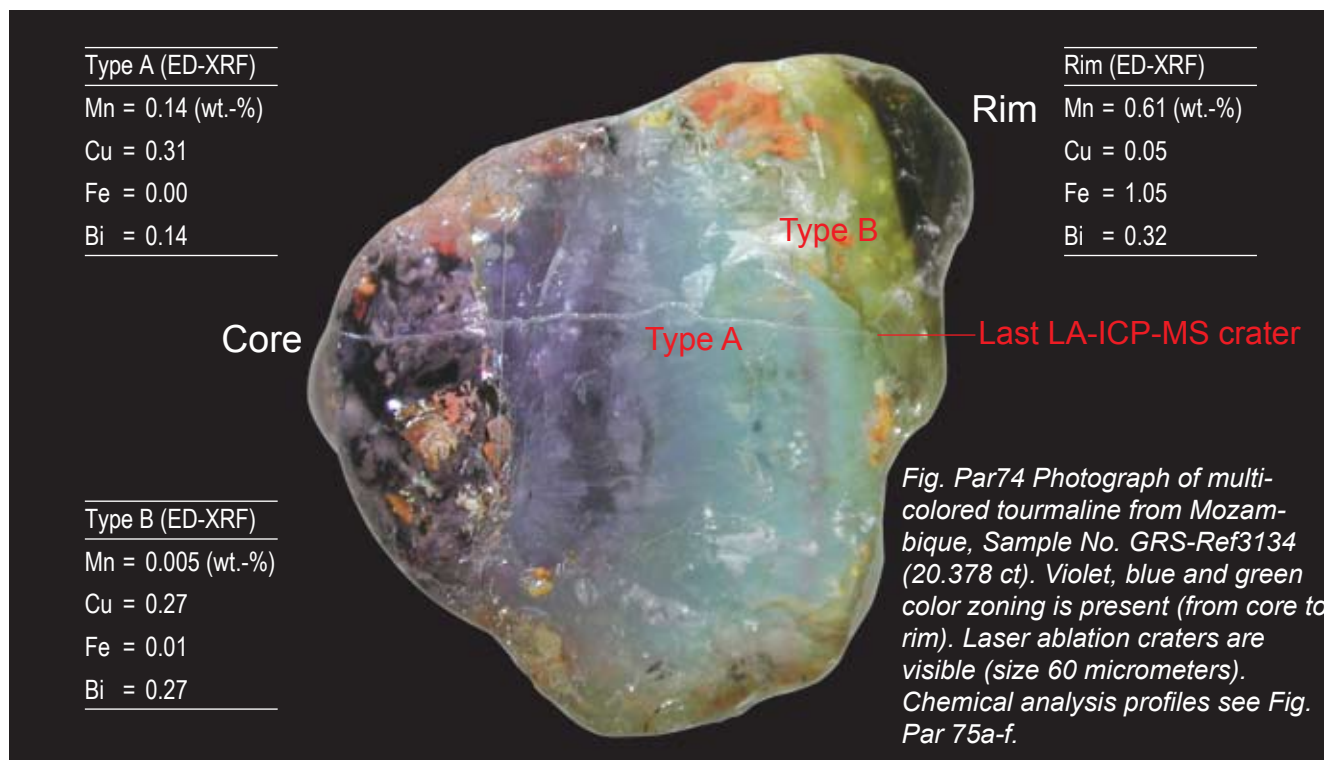


Fig. Par75a

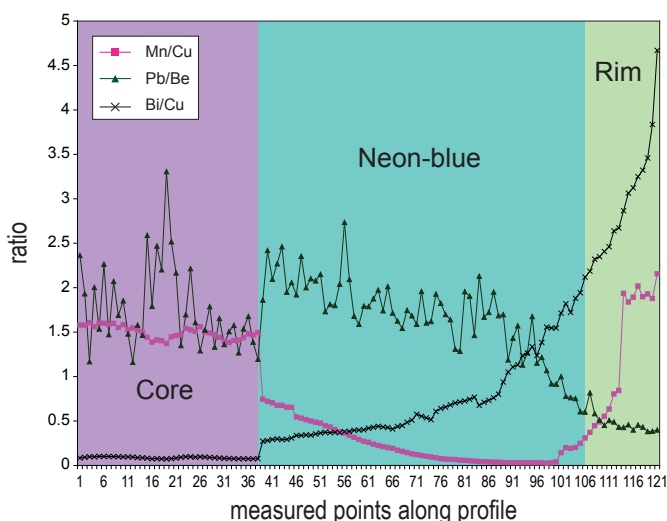


Fig. Par75b

Fig. Par 75a Variation in Cu-, Mn- and Bi-concentrations.

The color-zoning can be correlated with the chemical variations as measured by LA-ICP-MS (in ppm) and by ED-XRF (Fig. Par74, 75a-b and 76a-f).

Low Cu-concentrations are found in the purple core. They increase towards the blue part of the crystal and decrease towards the rim.

Mn-concentrations are high in the purple core and decrease towards the blue color zone. In the rim, they increase to the highest measured value in the entire profile. Highest Mn/Cu-ratios are found in the purple core and in the outer rim (Fig. Par75b).

Lowest Bi-concentrations are found in the core of the crystal. Towards the rim, the Bi-concentrations constantly increase. Highest Bi/Mn-ratios are found in the transition from the blue to the green color zone

The trend of variations in Bi-concentrations is opposite to the trend observed in tourmalines from Brazil (See Fig. Par59a, 62a and 66a).

In the outer dark green rim of the crystal, the Mn-concentrations increase along with Fe-concentrations (not measured by LA-ICP-MS, ED-XRF data, see Fig. Par74).

Fig. Par75b Variation in Mn/Cu-, Bi/Cu- and Pb/Be-ratios

Pb/Be-ratio decrease toward the rim and an opposite trend is observed for the Mn-Cu-ratio and Bi/Cu-ratio. They increase towards the rim. Note a sudden change of ratios is found at the transition zone from the purple core to the "neon"-blue color zone.

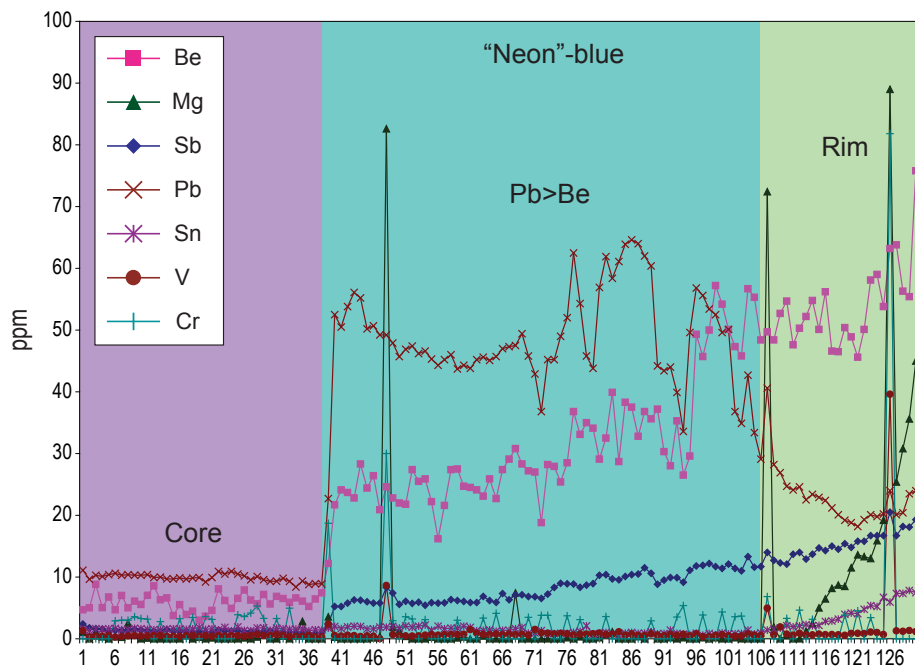


Fig. Par76a

Fig. Par76a-b Variation in chemical compositions of minor and trace elements in relation to color zoning (LA-ICP-MS analyses)

Regarding the concentrations of Be and Pb, a sudden change can be observed from the purple core to the violet/blue part of the crystal. Both elements increase in concentrations in this part of the crystal. Towards the green rim, Pb-concentrations decrease and Be-concentrations increase.

Mg-values remain at or below the detection limit in large parts of the crystal. In the outer rim, however, the Mg-concentrations increase. In the green rim Mg-concentrations increase along with Sn (Fig. Par76a).

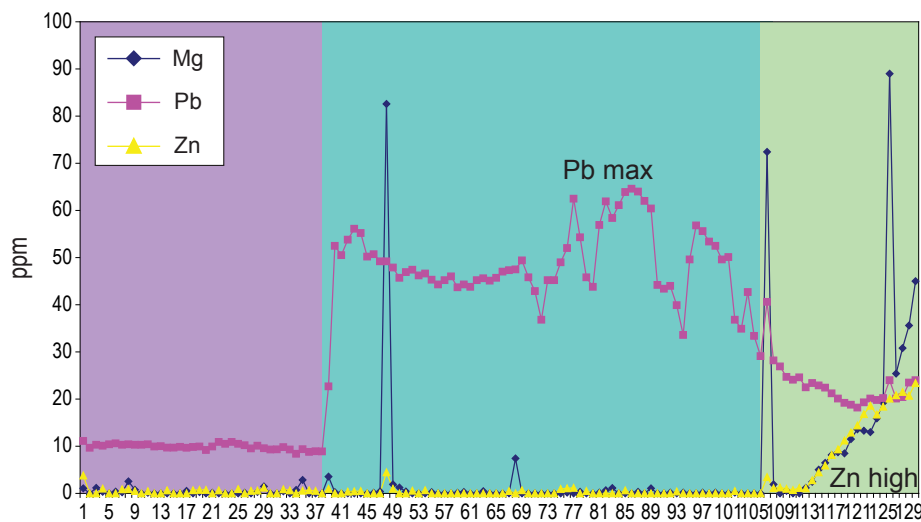


Fig. Par76b

Fig. Par76b-c Variation in Fe-, Zn- and Ti-concentrations

Fe-, Zn- and Ti-concentrations are enriched in the green rim of the tourmaline crystal. At isolated positions, they are enriched to relatively high values. These concentrations can be correlated with contaminated orange cracks or tubes.

Traces of V and Cr are not present as in the tourmaline. They are restricted to contaminated tubes or cracks as well (Fig. Par76a).

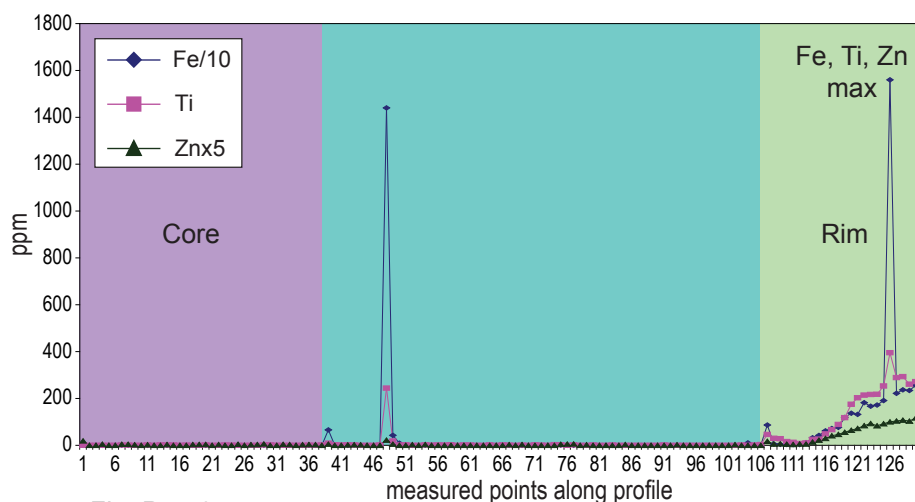


Fig. Par76c

Variation in Ge- and Sc-concentrations (See Tab. Par05)

Ge-concentrations constantly increase from the core to the rim. Sc remains low over the entire profile and increase towards the outer rim only (Ge- and Sc-concentrations see Tab. Par05). The increase of Sc in the green rim can be correlated with the increase of Mg- and Sn-concentrations.

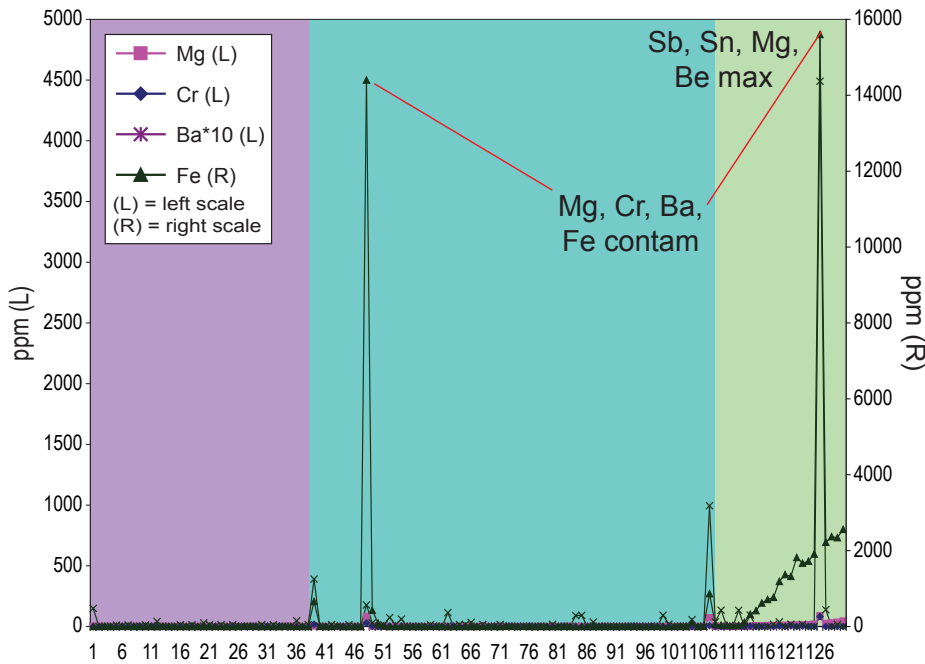


Fig. Par76d

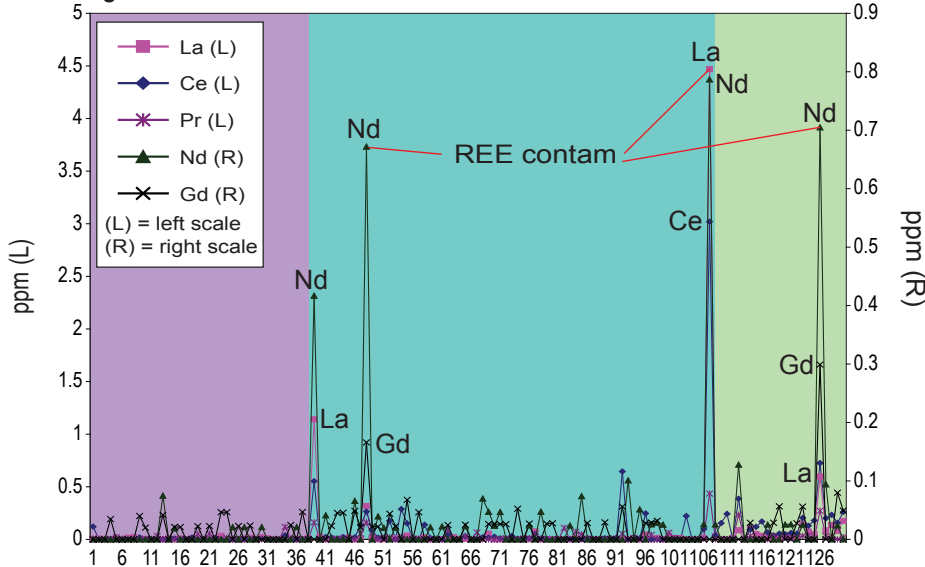


Fig. Par76e

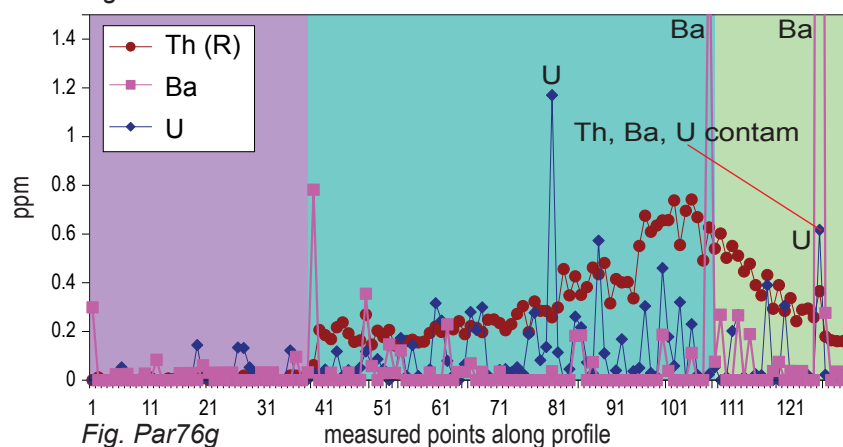


Fig. Par76g

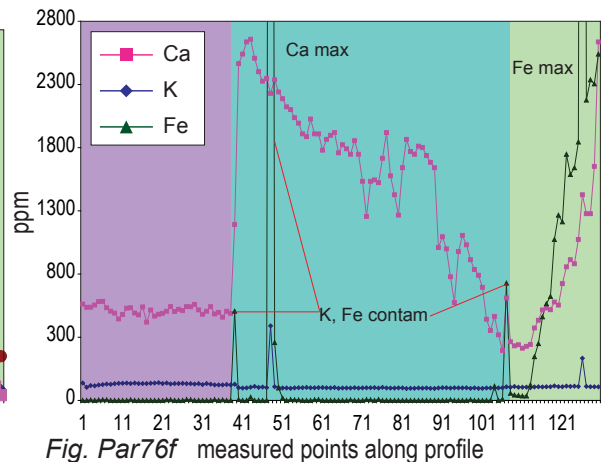


Fig. Par76f

Fig. Par76d-g. Variations of chemical compositions in correlation to color zoning.

Very high Fe-concentrations are found in tubes and cracks in several positions inside the tourmaline. They are not part of the chemical composition of tourmaline. These localized "contaminated zones" do also contain higher concentrations such as Ba and REE (Rare earth elements). These element concentrations are not correlated to the color zoning in the tourmaline. Other changes in element concentrations, however, can be correlated with the different growth zones in the tourmaline:

An increase in Ca is found at the transition from the purple core to the bluish part of the crystal. In the rim, the concentrations of Ca strongly increase (Fig. Par76f). This increase in Ca-concentrations in the rim is correlated with an increase of Fe- and Mg-concentrations (Fig. Par76d).

REE elements increase slightly in the outer rim.

Among the rare earth elements present, La, Ce and Nd are dominant (Fig. Par76e). Localized enrichments can be correlated with orange cracks and tubes.

Fig. Par78g Variation in Ba-, Th- and U-concentrations

Th-concentrations can be correlated with the color zoning in the tourmaline. Lowest Th-concentrations are found in the purple growth zone. They increase in the "neon"-blue growth zone. The U-concentrations are located at extremely small isolated areas that may also contain concentrations of Ba, REE (La, Ce, Nd and Gd, see Fig. Par76e), as well as Fe, Cr, Mg (Fig. Par76d), Pb, V (Fig. Par76a), Ti (Fig. 76c) and K (Fig. Par76f). These element concentrations are localized in areas with orange cracks or tubes in the tourmaline.



Fig. Par77 Photograph of a multi-colored tourmaline from Mozambique, Sample No. GRS-Ref3134. Violet, greenish-blue and green color zoning is present (from core to rim). Laser ablation craters are visible (size 60 micrometers). Chemical analysis profiles see Fig. Par78a-f.

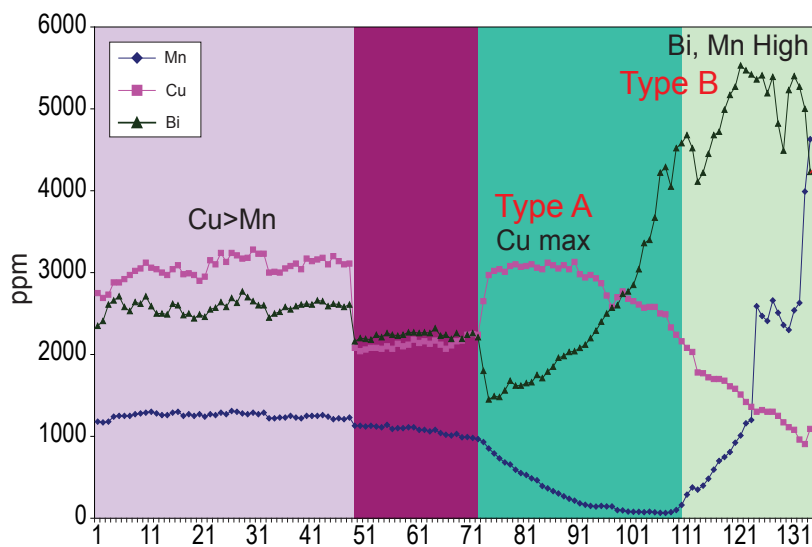


Fig. Par78a

Bi dropping, Mn increasing:
Trend to Type C

Fig. Par78a Variations in Cu-, Mn and Bi- concentrations

Concentrations of Cu, Mn and Bi are shown in a profile across a Mozambique tourmaline. From the core to the rim the following chemical variations are observed:

Cu-concentrations are high in the purple core. Abrupt increase in the violet to greenish-blue part of the crystal and decreasing concentrations towards the rim.

Mn-concentrations are relatively high in the core and decrease towards the middle part of the tourmaline. In the rim, manganese values increase to their highest measured values.

Bi-concentrations are high over the entire measured profile. Highest concentrations are found in the rim of the crystal. Lowest Bi concentrations are found along with low Mn-concentrations in the greenish-blue part of the crystal.

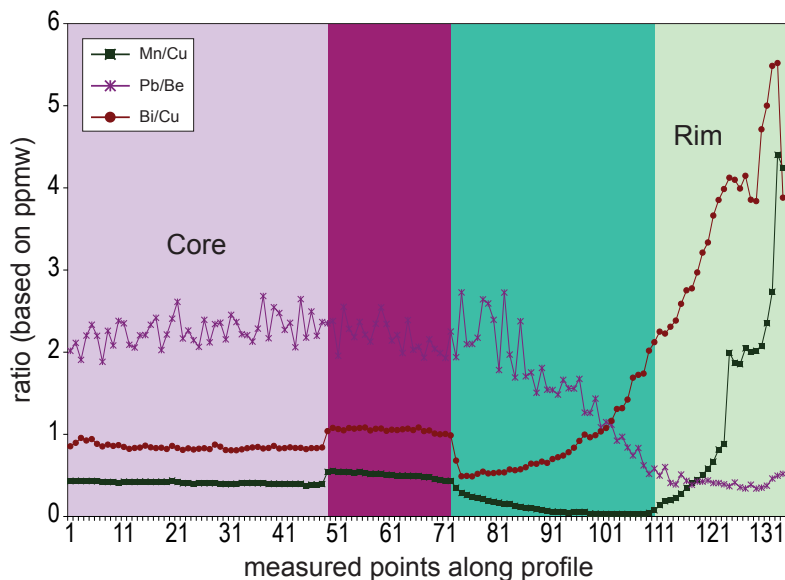


Fig. Par78b

Fig. Par78a Variations in Mn/Cu-, Bi/Cu-and Pb/Be-ratios

High Mn/Cu-ratios are measured in the green colored rim. Lowest Mn/Cu-ratios are formed in the greenish-blue color zone. Bi/Cu-ratios continuously increase from the core to the rim. In the middle of the blue color zone, Bi/Cu-ratios are continuously increasing towards the rim. Highest Bi/Cu-ratios are found in the green rim.

Pb/Be-ratios are well above 1 (Pb higher than Be). During the growth phase producing green colors, Be dominates Pb and therefore, Pb/Be-ratios are decreasing (Fig. Par78b).

**LA-ICP-MS Analysis Profiles of Copper-Bearing Tourmaline from Mozambique
Sample No. GRS-Ref7782**

Fig. Par78c-f Variations of chemical element concentrations in relation to color zoning.

In the chemical profile analysis of the Mozambique tourmaline GRS-Ref7782, the following elements increased in the rim: Fe, Ti, Zn (Fig. Par78d), REE-elements (Fig. Par78d) and Mg (Fig. Par78c).

Extremely low Mg-concentrations were present in the greenish-blue and purple color zones. Among the REE-elements, Ce shows the highest concentrations. However, in comparison to the concentrations found in Brazil, the Mg- and REE-concentrations found in the samples from Mozambique are low.

Isolated high concentrations of Fe, Ti, Zn, Mg, Cr and Ba are found in the area of the orangy zones, which are interpreted as contaminations that occurred after the formation of the tourmalines (Fig. Par78e; See also Box Par1). A similar situation was found in the other sample from Mozambique (Sample No. GRS-Ref3134, e.g. See Fig. Par76g).

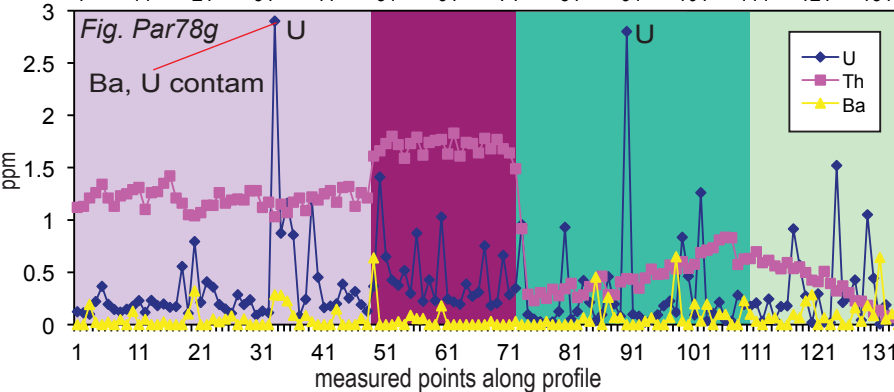
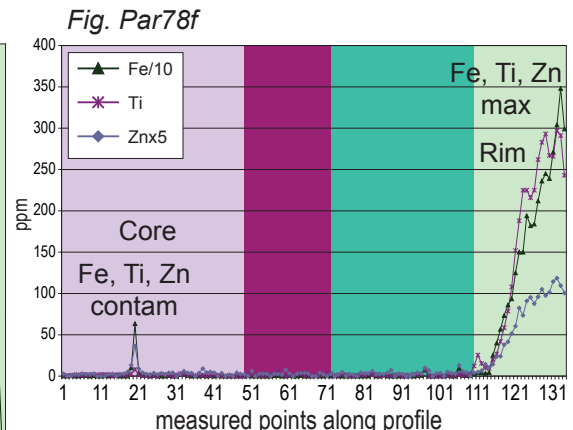
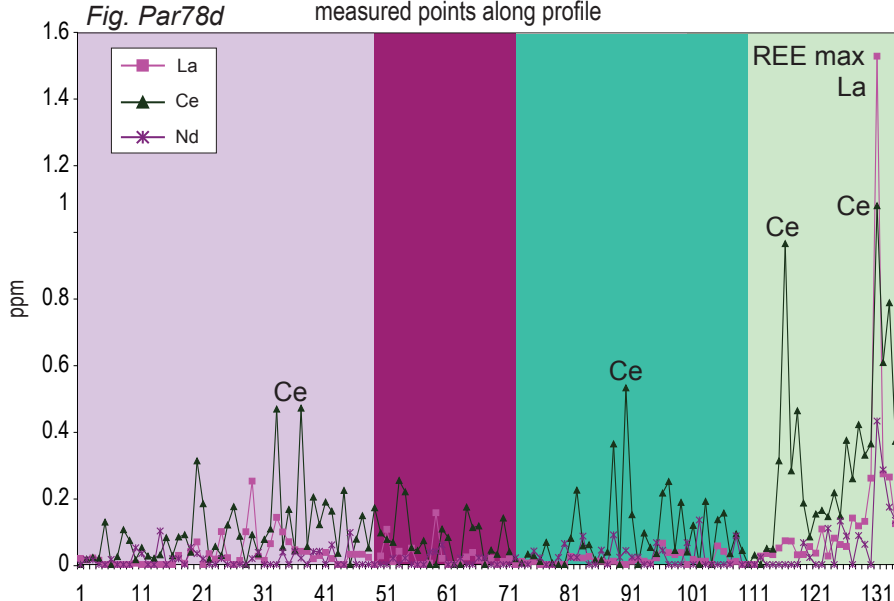
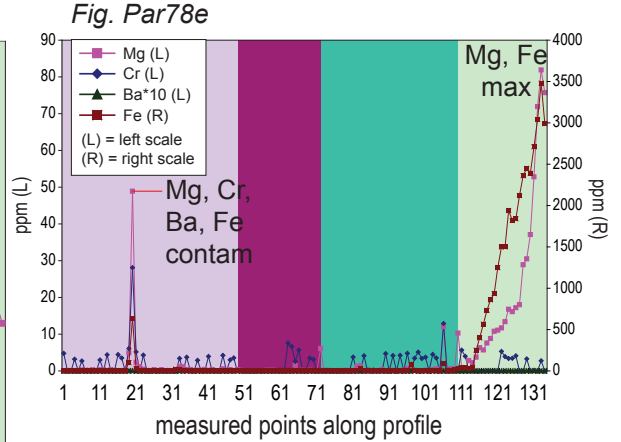
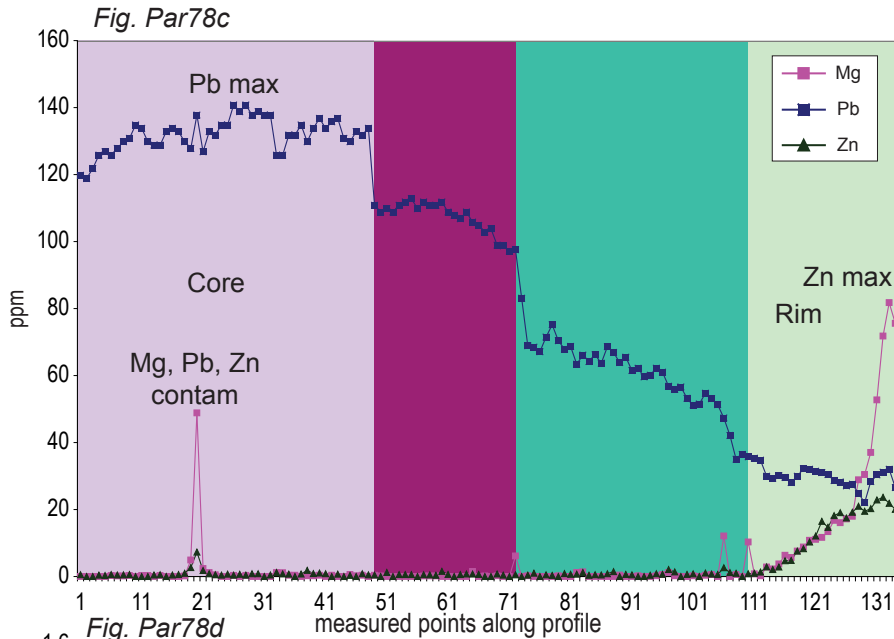


Fig. Par78g Variations in Th- and U-concentrations

Th-concentrations can be correlated with the color zoning in the tourmaline. Highest concentrations are found in the purple growth zone. The U-concentrations are found at extremely small isolated areas along with other elements not related to tourmaline (Fig. Par78c-f) and are localized in the areas of orangy contaminated cracks and tubes. Isolated enrichments of the REE elements Ce and La (Fig. Par78d) occur in the isolated zones containing U.

BOX Par2

COMPARISON OF VARIATION OF Pb- AND GA-CONCENTRATIONS IN MULTICOLORED COPPER-BEARING TOURMALINES FROM BRAZIL AND MOZAMBIQUE

Brazil (Paraiba)

Mozambique

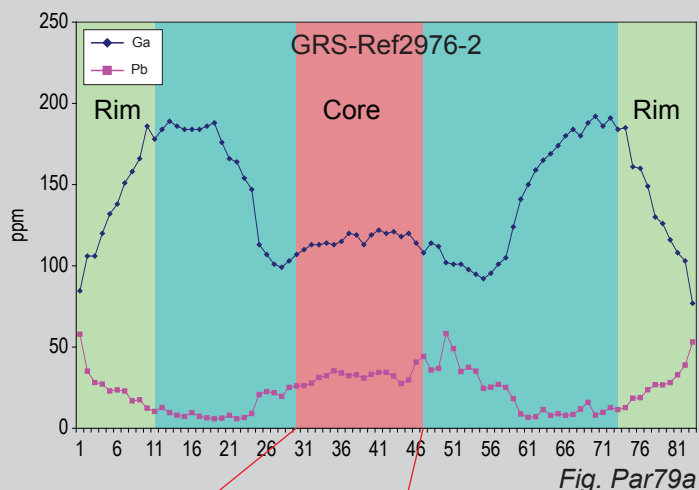


Fig. Par79a

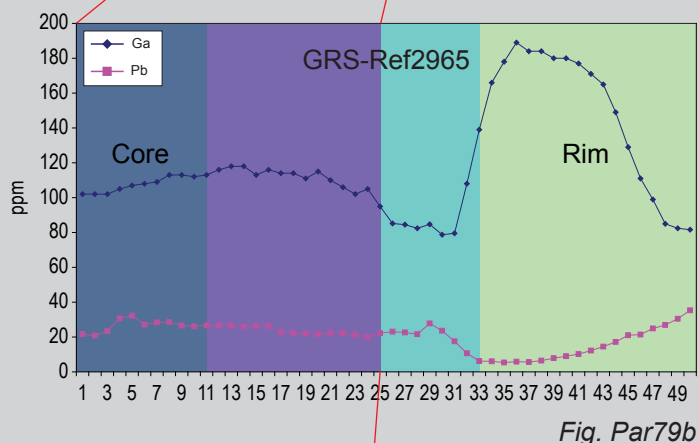


Fig. Par79b

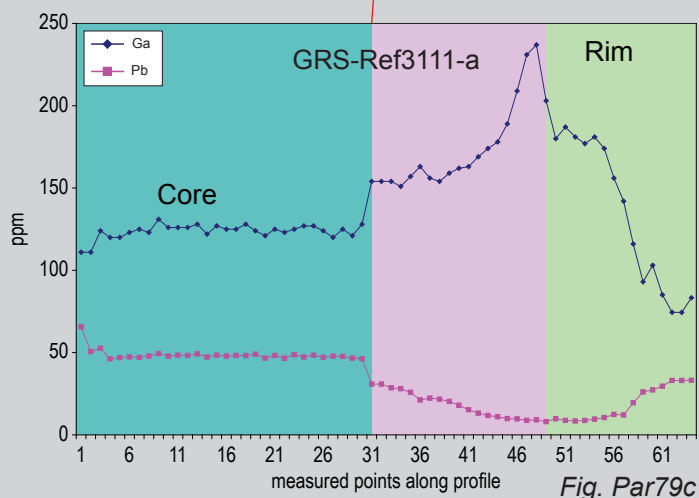


Fig. Par79c

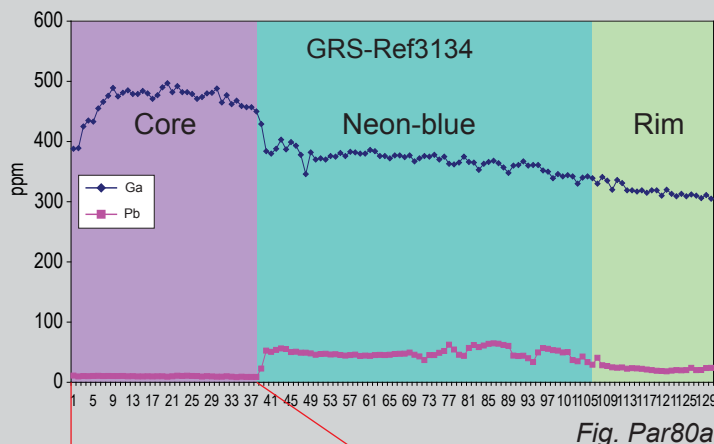


Fig. Par80a

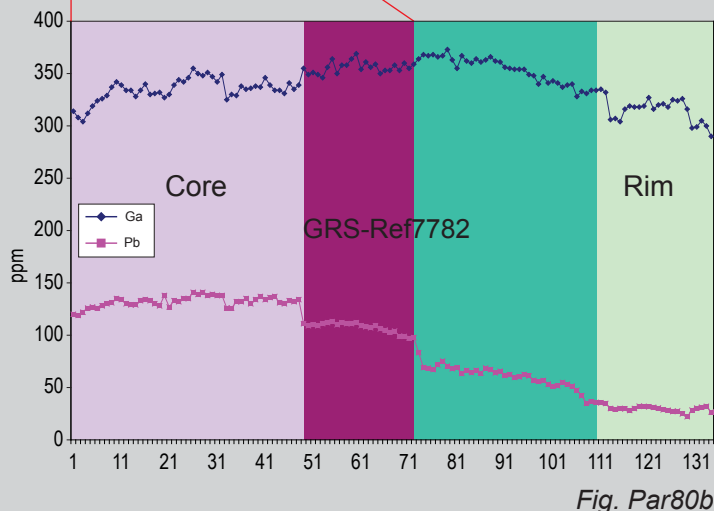


Fig. Par80b

Fig. Par79a-c and 80a-b Chemical profile analysis of 2 copper-bearing tourmalines from Mozambique and 3 samples from Brazil (Paraiba) are shown. A different trend in the concentrations of Pb and Ga was found. The minimum of the Ga-concentrations is found in the bluish-green growth zones of the Brazilian tourmalines. This is not observed in tourmalines from Mozambique. In general, higher Ga-concentrations are found in the Mozambique tourmalines. The highest Ga-concentrations in the Brazilian tourmalines are found in the transition zone of the bluish-green to green growth sectors (overlapping area see Fig. Par79a-b). Pb-concentrations are highest in the purple core of the Brazilian tourmalines. In Mozambique tourmalines, the Pb-concentrations are at its maximum in the greenish-blue growth zone. Ga and Pb-concentrations are therefore useful for the distinction of these two tourmaline groups from the two different origin (Fig. Par81 and 82). However, the sum of the concentrations (Ga+Pb) as proposed in the literature (Lit. Par11) may not always be sufficient for origin determination.

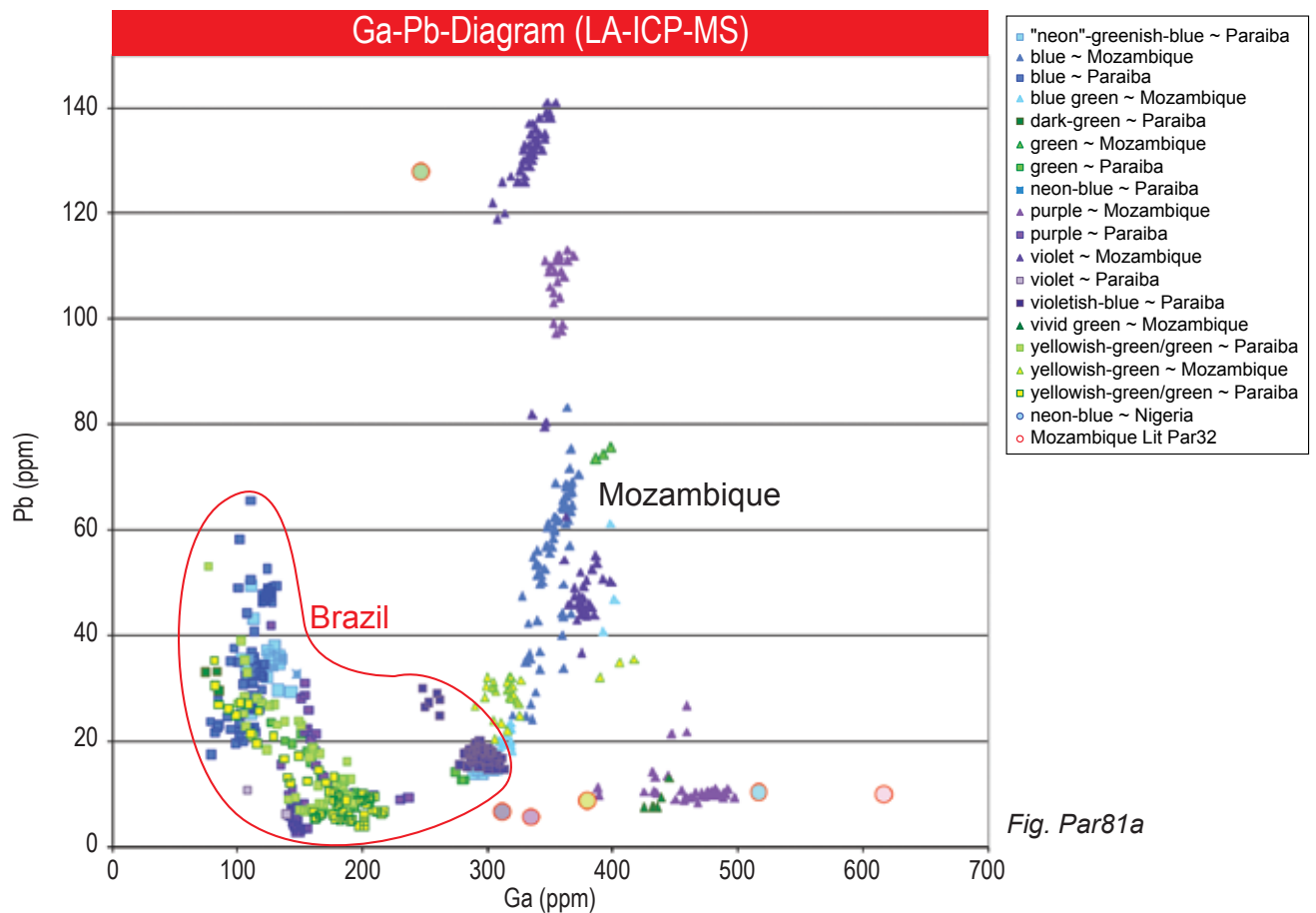


Fig. Par81a

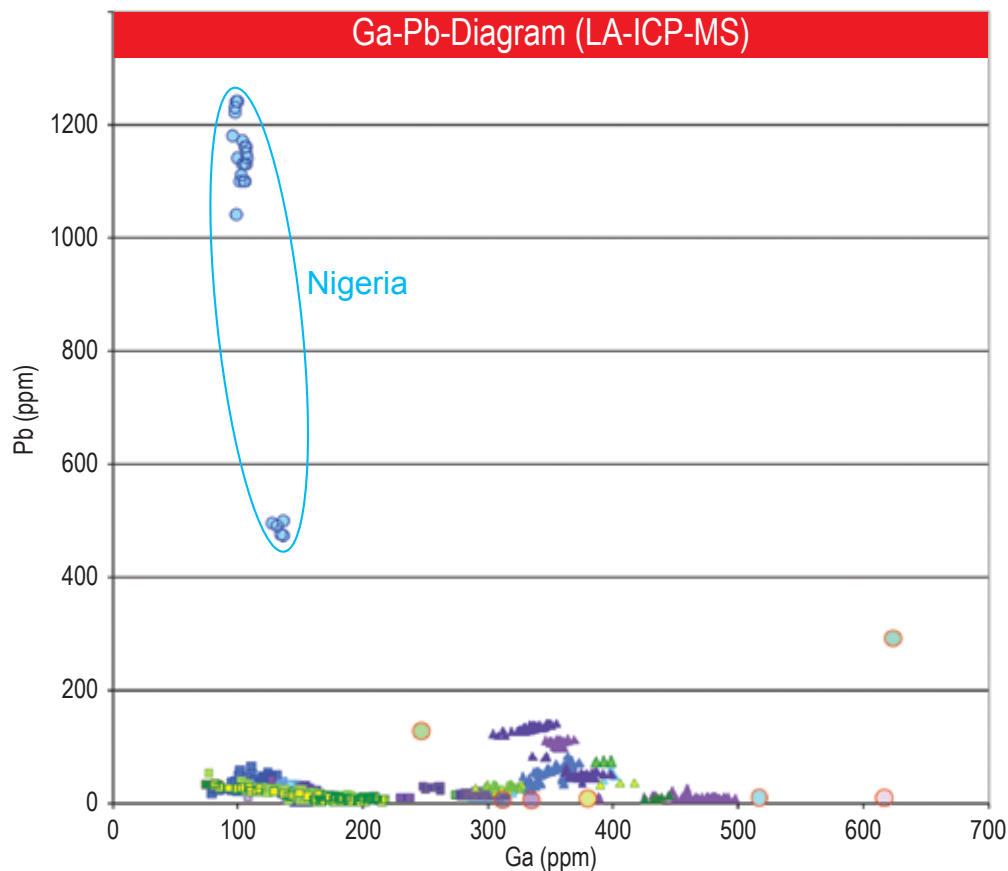


Fig. Par81b

Fig. Par81a-b Pb-Ga diagram of different tourmalines from Brazil, Mozambique and Nigeria. The two elements Pb and Ga were found to be suitable for origin determination of copper-bearing tourmalines, provided the color-zones are separately considered. Pb-concentrations are considerable higher in Nigerian tourmalines (Fig. Par81b and Par82a).

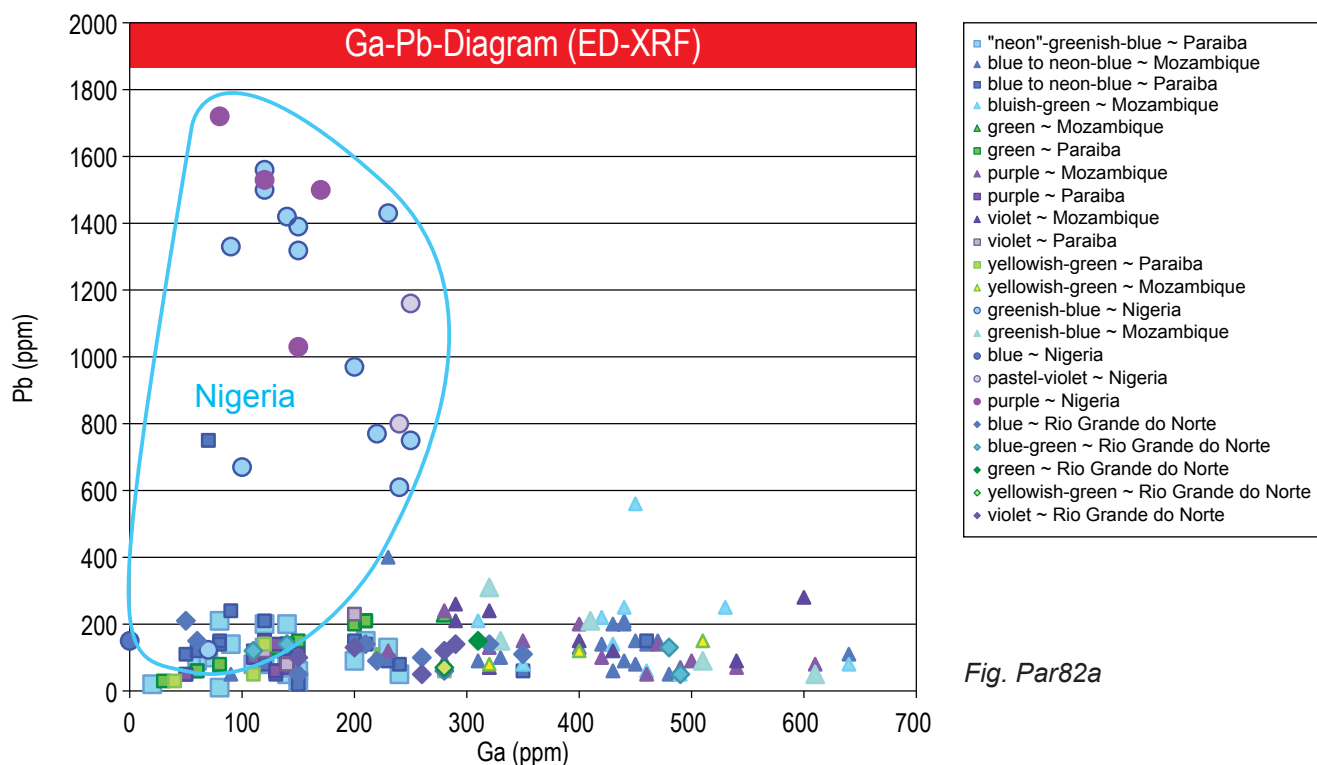


Fig. Par82a

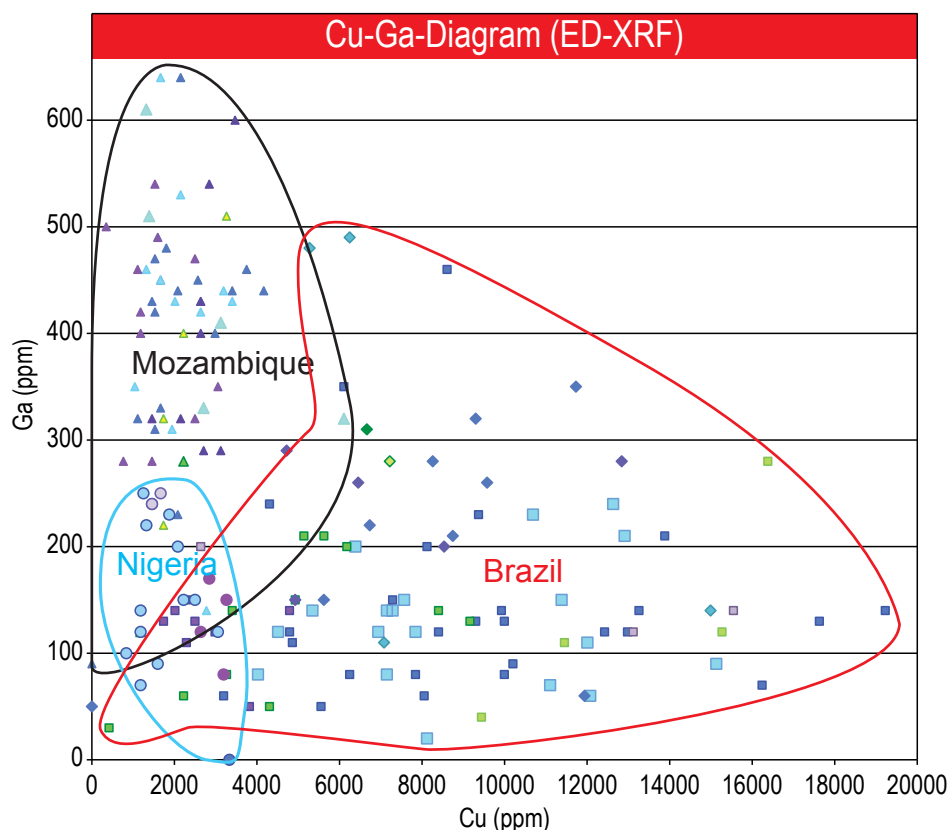


Fig. Par82b

Fig. Par82a-b Pb-Ga and Cu-Ga diagram based on ED-XRF analysis (in ppm) after correction against LA-ICP-MS analysis (See Fig. Par82d). The number of samples was extended with this method to 112 samples. The measured area for ED-XRF analysis was between 0.2 and 2mm for ED-XRF analysis and 60 microns for LA-ICP-MS analysis. More spots were measured on same samples by LA-ICP-MS analysis and more samples by ED-XRF (112 samples, 172 measured spots). Maximum Cu-concentrations were measured by ED-XRF in a tourmaline from Brazil (Batalha, Paraiba) with almost 2 wt.-%. The results of the ED-XRF analysis are in good agreement with those of the LA-ICP-MS analysis (compare Fig. Par82b with Fig. Par82c and Fig. Par81b with Fig. Par82a).

The Cu-Ga-Diagram for Origin Determination of Tourmalines
Comparison of ED-XRF with LA-ICP-MS Analysis

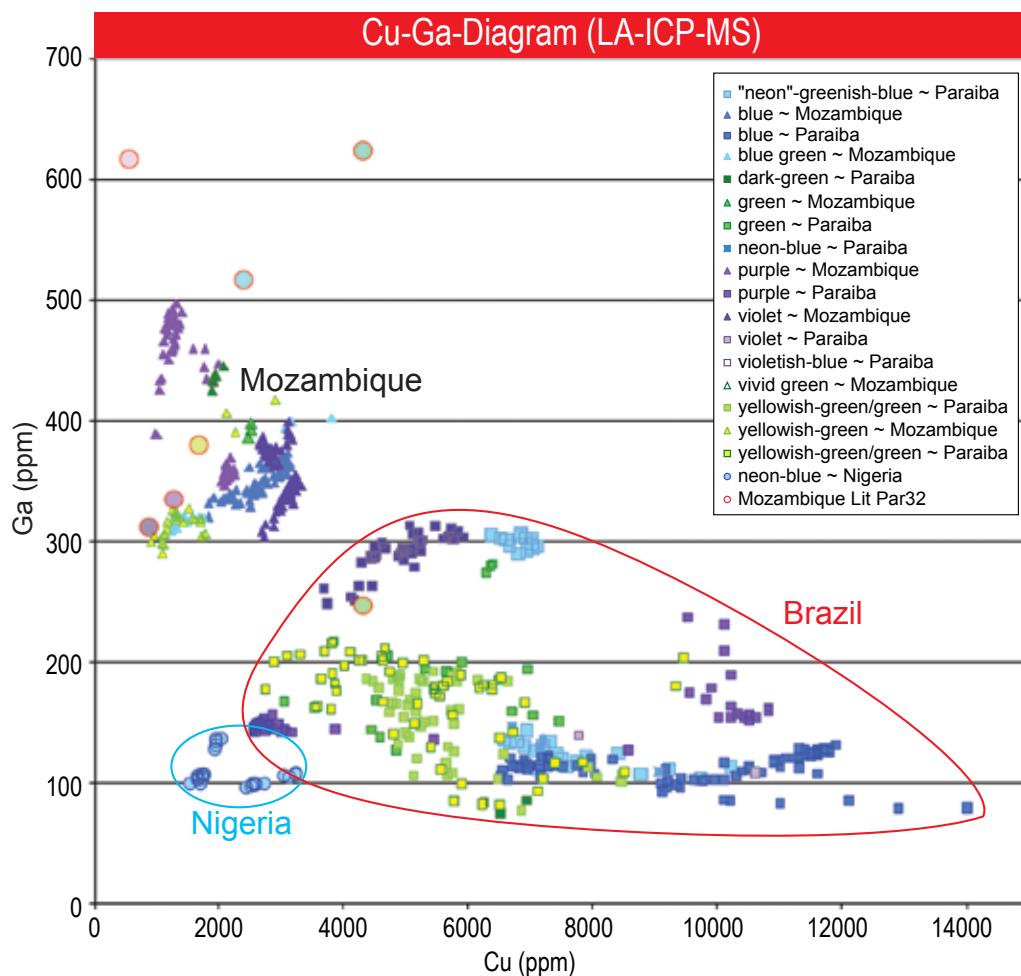


Fig. Par82c The Cu-Ga diagram based on LA-ICP-MS analysis (Averages see Tab. Par03-06).

This test was found to be useful, because the Cu-concentrations are often higher in the Brazilian tourmalines than in the counterparts from Mozambique. An opposite trend was observed for the Ga-concentrations. (See Box Par2).

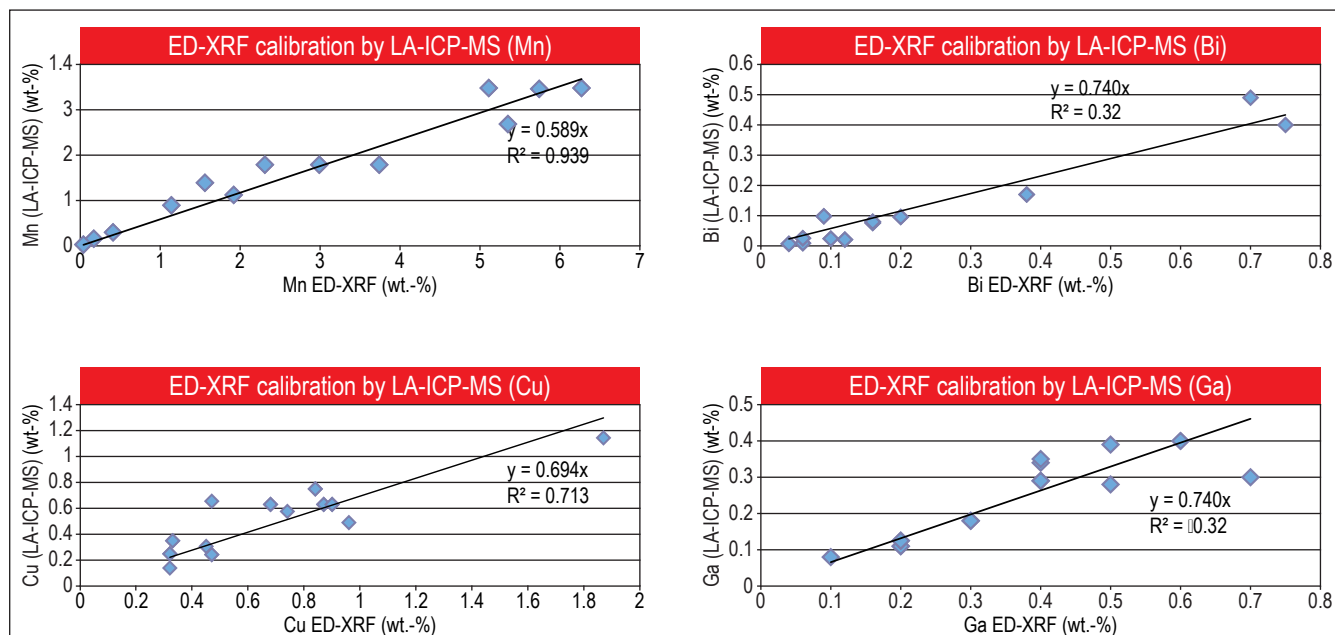
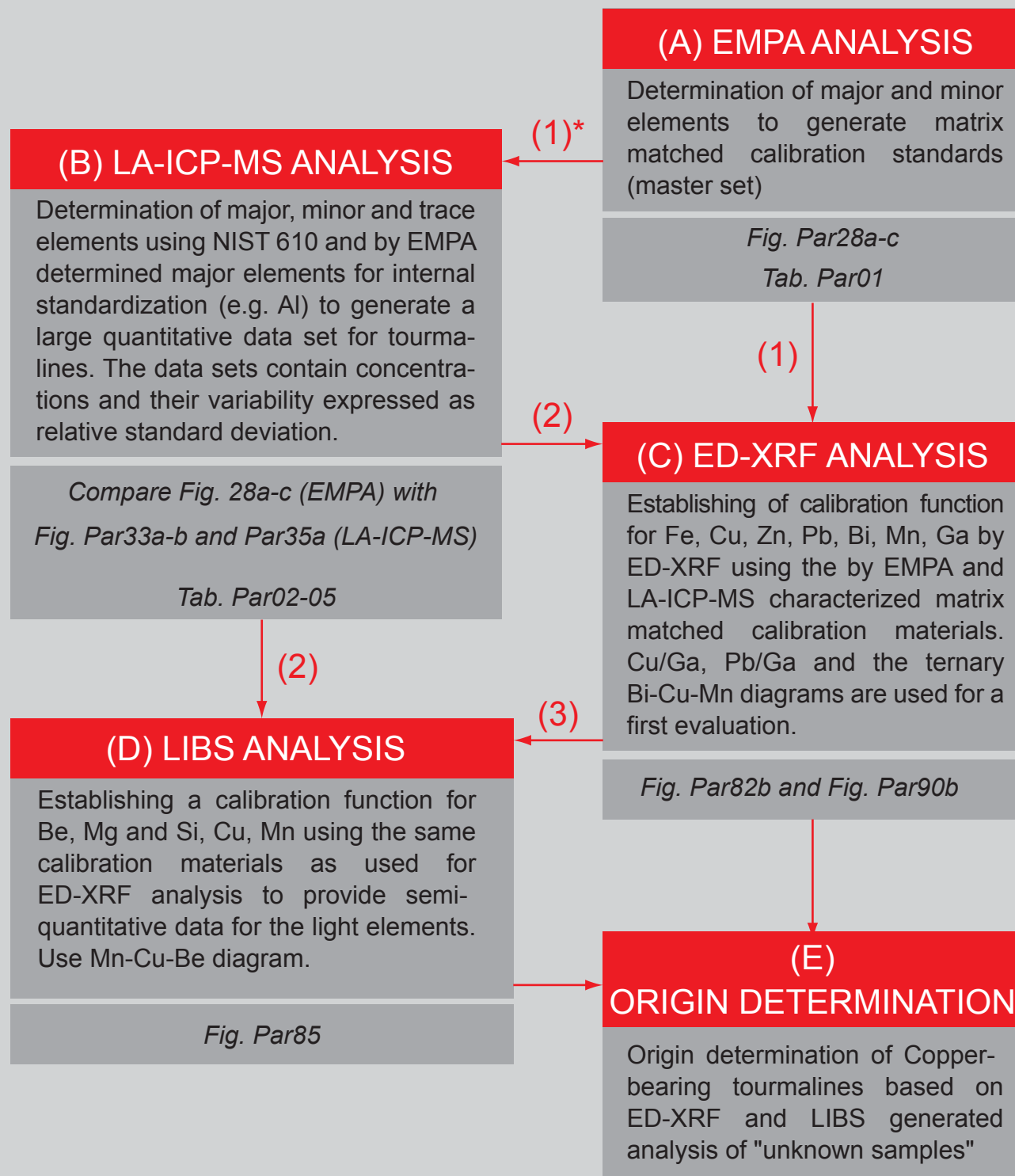


Fig. Par82d Shows the linear regression of ED-XRF concentrations against LA-ICP-MS data from the same measuring spot. The ED-XRF needed to be corrected to lower values by a factor (0.6-0.7) due to the technical specifications and the calculation routine of the particular ED-XRF instrument. The LA-ICP-MS standard set was used to calibrate the ED-XRF data (See methods and calibration protocol in Box Par03). Similar regression slopes were found for different elements (slightly different for the element Mn).

BOX PAR3

CALIBRATION FLOW CHART FOR DIFFERENT METHODS (A-D) USEFUL FOR ORIGIN OF COPPER-BEARING TOURMALINES (E)



* (1)-(3)

Legend: Step 1 and 2 are based on a research project to generate a large data set on selected tourmaline samples, which can be successively used for major, minor and trace element determinations by analytical techniques well known in gemology.

BOX PAR4

COMPARISON OF PB- AND BE-CONCENTRATIONS IN MULTICOLORED COPPER-BEARING TOURMALINES FROM BRAZIL AND MOZAMBIQUE

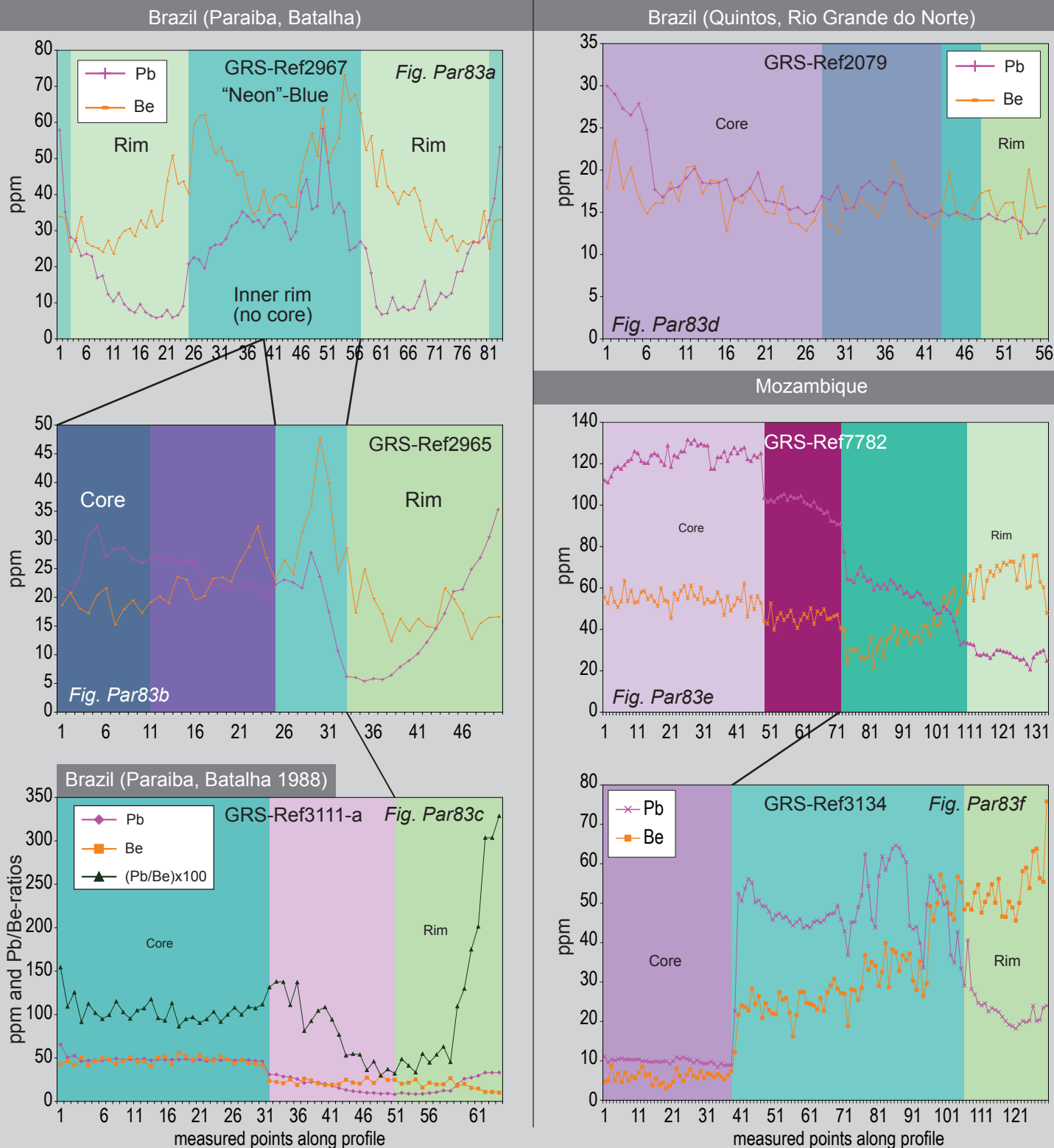


Fig. Par83a-f Comparison of Variation of Be- and Pb-concentrations in tourmalines from different origins. Pb- and Be-concentrations vary within the samples and are different between samples from different origins. This results in different ratios of Pb/Be within the same sample. The use of Pb/Be-ratios as a critical value for origin determination (See Fig. 88a-d) as published in the literature (Lit. Par11) must be therefore used with caution. For the variations of Be-concentrations in different color zones see Fig. Par84a-c and Fig. Par86.

(Cu+Mn)-Be-Diagram: Violet and Purple Colors (LA-ICP-MS)

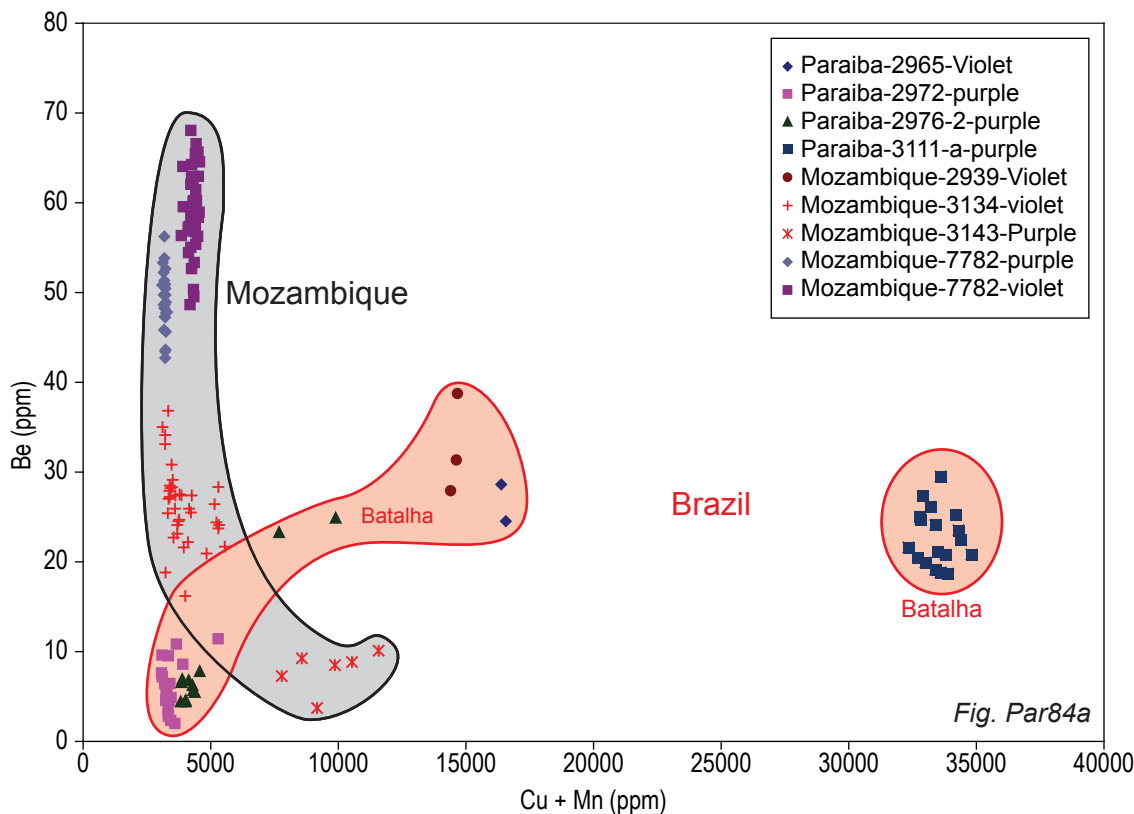


Fig. Par84a-c
Cu+Mn-Be-Diagram separated for different color groups of copper-bearing tourmalines from Brazil, Mozambique and Nigeria (LA-ICP-MS, in µg/g). The fields of two different mining areas in Brazil (Batalha and Quintos) are separately shown.

Note that the samples from the Batalha mine have highest Cu+Mn-concentrations in the group of purple and blue colors (Fig. 84a-b).

The highest Cu+Mn-values in the samples from Mozambique are found in the group of various green colors (Fig. Par84c).

The Be-concentrations are different according to the color-zone of the measured tourmaline:

In the group of violet to purple colors, the tourmalines from Mozambique had higher Be-values than the Brazilian counterparts (Fig. 84a).

Lower Be-concentrations were found in the blue and greenish-blue colored tourmalines from the Quintos mine (Brazil) in comparison to the concentrations found in the samples from Mozambique (Fig. Par84b).

(Cu+Mn)-Be-Diagram: Greenish-Blue, Violetish-Blue and Blue Colors (LA-ICP-MS)

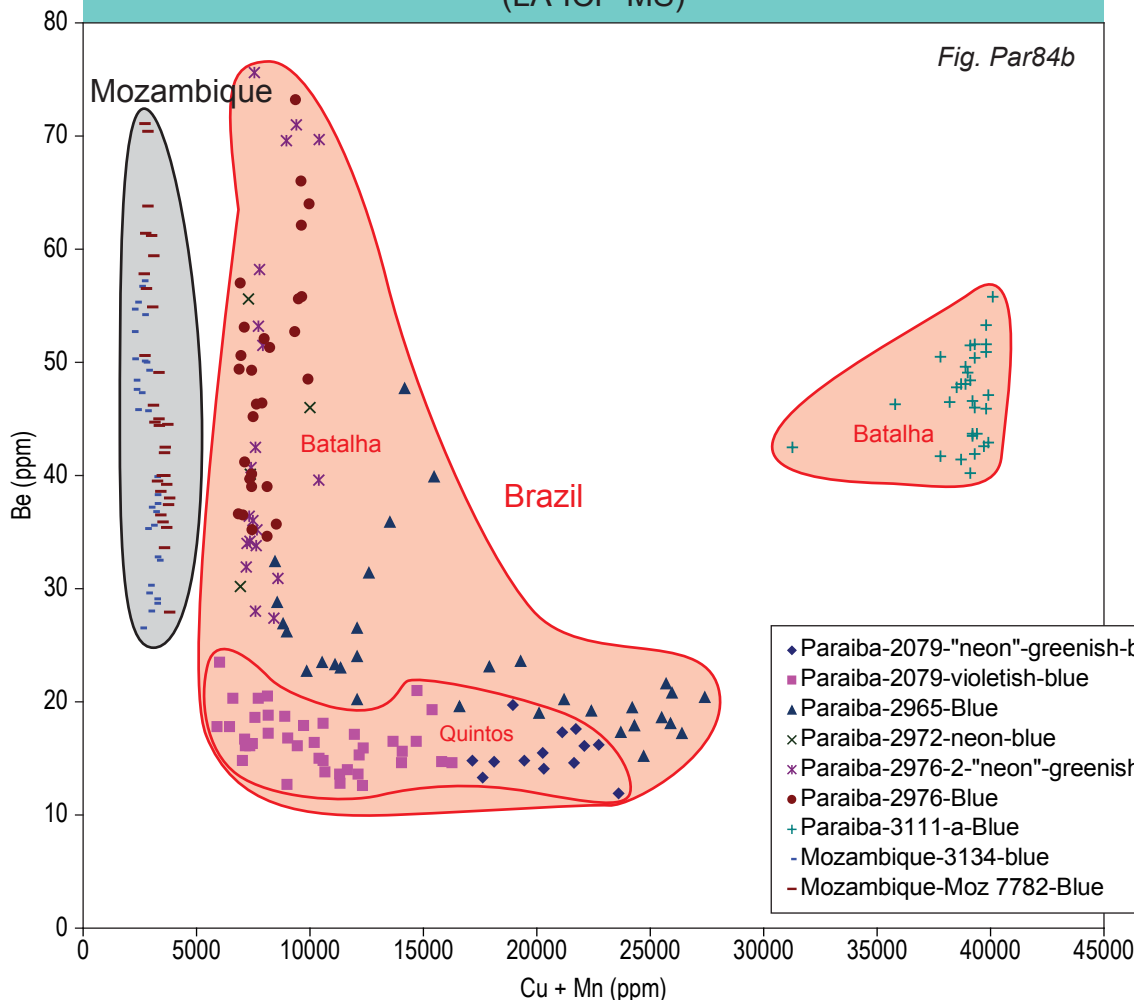
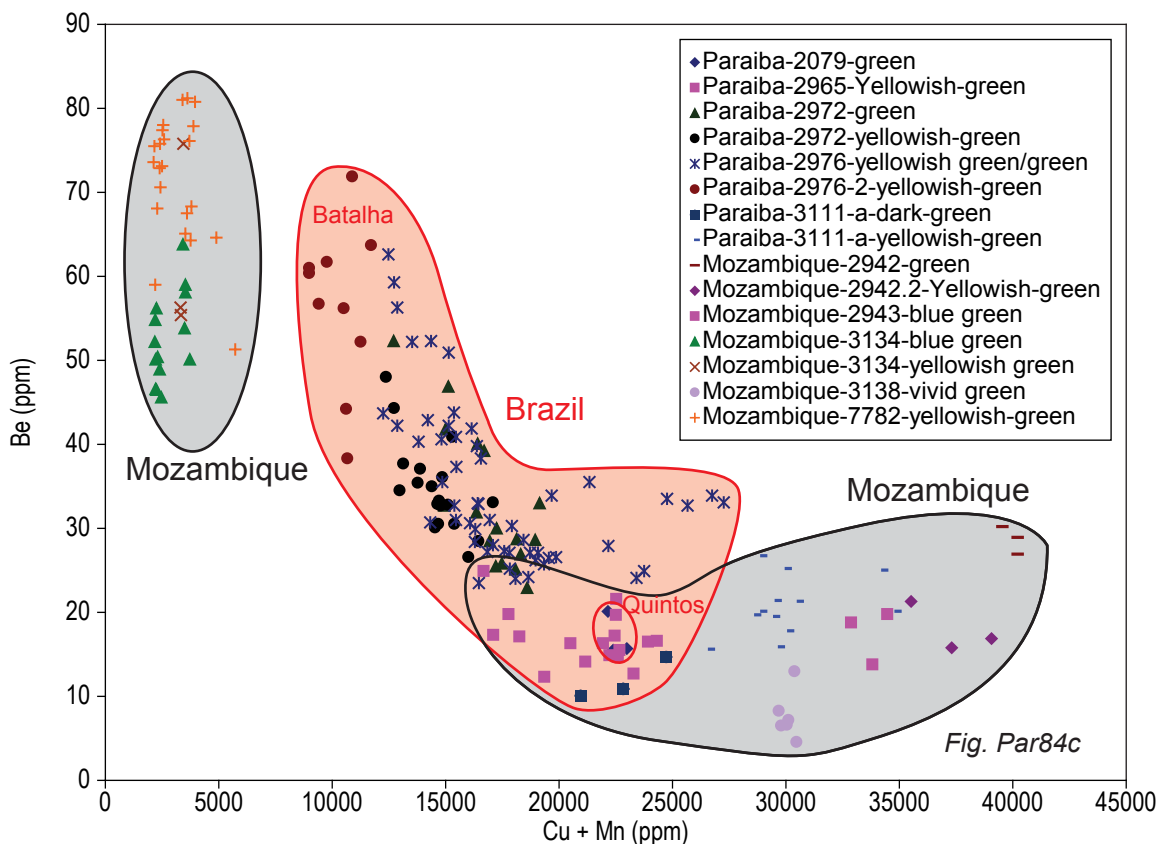


Fig. Par84b

**Ternary Be-Mn-Cu Diagram for Origin Determination of Copper-Bearing Tourmalines
(LA-ICP-MS Analysis)**

(Cu+Mn)-Be-Diagram: Yellowish-Green and Green Colors (LA-ICP-MS)



Cu-Mn-Be-Diagram: LIBS

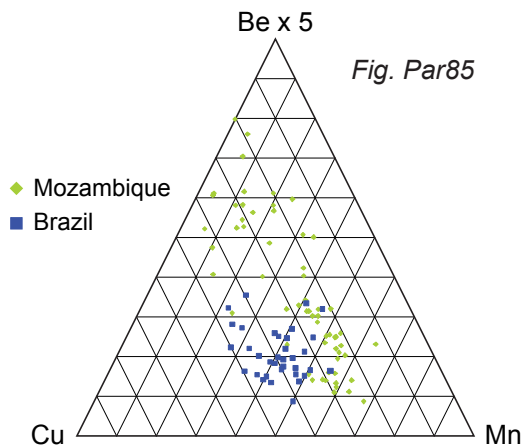
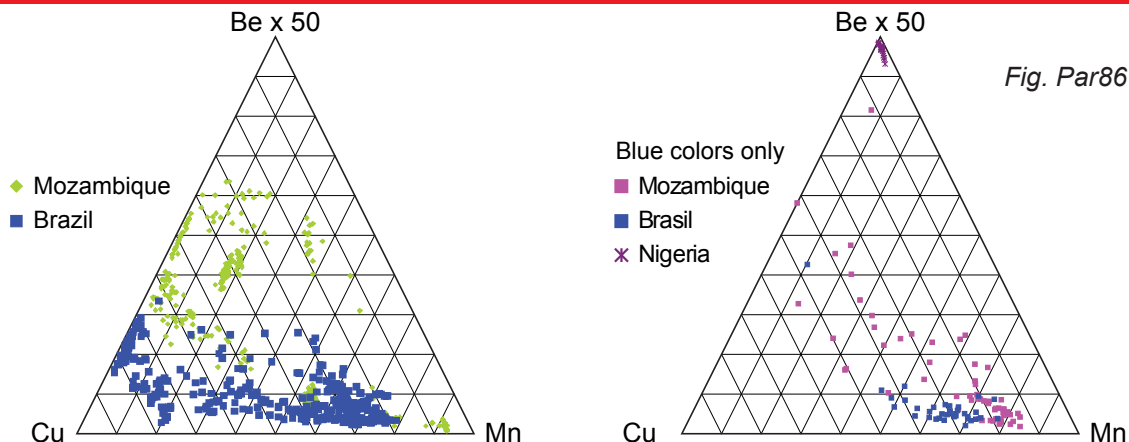


Fig. Par85 and 86 Shows the ternary Cu-Mn-Be-diagram based on all data measured with LA-ICP-MS (in $\mu\text{g/g}$, Be-concentrations are multiplied by 50) and by LIBS-analyses of same samples with less measuring points (in counts, Be-concentrations are multiplied by 5). Comparing the two methods, it can be seen that the LIBS counts for Be (relative to those of Cu and Mn) was much higher than those obtained by LA-ICP-MS analysis. Therefore, a series of LA-ICP-MS analyzed standards are needed if semi-quantitative data from LIBS-analysis are required (Box Par3). It can be seen in Fig. Par85, 86 that a field of high Be-concentrations in relation to Cu- and Mn-concentrations is occupied by samples from Mozambique. For certain samples, this provides additional information for origin determination.

Cu-Mn-Be-Diagram: LA-ICP-MS



Be-Mg-Diagram (LA-ICP-MS)

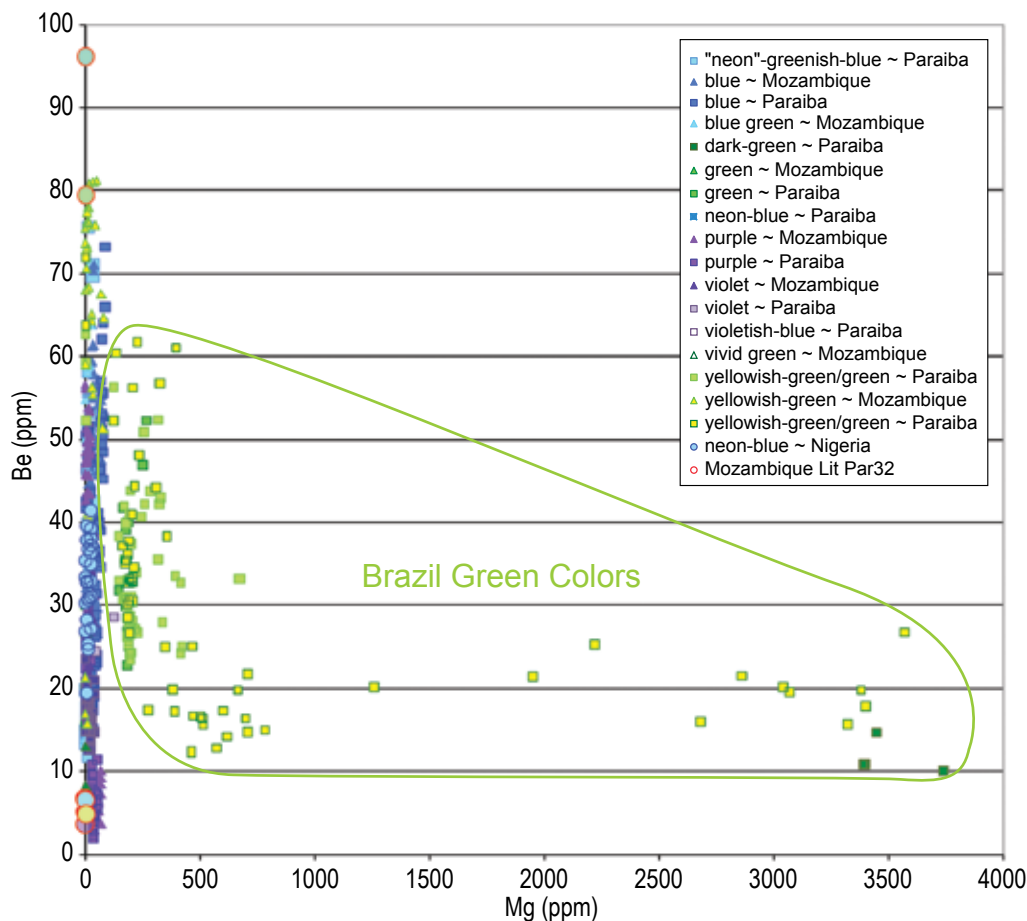


Fig. Par87 In addition to differences in Be-concentrations, the Mg-concentrations are helpful in separating green copper-bearing tourmalines from those of Mozambique with same color. Mg-concentrations were found to be higher in green copper-bearing tourmalines from Brazil.

Fig. Par87

(Cu+Mn)-Pb/Be-Diagram (LA-ICP-MS)

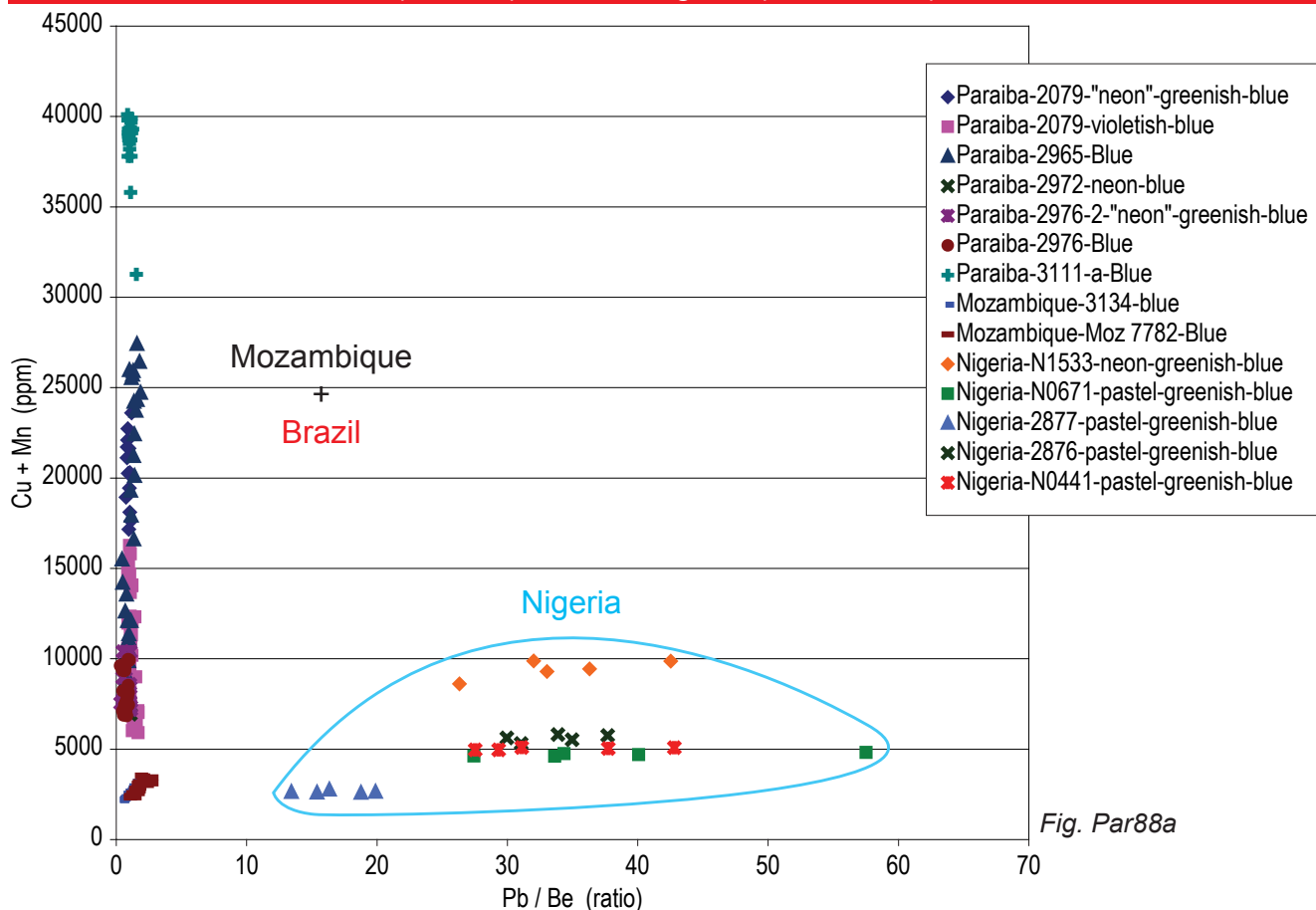


Fig. Par88a

The (Cu+Mn)-Pb/Be-Diagram for Origin Determination of Copper-Bearing Tourmalines:
Different Color Groups (LA-ICP-MS Analysis)

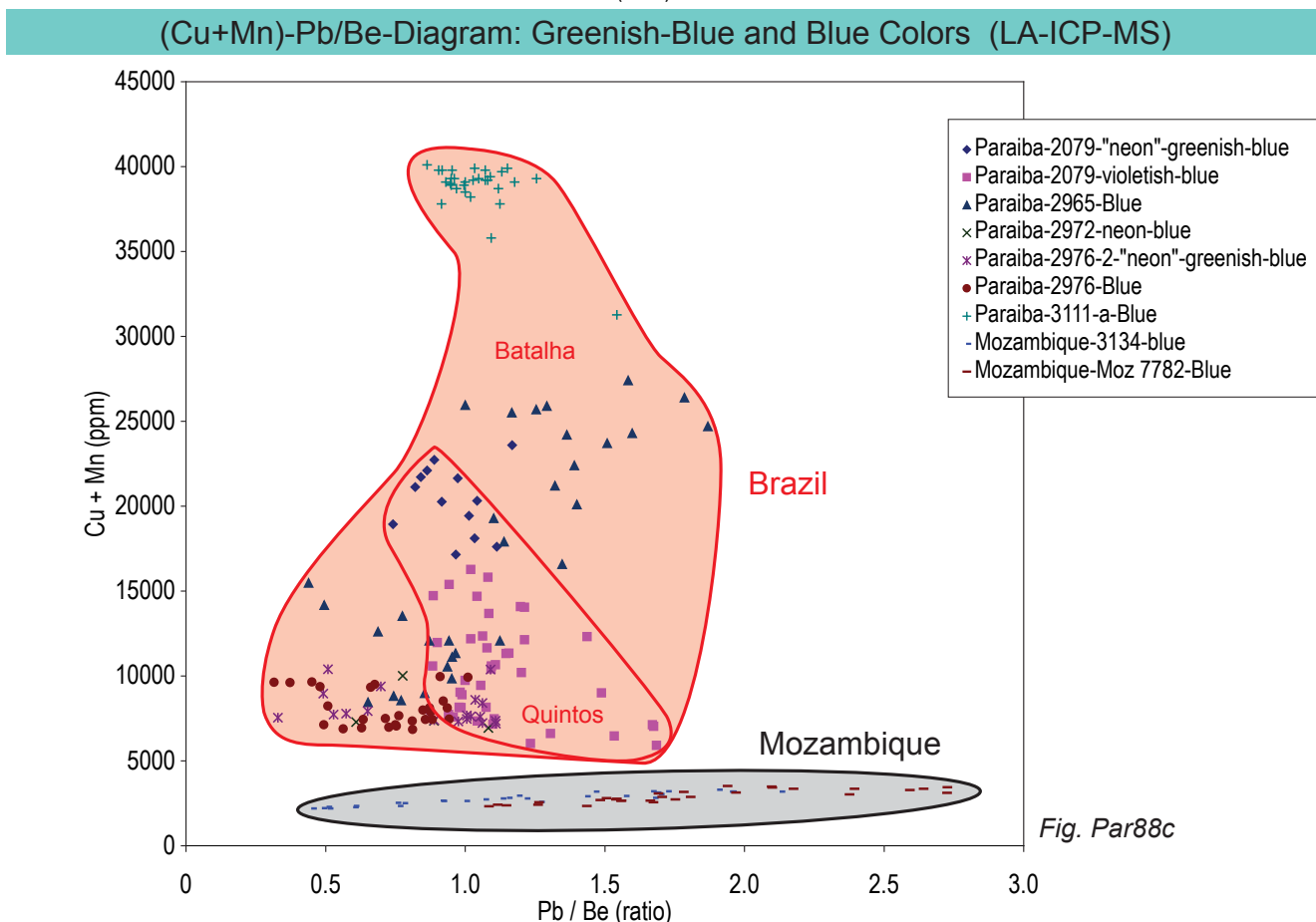
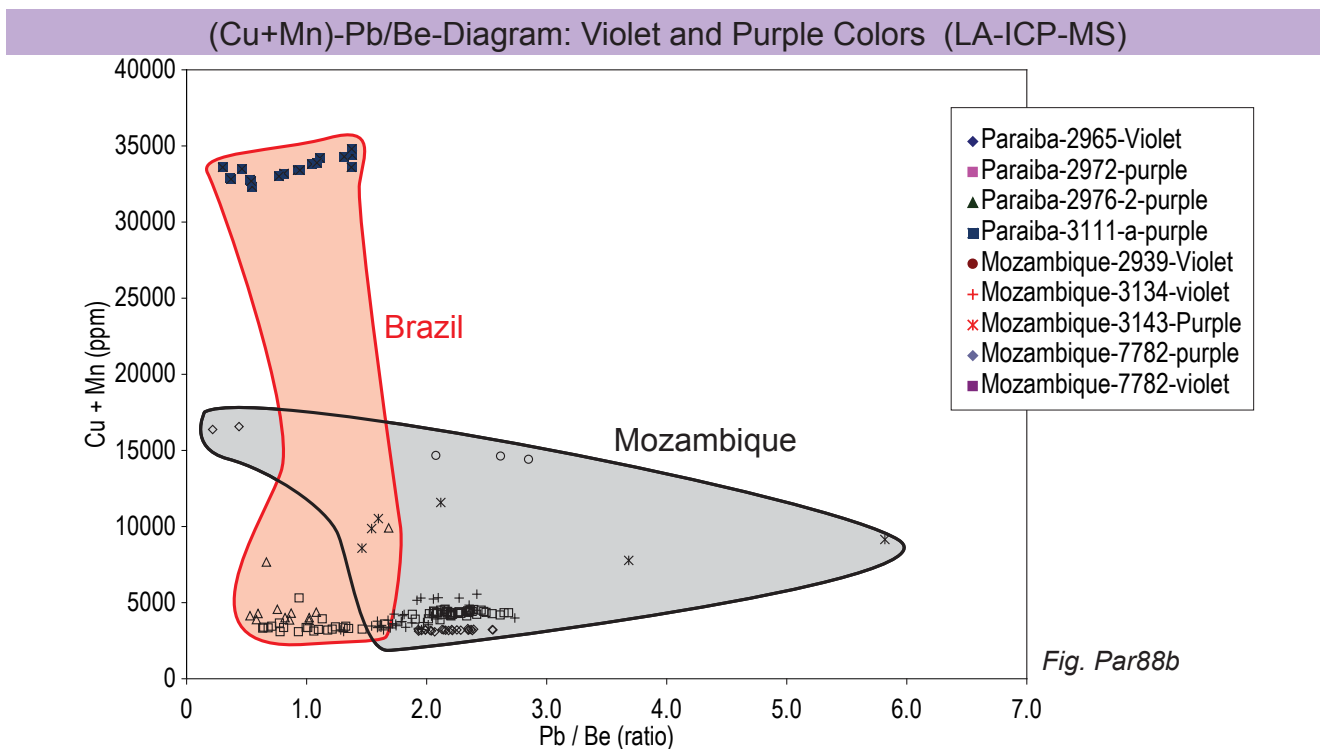


Fig. Par88a-d The Cu+Mn versus Pb/Be-diagram from the literature (Lit. Par 11) was tested. It is seen, that distinctive fields for Mozambique, Brazil and Nigeria can be defined. It is important to separate the plots according to color of the tourmalines. High Pb/Be-ratio characterize the bluish Nigerian and Mozambique tourmalines of green colors split into two fields and can be separated from the Brazilian counterparts. This is mostly due to the fact that the Mn-concentrations in the green rim are strongly increasing (See Fig. Par75a, 78a). In the greenish-blue to blue colors, the Mozambique tourmalines have distinctive lower Cu+Mn-concentrations at overlapping Pb/Be-ratios. This observation may also explain the same spread of the data that were reported in the literature (Lit. Par11).

(Cu+Mn)-Pb/Be-Diagram: Yellowish-Green and Green Colors (LA-ICP-MS)

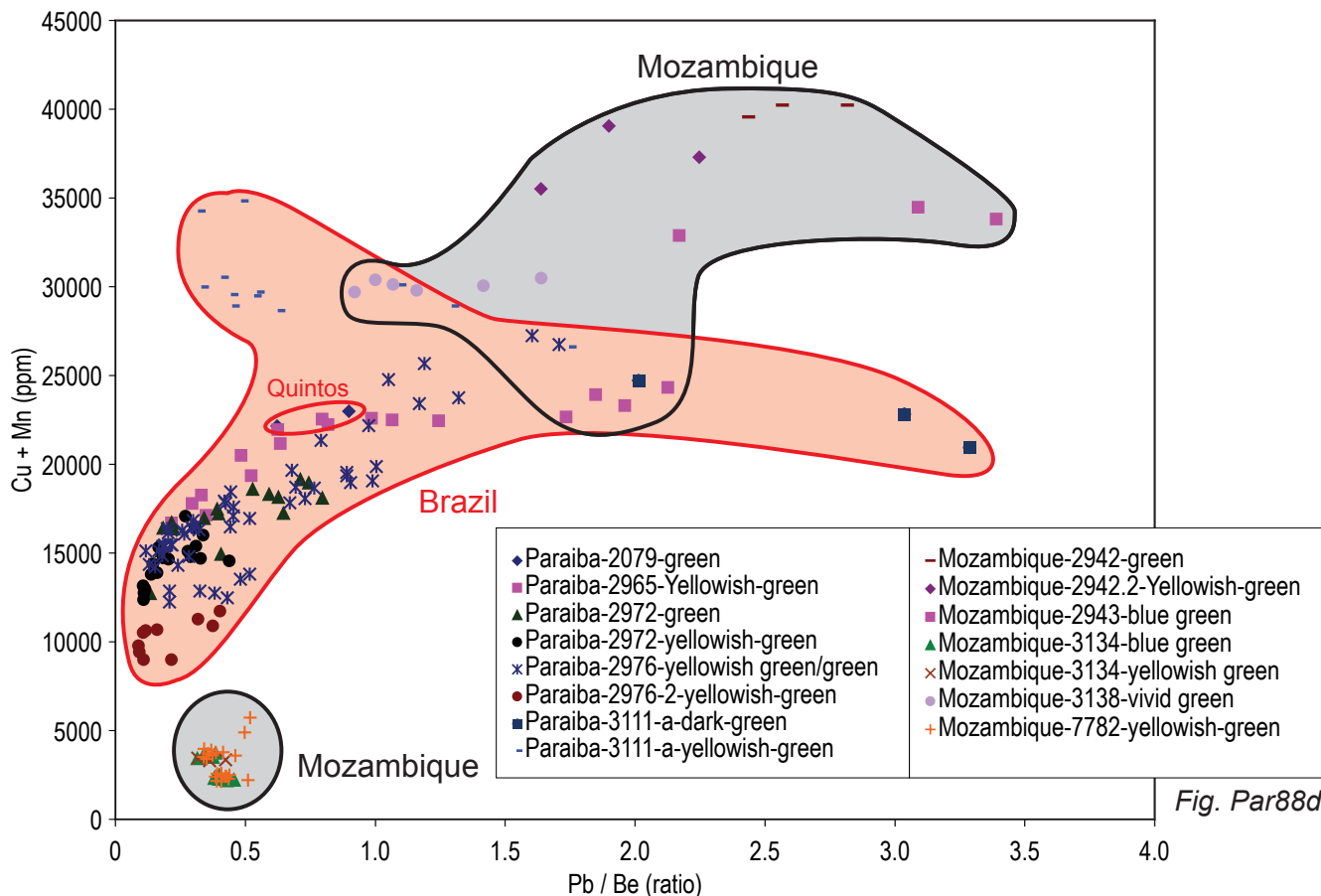


Fig. Par88d

(Ga+Pb)-(Cu+Mn)-Diagram: Violet and Purple Colors (LA-ICP-MS)

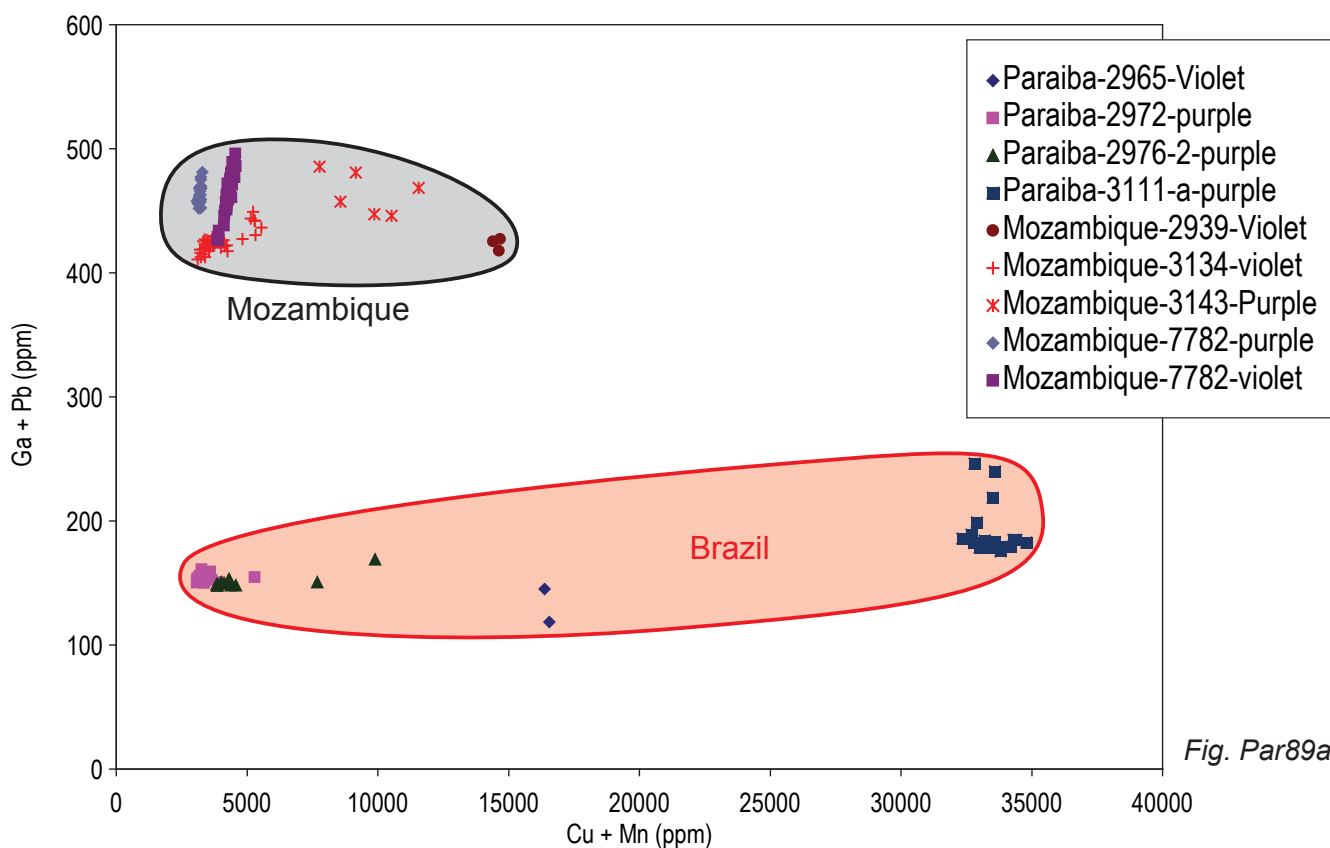


Fig. Par89a

*(Ga+Pb)-(Cu+Mn)-Diagram for Origin Determination of Copper-Bearing Tourmalines:
Different Color Groups (LA-ICP-MS Analysis)*

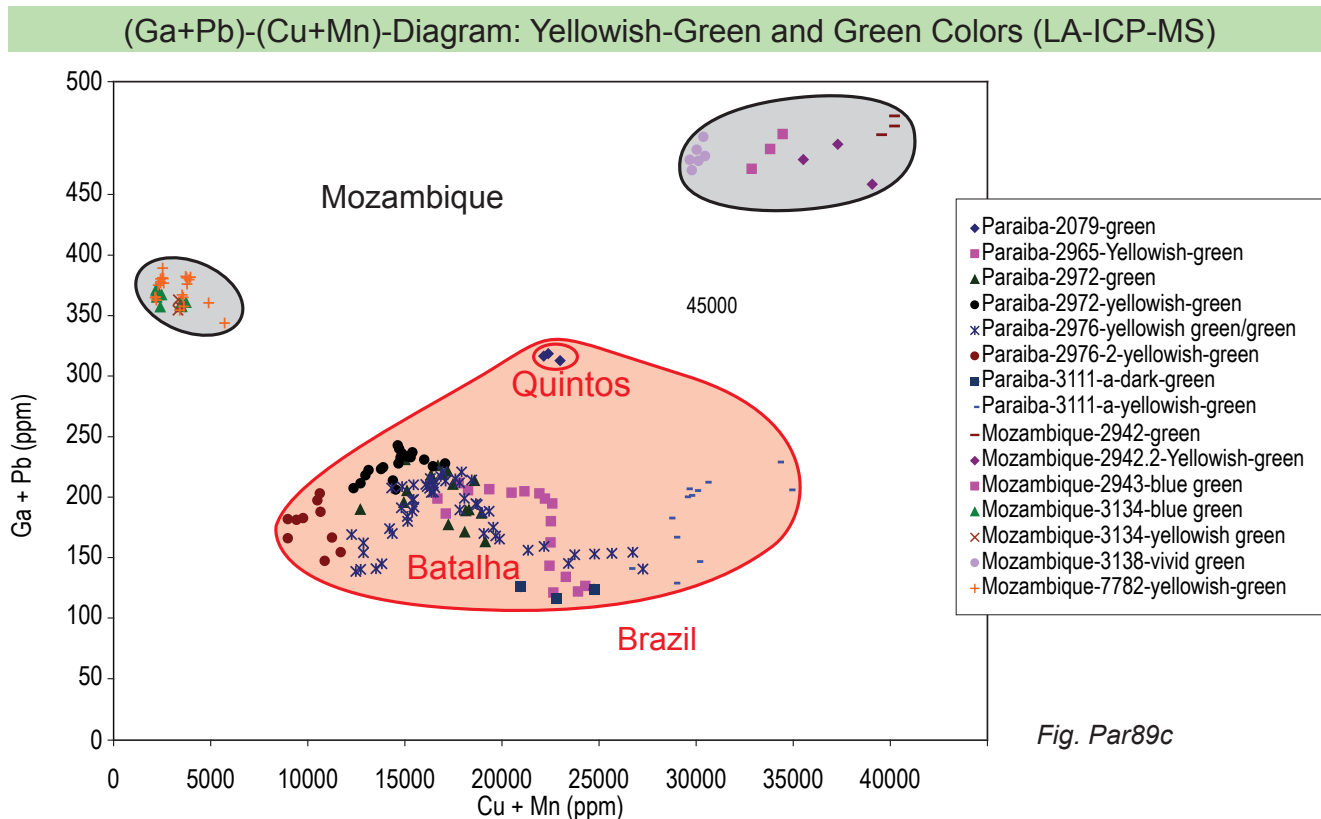
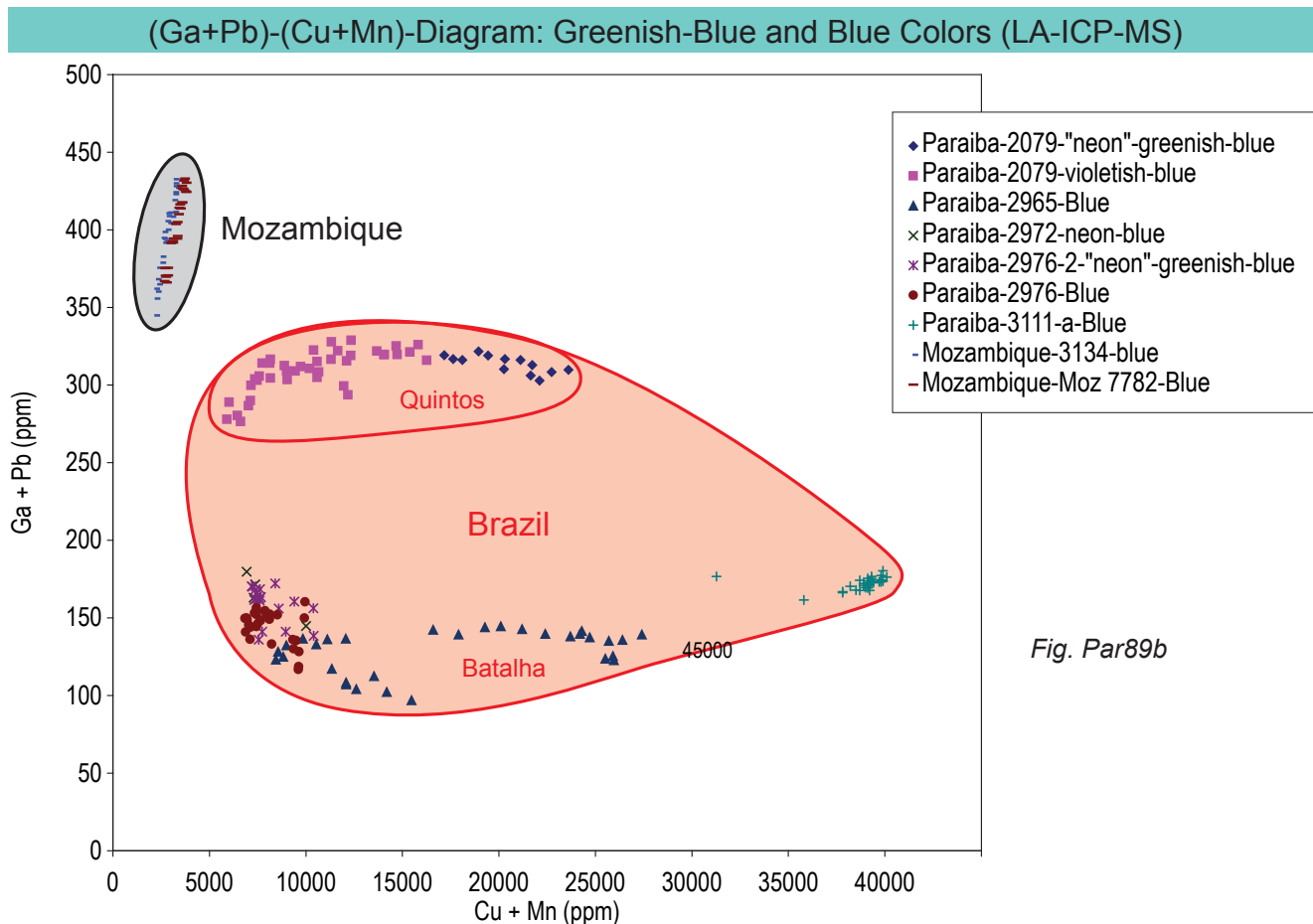


Fig. Par89a-c The (Ga+Pb)-(Cu+Mn) diagram for origin determination of copper-bearing tourmalines of different origin (Lit. Par11) is tested. This critical test was found to be useful if the data are arranged into different color groups. The values of Nigeria are out of the range at highest Ga+Pb-concentrations. The field of Mozambique tourmalines splits into two different fields for the yellowish green colors (Fig. Par89c).

Bi-Mn-Diagram for Classification of Copper-Bearing Tourmalines (LA-ICP-MS)

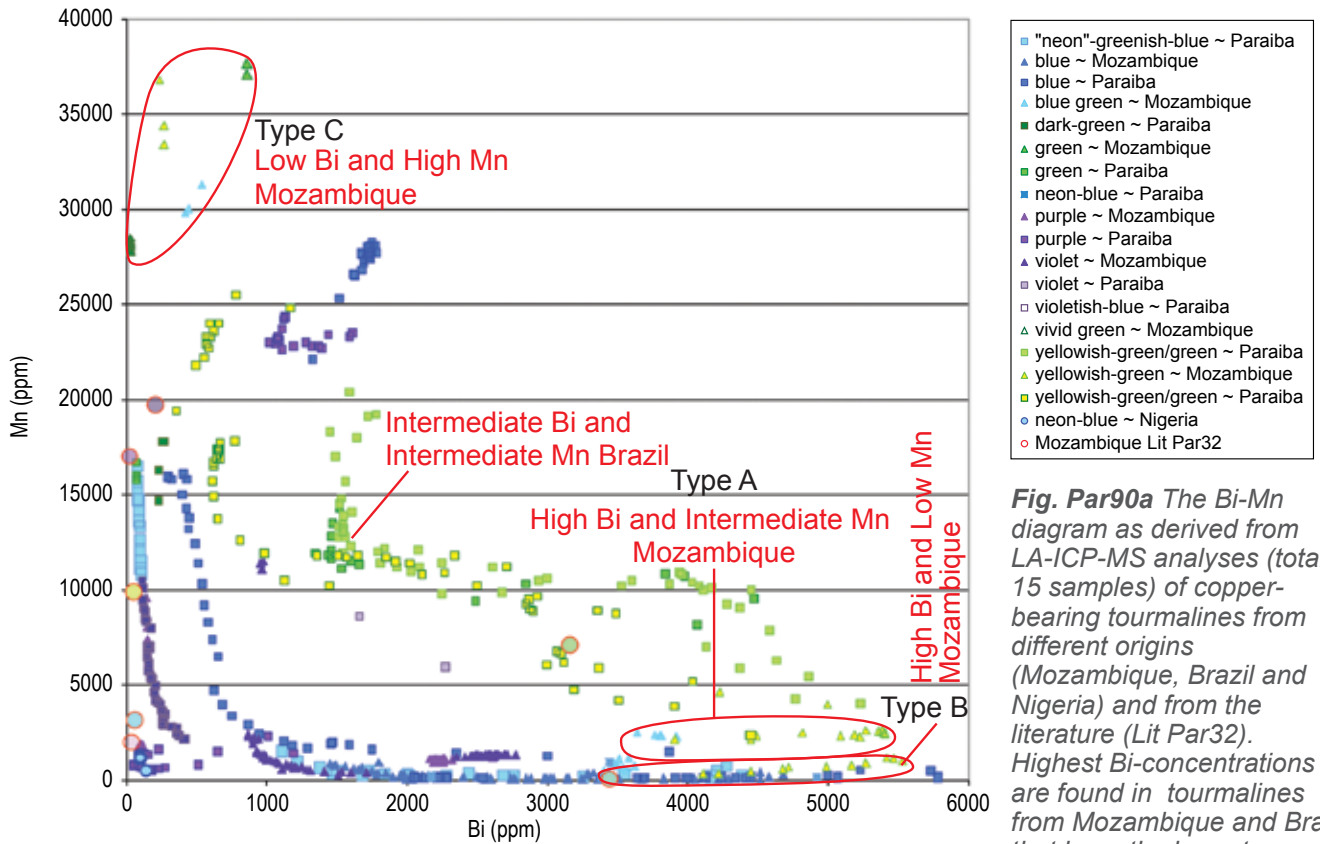


Fig. Par90a The Bi-Mn diagram as derived from LA-ICP-MS analyses (total 15 samples) of copper-bearing tourmalines from different origins (Mozambique, Brazil and Nigeria) and from the literature (Lit Par32). Highest Bi-concentrations are found in tourmalines from Mozambique and Brazil that have the lowest

Mn-concentrations. Three different types of Mozambique tourmalines have been indicated based on Bi- and Mn-concentrations (Type A, B and C). Type B is found in the samples with low Cu-concentrations in the outer green rim of the crystals (Tab. Par05, Fig. Par74 and Fig. Par78a) and has low Mn- and high Bi-concentrations. Intermediate Mn- and Bi-concentrations were observed in Brazilian tourmalines (rarely occupied by tourmalines from Mozambique and Nigeria). "Type C"-tourmalines are characterized by extremely high Mn- and low Bi-concentrations. This type of tourmaline is typically found in Mozambique.

Bi-Mn-Diagram for Classification of Copper-Bearing Tourmalines (ED-XRF)

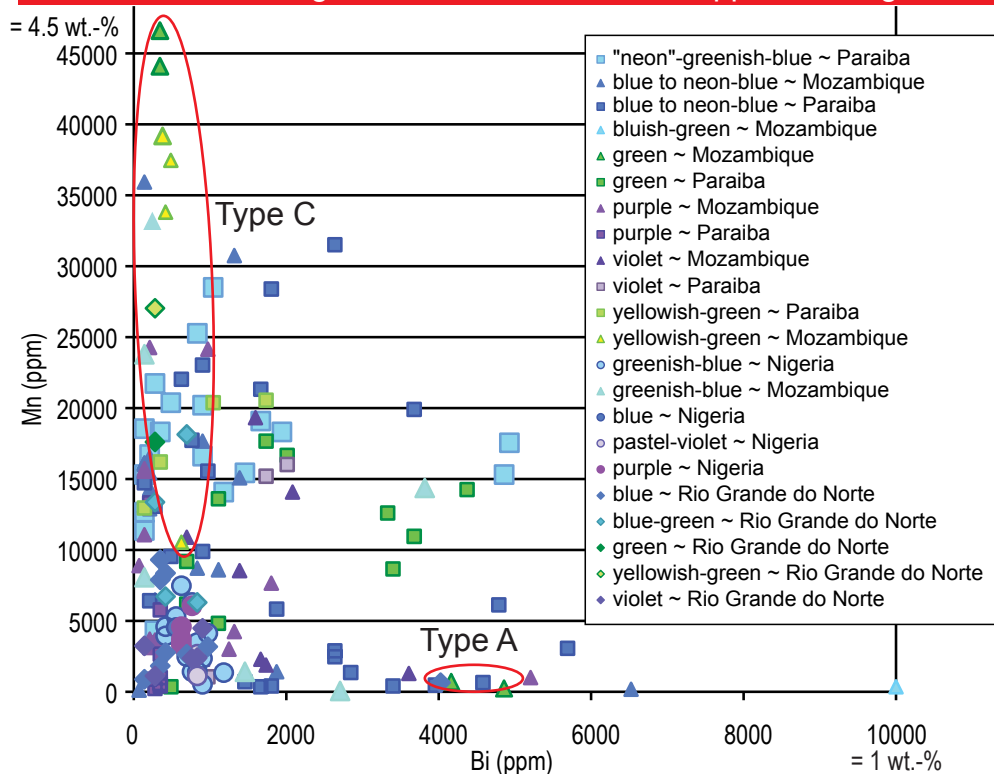


Fig. Par90b shows the Bi-Mn diagram based on ED-XRF analyses. In comparison to LA-ICP-MS analysis, a larger number of samples (over 112 samples, including those measured by LA-ICP-MS, total 174 analyses) were measured.

Note that the same trends are found by the two different methods LA-ICP-MS and ED-XRF. The samples from Nigeria occupy the area of low Mn- and Bi-concentrations. Definition of Type A and C see Fig. Par90a.

CONCLUSIONS

High valuable copper-bearing tourmalines occur in different color and large size and are produced in Brazil, Mozambique and Nigeria. The sizes and distribution of these gemstones in the gem market were studied and a statistic about the trade has been published in this report. These types of tourmalines include many different color varieties and are found as heated as well as unheated gems (Fig. Par07 and 12). Unusual large sizes have been found from the mines in Mozambique. The majority of the stones have been heat-treated in the greenish-blue to blue colors, whereas the purple and green colors are more frequently spared of thermal enhancement (Fig. Par07). These findings are in good agreement with the findings from heat-treatment experiments (Lit. Par33), which predicted that heat-treatment of green colors, is possible with limited success only. Copper-bearing tourmalines from Brazil such as from the state of "Paraiba" were more often found to be unheated than Mozambique tourmalines. Gem quality "Paraiba"-tourmalines does occur in much smaller sizes than the African counterparts, but they are generally more saturated in color. According to our opinion, large-sized unheated gem-quality tourmalines from Brazil (Paraiba or Rio Grande do Norte) with intense "neon"-blue colors can be described as extremely rare (See Fig. Par07, 08, 11 and 12).

We found it useful to investigate the origin based on chemical fingerprints using different methods, including EMPA, LIBS, LA-ICP-MS and ED-XRF analyses. Based on these analyses, it was found that the chemical composition of copper-bearing tourmalines from Mozambique, Nigeria and Brazil show distinct differences, which are sufficient selective to determine their origin. The findings on LA-ICP-MS-analyses are in agreement with earlier work in the literature (Lit. Par11 and Lit Par33). The usefulness of diagrams from these earlier works (Lit. Par11) were tested and found to be mostly applicable, such as the ternary diagram Mg-Zn-Pb (See Fig. Par 91a-b), the Cu+Mn versus Ga+Pb-diagram and the Cu+Mn versus Pb/Be-ratio-diagram

(Fig. Par88 and Fig. Par89). However, the data of Abduriyim et al. (Lit. Par11) could not be plotted in some of our diagrams as they did only publish concentration ranges and ratios and no individual quantitative results and the standard deviation, respectively. However, the trends between different colored copper-bearing Mozambique tourmalines including the variations in Fe and Ti as published in the literature (Lit. Par 33) were plotted in diagrams and confirmed (Fig. Par76c, 78f, 81, 82 and 88). Because we focused on chemical profile analyses (LA-ICP-MS) and chemical distribution mapping (EMPA-analyses) of chemical zoning within single tourmalines, however, it was possible to investigate the chemical evolution of the copper-bearing tourmalines of samples from Mozambique and Brazil (Fig. Par91) in more detail. We correlated different zones of different tourmalines with the chemical evolution within the tourmalines. Different evolution patterns were found in Brazilian and Mozambique tourmalines (Fig. Par91). This helped us to explain the spread of the data published elsewhere (Lit. Par 11), such as in the Mg-Zn-Pb ternary diagram that are proposed for use of origin determination. With chemical profile analyses it was possible to evaluate the limitations of the diagrams proposed for origin determination in the literature (Lit. Par11). It can be shown that sudden changes of ratios and sum of elements occurred within the same crystal depending on the different growth zones (e.g. see Box Par2 and 4). The diagrams based on Cu, Mn, Pb, Ga and Be should be used for each color group separately. In the light of strong variations within single tourmalines, the generalization about the chemical differences regarding Ga, Ge, Pb, Mg, Zn, Sb, Sc and Bi in tourmalines (See abstract Lit. Par 11) are not useful for origin determination purposes.

For example, due to the different approach of concentrating the research on studies within single crystals, it was possible to find different trends regarding the element Bi (See Fig. Par91d). High Bi-concentrations were found in tourmalines from both, Brazil and Mozambique, respectively. Different Bi-Cu-Mn-concentration trends were found in tourma-

Mg-Pb-Zn Chemical Evolution Trends in Tourmalines from Mozambique and Brazil (Pb-Mg-Zn-Diagram)

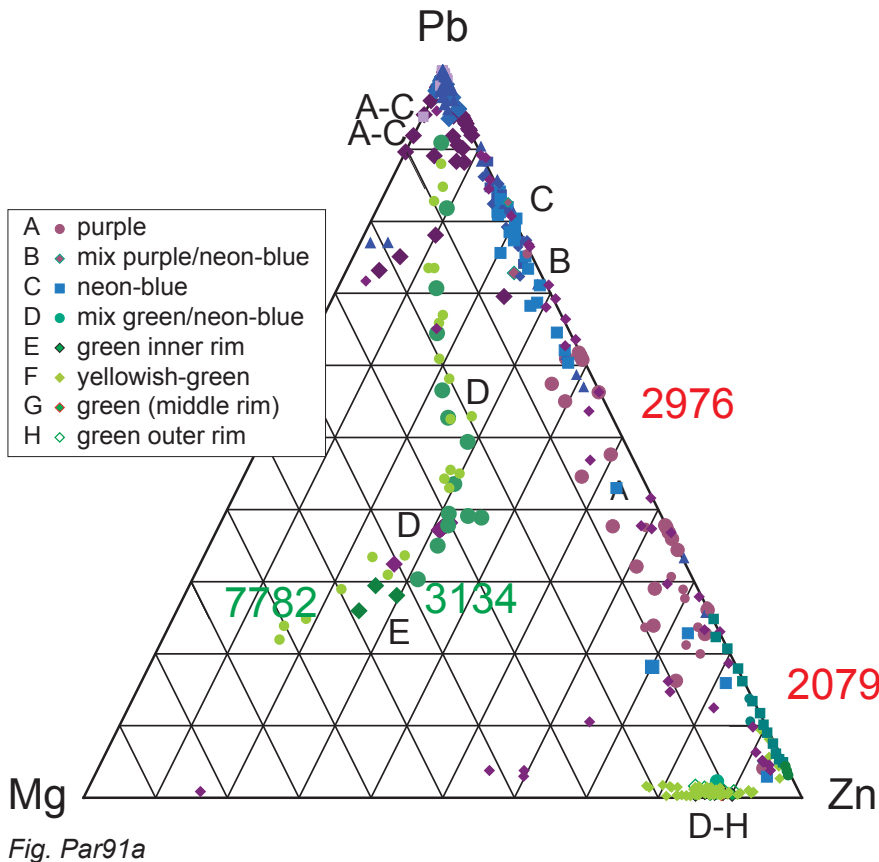


Fig. Par91a

Fig. Par91a-d
 Triangular plots of Mg-Pb-Zn (Fig. Par91a) and Mn-Bi-Cu (Fig. Par91c) of chemical compositions in multicolored copper-bearing tourmaline from Mozambique and Brazil are shown (LA-ICP-MS analysis, in $\mu\text{g/g}$). 5 chemical profile analysis of tourmalines from Brazil and 2 from Mozambique are shown in the same diagrams. Chemical compositions from the core to the rim are mapped (A-H). For each studied sample, a chemical trend is obtained that shows the chemical variations of the tourmalines from the core to the rim ("Chemical evolution trends" marked with red and green lines, Fig. Par91b and Par91d). The sample number is indicated.

Different chemical trends were found for tourmalines from Mozambique and Brazil.

As shown in Fig. Par91d, tourmalines from Mozambique evolve towards the Mg-corner.

Brazilian tourmalines show a relative trend towards higher Zn-concentrations during their growth. A 2-step trend was found. A chemi-

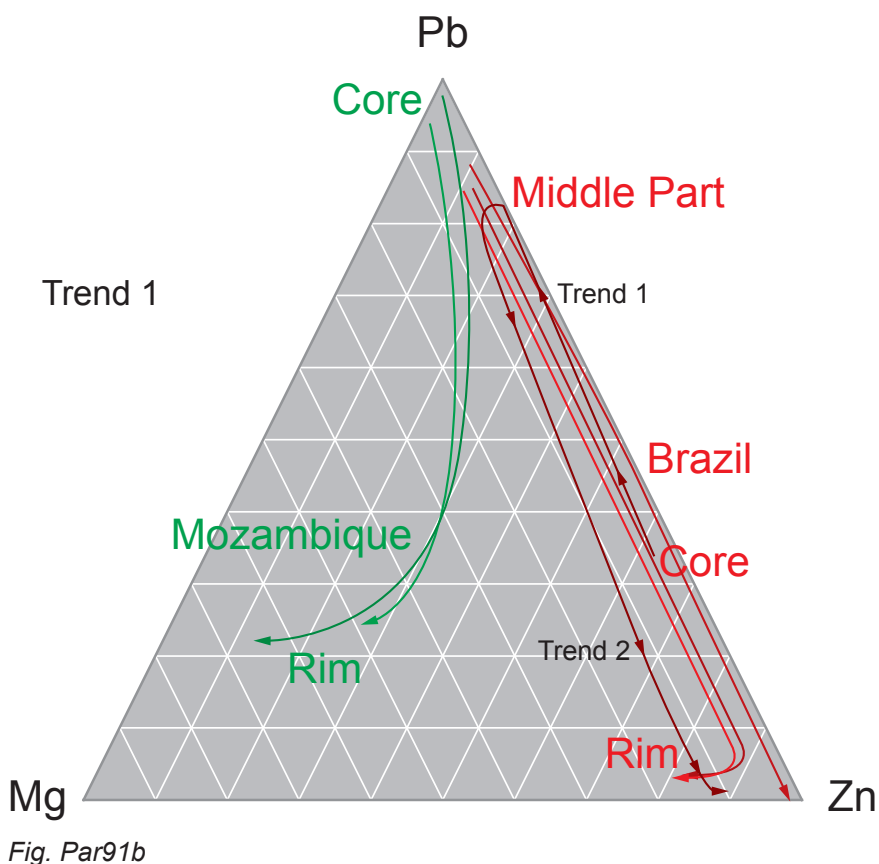


Fig. Par91b

Mn-Cu-Bi Chemical Evolution Trends in Tourmalines from Mozambique and Brazil (Mn-Cu-Bi-Diagram)

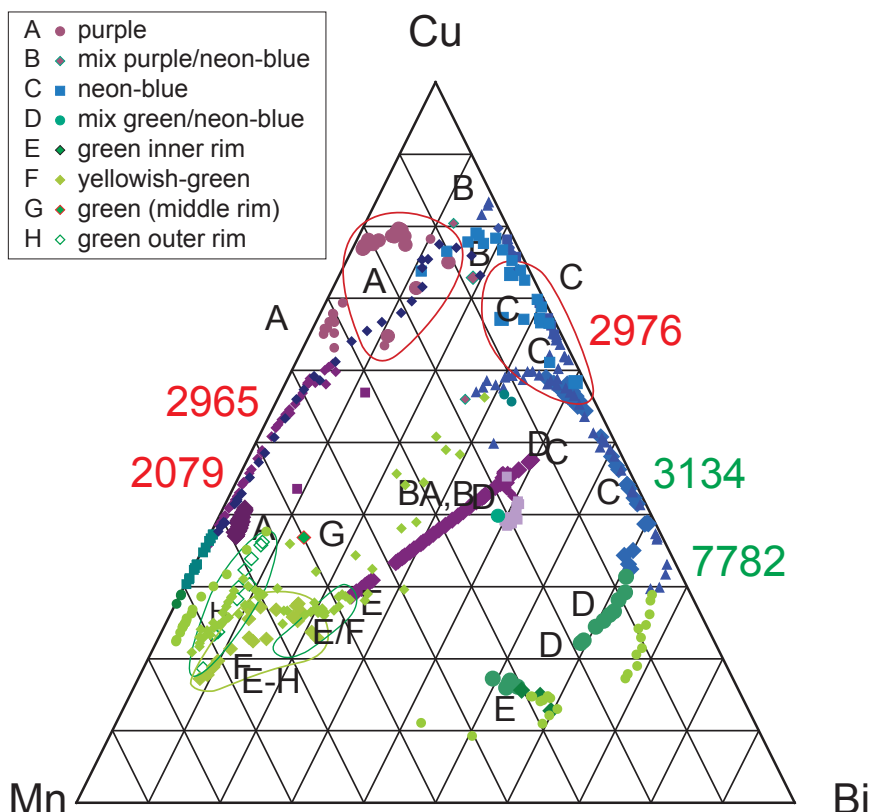


Fig. Par91c

cal trend towards higher Pb-concentrations is followed by a trend towards higher Zn-concentrations.

The spread of the data in the Mg-Pb-Zn-diagram as published in the literature (Lit Par11) can be explained by our profile analysis. The variation of the concentrations can be found within single tourmaline crystals.

The “chemical evolution path” of Cu, Mn and Bi is different for samples from Mozambique and Brazil (Fig. Par91d).

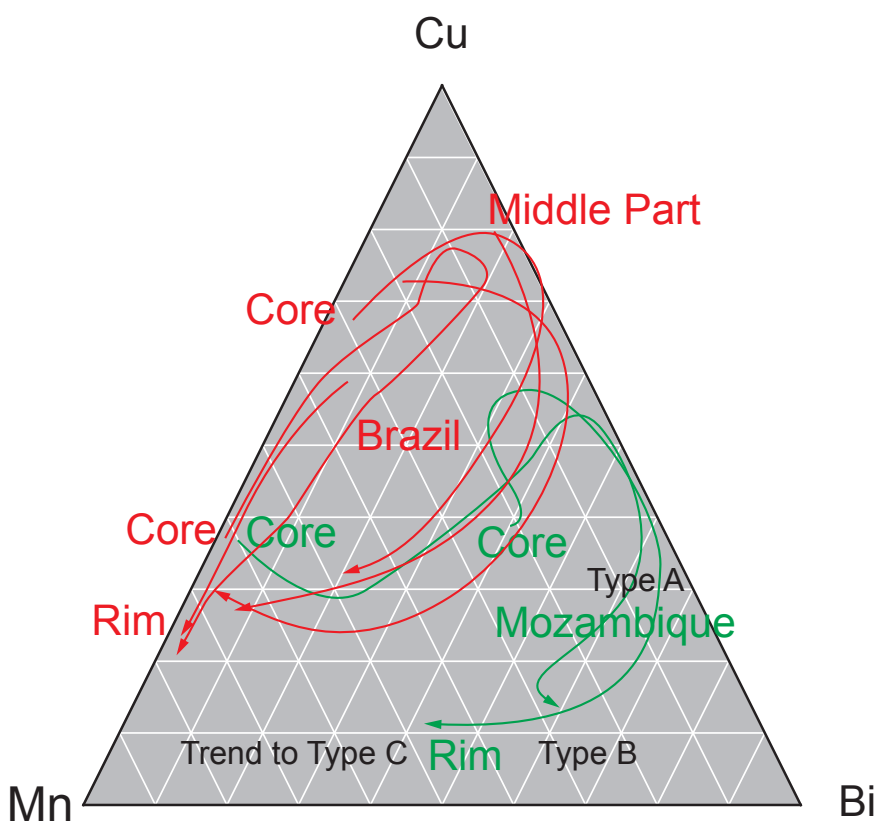


Fig. Par91d

The trends in Mozambique tourmalines are found to be similar but shifted towards higher Bi-concentrations. According to the Mn/Bi-ratio, the Mozambique tourmalines have been classified as Type A, B and C (Fig. Par90a-b). Type C is extremely Mn-rich at low Bi-concentrations.

The trends observed in the tourmalines from Brazil are centered towards the corner of Cu in the Cu-Mn-Bi-triangle. This due to the generally higher Cu-concentrations of the Brazilian tourmalines.

lines from the different locations and could be correlated to the different color zones in these tourmalines (Fig. Par91c-d). However, only Cu and Mn are responsible for the color, not Bi. The Bi-Cu-Mn trends can be combined with other elements, such as other minor or trace elements. For example, in general much higher Cu-concentrations are found in tourmalines from Brazil and much higher Ga-concentrations are found in Mozambique tourmalines. The Cu/Ga-ratio was found a very promising critical test. In a large number of samples (See Fig. Par82b-c for overlapping area), the Cu/Ga-ratios (in weight-ppm) were found to be greater than 12 in tourmalines from Brazil.

Based on our Mn-, Bi- and Cu-concentrations, it was possible to classify certain copper-bearing tourmalines as type A, B and C (Fig. Par90a). Of particular interest were "Type C"-tourmalines that are characterized by very high Mn-concentrations and low Bi- and Cu-concentrations. Different types of Mozambique tourmalines (Type A-C) were found within single multicolored crystals (Fig. Par72a) or as individual large samples almost entirely forming "Type C"-tourmalines (Fig. Par67). "Type C"-tourmalines were also discovered from one particular source in 2005 (Bank, Tab. Par05, Lit Par36). It is well possible that these Bi-poor tourmalines of high Mn-concentrations and low Cu-concentrations are more often found in some mining spots in Mozambique (Lit. 30, 33, 34, 36 and 39). Some inclusion features that we found in these tourmalines (e.g. purple halos around orange growth tubes and cracks, See Lit. Par48) have created some controversy on the issue of treatments of copper-bearing tourmalines. We have therefore included a case study focusing on these type of inclusions (Interpretations and summary, See Box Par1). With detailed pinpointing LA-ICP-MS analysis, we detected the presence of radioactive trace element concentrations of uranium in the orange cracks and tubes along with other element concentrations such as barium, iron and rare earth elements (Details See Fig. Par76 and 78). These findings support the recent theory that the purple "halos" in tourmalines from Mozambique are induced

by natural irradiation (Lit. Par48).

Ba-contaminations were also found on the surface of rough tourmalines from Mozambique (See Tab. Par05).

Our approach on chemical profile analyses allowed us furthermore to identify some new chemical evolution trends in copper-bearing tourmalines from different origins (e.g. REE-trends) that have not been reported in such details in the literature. For example, the occurrence of U and Th-concentrations appeared at different growth stages (Fig. Par41b) and increasing concentration of Rare Earth Elements (REE's) were measured in the tourmaline rims (Fig. Par40, 49a, 50, 63a-b, 76e and 78d). Furthermore, it can be shown that the growth of Brazilian tourmalines can be divided in a Nb and Ta-dominated growth phase (Fig. Par41c, 51c, 60b, 62d and 66g) and some other elements, such as Be and Pb, are differently enriched in various growth sectors (Fig. Par33a, 43b, 59d, 62e, 66d; Box Par2 and 4). The concentrations of Sb, Sc and Ge (Fig. Par33a, 43b, 60d, 62c, 66h and 76a) are also variable within single tourmaline crystals depending on measuring position in different growth and color zones.

Element distribution patterns as determined with EMPA analysis detected chemical variations within a single crystal of the elements Al, Ca, Na, Mg, Ti, Zn, F, Mn, Cu and Bi. The variations detected by this method can provide additional important information on the genesis of copper-bearing tourmalines. For example, it was found that the tourmalines have a distinct chemical zoning in fluorine, along with other elements (Fig. Par28c and 31i). The F-concentrations increased with the concentrations of heavy elements such as Cu, Mn and Bi. These observations will become important for the interpretation of the sudden enrichment of copper and other elements in copper-bearing tourmalines and for the interpretation of what kind of fluids were present (See Lit. Par09). While we have only reported on the example of a Brazilian tourmaline, such F-analysis can be expanded to copper-bearing tourmalines from other origins. For example, high F-concentrations

are also reported from Mozambique tourmalines (Lit. Par33). The element distribution mapping in tourmalines are also important to compare them with any future patterns that may occur in relation to potential new treatments.

Regarding the importance of different methods useful for provenance determination of tourmalines, the following conclusions can be made (See Box Par3). LA-ICP-MS in combination with EMPA analyses was most important for the creation of a sample set (matrix matched) applicable as calibration materials for other and more matrix-dependent techniques commonly used for gem testing. We found that heavy elements such Ti, Fe, Cu, Zn, Mn, Bi, Pb and Ga can be routinely measured by ED-XRF analyses, while light elements such as Be and Mg can be measured by LIBS, which has been more recently introduced into gem testing. Box Par3 shows a test procedure that summarizes our protocol for chemical testing for tourmaline aiming at determining their origin and authenticity. For example, a test is based on the Cu/Ga- and Pb/Ga-ratios. The Cu-, Ga- and Pb-concentrations can be determined by ED-XRF analyses (C, Box Par3). This test can be combined with LIBS-analyses to determine Be-concentrations (D, Box Par3). For example, Cu and Mn-values are measured first by ED-XRF. The obtained Cu- and Mn-values can then be re-measured by LIBS-analysis along with light elements such as Be. Based on the calibrated LIBS-analyses and on LA-ICP-MS generated in-house and matrix matched calibration materials, a ternary Mn-Cu-Be diagram can be obtained that provides additional results useful for origin determination (See Fig. Par85 and 86). Further combinations of light and heavy element analyses may be necessary, depending on the color variety of the copper-bearing tourmalines. In conclusion, with the combined use of LIBS- (for testing of light elements such as Mg and Be), and ED-XRF analyses (for testing of elements at concentrations higher than 0.001%, such as Pb, Zn, Bi, Cu, Mn, Fe and Ga), it is possible to derive a conclusive information about the origin of copper-bearing tourmalines in most cases (See overlapping

areas in critical diagrams, See Fig. Par82a-b). It is important, however, that a "Standard-Set" (matrix matched calibration materials) is available that has been measured by both, EMPA and LA-ICP-MS (See Box Par3). We have presented only the data on unheated samples in our charts and classified them according to color. It must be kept in mind that heat-treatment may have been applied to tourmalines that may have changed their original color (See for example Lit. Par11 and 33). Based on the experiments published in the literature and observations that can be made using a microscope (e.g. heated tourmalines have extensive cracks around tubes and fluid inclusions), it is possible, according to our experience, to reconstruct these color-changes. Our test procedure is presented as flow chart in Box Par3 for laboratories that do not have routinely access to LA-ICP-MS or EMPA.

This study indicates that the general conclusion made in the literature (Lit. Par11) that the origin of tourmalines can only be determined by LA-ICP-MS is not valid anymore. Our EMPA and LA-ICP-MS generated database allows using commonly applied gem-testing methods (ED-XRF and LIBS) for origin determinations of copper-bearing tourmalines.

Acknowledgments

We would like to thank the P. Wild company (Idar-Oberstein, Germany) for providing us with numerous pictures from the mines and supporting us with samples for this research project. Marcus Paul Wild explained us the geological background of some Brazilian tourmaline mines. Brian Pavlik from Brian's Fine Gems (Austria) granted us permission to use pictures from the Pavlik Gem History Archive (Vienna, Austria) and donated Paraiba tourmalines from the first production years (1988). Gebr. Bank (Idar Oberstein) donated samples from the first mining period in Mozambique and obtained further samples from Paraiba from Bob von Wagoner (Beija-Flor Gems). Tourmalines from Nigeria were received from Steve Jaquith and Arnold Silverberg in Bangkok. Hatta New World company provided us professional jewelry photography and valuable jewelry sets for testing purposes. Without the support from African miners and dealers, we would not have been able to acquire multi-colored tourmaline samples from Mozambique. C.H. Lapidaries from Bangkok assisted us for faceting our own rough materials. Miriam Peretti helped for presentation of jewelry sets and Elia Menghini assisted in ED-XRF analysis.

Many thanks to Mr. Tanthadilok for graphic and artwork, Ms Anong Kranpaphai from Anong Imaging for photography and Mr. Michael for preparing this report for the Internet online version, now in translation mode for over a dozen languages (www.gemresearch.ch).

About the Authors

Dr. Peretti is Director of the GRS Gemresearch Swisslab Ltd., Lucerne, Switzerland
Adolf@Peretti.ch

Dr. Günther is Professor for Trace Elements and Microanalysis at the Laboratory for Inorganic Chemistry, ETH Zurich, Switzerland
guenther@inorg.chem.ethz.ch

K. Hametner is Research Assistant for Trace Elements and Microanalysis at the Laboratory for Inorganic Chemistry, ETH Zurich, Switzerland
hametner@inorg.chem.ethz.ch

W. Bieri (Bsc. EarthSc.) is Research Gemologist at GRS (Thailand) in Bangkok, Thailand.
wbieri@gemresearch.ch

Dr. Reusser is Research Scientist at Institute of Mineralogy and Petrography, ETH Zentrum, CH-8092 Zurich, Switzerland
eric.reusser@erdw.ethz.ch

An extended scientific report of this book is published under:

Lit Par01 Peretti A., Reusser E., Bieri W., Hametner K. and Guenther D. (in prep.) Provenance studies of "Paraiba" tourmalines using EMPA and LA-ICP-MS analysis. *Analytical and Bioanalytical Chemistry*.

Literature review on methods

Lit Par02 Armstrong J.T., Caltech 1993, Jeol license of CITZAF version 3.5.

Lit Par03 Gao, S., Liu, X., Yuan, H., Hattendorf, B., Günther, D., Chen, L., Hu, S. 2002 Analysis of forty-two major and trace elements of USGS and NIST SRM Glasses by LA-ICPMS *Geostandard Newsletters*, Vol. 26, 181-195

Lit Par04 Guillong M., Günther D. (2001) Quasi 'non-destructive' laser ablation-inductively coupled plasma-mass spectrometry fingerprinting of sapphires. *Spectrochimica Acta Part B*, Vol. 56, pp. 1219-1231.

Lit Par05 Günther D., Hattendorf B. (2005) Solid sample analysis using laser ablation inductively coupled plasma mass spectrometry. *Trends in Analytical Chemistry*, Vol.24, No. 3, pp. 255-265.

Lit Par06 Leach A.M., Hieftje G.M. (2002) Factors affecting the production of fast transient signals in single shot laser ablation inductively coupled plasma mass spectrometry. *Applied Spectroscopy*. Vol. 56, No. 1, pp. 62-69.

Lit Par07 Longerich H.P., Jackson S.E., Günther D. (1996) Laser ablation inductively coupled plasma mass spectrometric transient signal data acquisition and analyte concentration calculation. Winter Conference on Plasma Spectrochemistry. 1996. Ft Lauderdale.

Lit Par08 Pearce N. J. G., Perkins W. T., Westgate J. A., Gorton M. P., Jackson S. E., Neal C. R., Chenery S. P. (1996) Application of new and published major and trace elements data for NIST SRM 610 and NIST SRM 612 glass reference materials. *Geostandards Newsletter*, Vol. 20, No. 2, pp. 115-144.

Lit Par09 Peretti A., Mullis J., Mouawad F. (1996) The role of fluorine in the formation of color zoning in rubies from Mong Hsu (Myanmar, Burma). *J. Gemmol.* 25: p. 3-19.

Lit Par10 Rossman G. R., Mattson S. M. (1986) Yellow, Mn-rich elbaite with Mn-Ti intervalence charge transfer. *American Mineralogist*, Vol. 71, pp. 599-602.

Literature review on tourmalines from Brazil

Lit Par11 Abduriyim A., Kitawaki H., Furuya M., Schwarz D. (2006) "Paraiba"-type copper-bearing tourmaline from Brazil, Nigeria, and Mozambique: Chemical fingerprinting by LA-ICP-MS. *Gems & Gemology*, Vol. 42, No. 1, pp. 4-21.

Lit Par12 Bank H., Henn U. (1990) Paraiba tourmaline: Beauty and rarity. *Jewellery News Asia*, No.70, 1990, pp. 62, 64.

Lit Par13 Bank H., Henn U., Bank F. H., von Platen H., Hofmeister W. (1990) Leuchtendblaue Cu-führende Turmaline aus Paraiba, Brasilien. *Zeitschrift der Deutschen Gemmologischen Gesellschaft*, Vol.39, No. 1, pp. 3-11.

Lit Par14 Brandstätter F., Niedermayr G. (1994) Copper and tenorite inclusions in cuprian-elbaite tourmaline from Paraiba, Brazil. *Gems & Gemology*, Vol. 30, No. 3, pp. 178-183.

Lit Par15 Federman D. (1990) Gem profile. Paraiba tourmaline: Toast of the trade. *Modern Jeweler*, Vol.89, No. 1, p. 48.

Lit Par16 Fritsch E., Shigley J. E., Rossman G. R., Mercer M. E., Muhlmeister S., Moon M. (1990) Gem-quality cuprian-elbaite tourmalines from São José da Batalha, Paraiba, Brazil. *Gems & Gemology*, Vol. 26, No. 3, pp. 189-205.

Lit Par17 Furuya M. (2004) Electric blue tourmaline from Nigeria: Paraiba tourmaline or new name? Proceedings of the 29th International Gemmological Conference 2004, Wuhan, China, September 13-17, China University of Geosciences (Wuhan) and Hong Kong Institute of Gemmology, pp. 111-112.

- Lit Par18 Furuya M., Furuya M. (2007) Paraiba Tourmaline-Electric Blue Brilliance Burnt into Our Minds. Japan Germany Gemmological Laboratory, Kofu, Japan, 24 pp.
- Lit Par19 Kane R.E. (1989) Gem trade lab notes: Blue tourmaline from Brazil. *Gems & Gemology*, Vol. 25, No. 4, pp. 241-242.
- Lit Par20 Karfunkel J., Wegner R. R. (1996) Paraiba tourmalines: Distribution, mode of occurrence, and geologic environment. *Canadian Gemmologist*, Vol.17, No. 4, pp. 99-106.
- Lit Par21 Kitawaki H. (2005) Journey through Brazil mines: Hometown of "Paraiba" tourmaline. *Gemmology*, Vol.36, No. 435, pp. 19-23.
- Lit Par22 Koivula J. I., Kammerling R. C., Eds. (1989) Gem News: Unusual tourmalines from Brazil. *Gems & Gemology*, Vol. 25, No. 3, pp. 181-182.
- Lit Par23 Koivula J. I., Kammerling R. C., Eds. (1989) Gem News: Paraiba tourmaline update. *Gems & Gemology*, Vol. 25, No. 4, pp. 248-249.
- Lit Par24 Koivula J. I., Kammerling R. C., Eds. (1990) Gem News: Treated Paraiba tourmaline. *Gems & Gemology*, Vol. 26, No. 1, pp. 103-104.
- Lit Par25 Koivula J. I., Kammerling R.C. (1990) Gem news: The discovery of the Paraiba tourmaline mine. *Gems & Gemology*. Vol. 26, No.2, pp. 164-165.
- Lit Par26 Koivula J. I., Kammerling R. C., Fritsch E., Eds. (1992) Gem News: Tourmaline with distinctive inclusions. *Gems & Gemology*, Vol. 28, No. 3, pp. 204-205.
- Lit Par27 Milisenda C. C. (2005) "Paraiba-Tourmaline" aus Quintos de Baixo, Rio Grande do Norte, Brasilien. *Gemmologie: Zeitschrift der Deutschen Gemmologischen Gesellschaft*, Vol. 54, No. 2-3, pp. 73-84.
- Lit Par28 Shigley J. E., Cook B. C., Laurs B. M., Oliveira Bernardes M. (2001) An update on "Paraiba" tourmaline from Brazil. *Gems & Gemology*, Vol. 37, No. 4, pp. 260-276.
- Literature review on tourmalines from Africa**
- Lit Par29 Abduriyim A., Kitawaki H. (2005) Cu- and Mn-bearing tourmaline: More production from Mozambique. *Gems & Gemology*, Vol. 41, No. 4, pp. 360-361.
- Lit Par30 Bettencourt Dias M., Wilson W. E. (2000) Famous mineral localities: The Alto Ligonha pegmatites, Mozambique. *Mineralogical Record*, Vol. 31, pp. 459-497.
- Lit Par31 Breeding C. M., Rockwell K., Laurs B. M. (2007) Gem News International: New Cu-bearing tourmaline from Nigeria. *Gems & Gemology*, Vol. 43, No. 4, pp. 384-385.
- Lit Par32 Henricus J. (2001) New Nigeria tourmaline find excites trade interest. *Jewellery News Asia*, No.207, pp. 77-78, 87.
- Lit Par33 Laurs, B.M., Zwaan J.C., Breeding C.M., Simmons W.B., Beaton D., Rijdsdijk K.F., Befi R., Falster A.U. (2008) Copper-bearing (Paraiba-type) tourmaline from Mozambique. *Gems & Gemology*, 2008. Vol. 44, No. 1: pp. 4-30.
- Lit Par34 Lächelt S. (2004) The Geology and Mineral Resources of Mozambique. National Directorate of Geology, Maputo, Mozambique, 515 pp.
- Lit Par35 Milisenda C. C. (2001) GemmologieAktuell: Cuprian tourmaline from Nigeria. *Gemmologie: Zeitschrift der Deutschen Gemmologischen Gesellschaft*, Vol. 50, No. 3, pp. 121-122.
- Lit Par36 Milisenda C. C., Horikawa Y., Emori K., Miranda R., Bank F. H., Henn U. (2006) Neues Vorkommen kupferführender Turmaline in Mosambik [A new find of cuprian tourmalines in Mozambique]. *Gemmologie: Zeitschrift der Deutschen Gemmologischen Gesellschaft*, Vol. 55, No. 1-2, pp. 5-24.
- Lit Par37 Mozambique Paraiba tourmaline hot in Tucson (2007) *jewellery News Asia*, No. 272 (April), p. 56.
- Lit Par38 Petsch E. J. (1986) Riesen in Rot, Grün und Blau—Die Turmalin-Vorkommen in Mosambik. *Mineralientage München 85—Turmalin*, Oct. 18-20, Munich, Germany.
- Lit Par39 Rondeau B., Delaunay A. (2007) Les tourmalines cuprifères du Nigeria et du Mozambique [Cuprian tourmalines from Nigeria and Mozambique]. *Revue de Gemmologie*, No. 160, pp. 8-13.
- Lit Par40 Smith C. P., Bosshart G., Schwarz D. (2001) Gem News International: Nigeria as a new source of copper-manganese-bearing tourmaline. *Gems & Gemology*, Vol. 37, No. 3, pp. 239-240.
- Lit Par41 Wentzell C. Y. (2004) Lab Notes: Copper-bearing color-change tourmaline from Mozambique. *Gems & Gemology*, Vol. 40, No. 3, pp. 250-251.
- Lit Par42 Wentzell C. Y., Fritz E., Muhlmeister S. (2005) Lab Notes: More on copper-bearing color-change tourmaline from Mozambique. *Gems & Gemology*, Vol. 41, No. 2, pp. 173-175.
- Lit Par43 Wise R. W. (2007) Mozambique: The new Paraiba? *Colored Stone*, Vol. 20, No. 2, pp. 10-11.
- Lit Par44 Zang J. W., da Fonseca-Zang W. A., Fliss F., Höfer H. E., Lahaya Y. (2001) Cu-haltige Elbaite aus Nigeria. *Berichte der Deutschen Mineralogischen Gesellschaft, Beihefte zum European Journal of Mineralogy*, Vol. 13, p. 202.
- Literature arrived at printing date**
- Lit Par48 Koivula J. I., Nagle K., Shen A. H-T., Owens P. (2009) Solution-Generated Pink Color Surrounding Growth Tubes and Cracks in Blue to Blue-Green Copper-Bearing Tourmalines from Mozambique. *Gems & Gemology*, Vol. 40, No.1, pp. 44-47.

Origin	Brazil																				
Sample	3111-a						2079						2079 47	2965							
Color	blue		purple		yellowish-green		dark-green		violetish-blue		"neon"-greenish blue		green		"neon"-greenish-blue	Blue		Violet		Yellowish-green	
Qty	30		18		12		4		40		13		3		1	31		2		17	
	Avg	St Dev	Avg	St Dev	Avg	St Dev	Avg	St Dev	Avg	St Dev	Avg	St Dev	Avg	St Dev	Single	Avg	St Dev	Avg	St Dev	Avg	St Dev
Al	210000		210000		210000		210000		210000		210000		210000		210000	210000	210000	210000		210000	
Si	190807	6017	185328	2782	190583	5228	182675	2304	169928	4456	169423	1150	156200	2138	167600	176900	6421	178300	4525	178547	6582
B	39230	1217	37378	994	37908	994	36350	465	34978	1373	35638	681	33567	643	35000	37465	1347	37800	1273	37159	1906
Li	9804	379	9089	182	8952	261	8335	64	9679	340	9239	142	8453	85	9160	10009	654	10400	424	9794	450
Na	19017	521	17494	333	19158	399	20450	238	13143	536	14262	293	13767	115	14000	14806	800	14900	141	16524	710
Mn	27357	1161	23278	554	23125	1566	16275	1266	5379	2413	13546	1832	16167	473	13600	7609	5774	7285	1874	15371	2594
Cu	11439	506	10202	371	6995	1250	6555	281	4955	574	6819	223	6343	50	6660	9839	1965	9185	2001	5763	467
Be	47.0	4	22.7	3	20.69	3	11.7	2.1	16.6	2.5	15.4	2.0	17.1	2	15.5	24.0	7.2	26.6	2.9	16.9	3
Mg	59.65	256	15.8	46	2602	958	3495	165	bd to 1530		bd to 1.40		0.94	0.7	bd	4.44	4.3	86.3	53	543	145
K	153	6	137	3	175	62	164		93.5	58	98.6	5.4	103	1	97.2	115	39	114	7	126	8
Ca	2679	52	1316	210	1098	124	715	59	2047	253	1962	75	1897	25	1930	2107	195	2485	134	2014	166
Sc	0.426	0.07	0.380	0.1	0.36	0.1	0.322	0.1	0.449	0.06	0.541	0.09	0.519		0.473	0.411	0.05	0.547	0.08	0.456	0.09
Ti	22.3	18	36.8	52	517	109	953	33	bd to 80.5		174	59	279	18	175	5.15	3.3	332	122	389	163
V	0.742	0.6	1.92	1.8	7.44	1	18.9	3	0.546	0.24	0.694	0.15	0.976	0.1	0.661	0.483	0.1	1.82	0.9	3.00	1.1
Fe	55.0	157	22.8	40	2462	2133	18500	3676	bd to 189		84.1	43	201	55	74.7	bd to 79.80		784	320	1293	182
Zn	342	1399	49.3	88	4877	1798	5880	441	102	132	131	78	347	84	108	338	341	1845	912	9094	4118
Ga	124	4	173	27	158	36	79.3	5	290	17	299	5.4	278	3.6	296	104	12	124	22	148	40
Ge	37.0	1.9	51.9	11	41.5	9	18.8	2	11.6	2	8.04	0.5	7.51	0.2	7.15	22.8	11	53.5	0.57	33.4	14
Sr	0.617	0.2	0.256	0.05	2.12	3	16.9	2	bd to 1.36		bd to 0.41		0.030		bd	0.217	0.07	0.183	0.08	0.423	0.3
Nb	0.614	0.07	0.458	0.2	0.871	0.2	0.589	0.1	4.14	0.7	2.60	0.2	2.24	0.09	2.61	2.01	1.4	1.29	0.34	2.25	0.6
Sn	bd to 0.42		bd to 0.48		bd to 0.51		0.395	0.1	bd to 0.39		bd to 0.32		bd to 0.20		bd	bd to 1.25		bd to 0.35		0.438	0.1
Sb	4.57	0.4	3.54	0.9	5.22	0.7	4.31	0.6	7.46	33	0.525	0.07	0.832	0.3	0.598	4.11	4.4	14.3	1	13.6	2.2
Ta	5.77	0.2	1.00	0.25	0.375	0.1	0.121		4.34	1.3	2.28	0.1	2.04		2.24	2.08	0.50	0.934		0.886	0.3
Pb	48.6	3.5	18.7	7.9	13.4	6.9	32.3	1.8	18.8	4.0	14.5	0.4	13.0	0.9	14.2	24.4	3.3	8.5	3	15.3	9
Bi	1702	88	1228	184	630	197	239	16	217	82	91.5	10	70.0	0.8	89.2	980	829.1	1965	431	756	229
Th	0.3		0.04		bd to 0.17		bd to 0.01		0.19	0.1	0.1		0.1		0.10	0.16	0.1	0.15		bd to 0.21	
U	0.07		bd to 0.04		bd to 0.38		bd to 0.01		bd to 0.82		bd to 0.04		bd to 0.01		0.008	bd to 0.36		0.154	0.1	0.166	0.1
Cr	bd to 4.76		bd to 4.96		bd to 4.96		bd to 3.65		bd to 4.32		bd to 3.59		bd to 2.12		bd	bd to 5.48		3.65	0.28	bd to 4.65	
Co	bd to 0.65		bd to 0.09		0.720	0.7	7.17	1.8	bd to 0.17		bd to 0.62	0.30	bd		bd	bd tp 0.47	0.1	0.177	0.1	0.511	0.2
Rb	bd to 0.16		bd to 0.06		bd to 39.10		bd to 0.02		bd to 1.03		bd to 0.04		bd to 0.03		0.018	bd to 0.86	0.2	0.202	0.1	bd to 0.49	
Zr	bd to 0.33		bd to 0.04		bd to 0.02		bd to 0.01		bd to 0.33		bd to 0.03		bd tp 0.02		0.021	bd to 0.05		bd to 0.02		bd to 0.03	
Mo	bd to 1.06		bd to 0.86		bd to 0.45		bd to 0.32		bd to 0.24		bd to 0.28		0.242	0.07	0.280	bd to 0.079		0.173	0.1	0.267	0.1
Ag	bd to 0.28		0.136		0.179	0.07	0.242		0.140	0.05	0.15		0.162		0.086	0.178		0.115		0.169	
Cs	bd to 0.90		bd to 0.53		bd to 13.60		0.128	0.1	bd to 8.03		bd to 0.03		bd to 0.004		bd	bd to 1.06		bd to 0.11		bd to 0.28	
Ba	bd to 0.81		bd to 0.06		bd to 0.10		0.047		bd to 0.25		bd to 0.03		bd to 0.02		bd	bd to 0.20		0.373	0.4	bd to 0.16	
La	0.526	0.07	0.146	0.08	0.501	0.2	0.403		0.29	0.2	0.91	0.09	1.31	0.1	0.798	0.200	0.09	0.668	0.1	0.229	0.1
Ce	0.649	0.1	0.243	0.1	0.937	0.4	0.586	0.06	0.413	0.3	0.96	0.2	1.46	0.07	0.760	0.165	0.09	0.921	0.3	0.261	0.1
Pr	0.056		bd to 0.05		bd to 0.13		0.027		bd to 0.07		0.06		0.093		0.038	bd to 0.15		0.090	0.1	bd to 0.09	
Nd	bd to 0.36		bd to 0.18		bd to 0.36		0.096		bd to 0.21		bd to 0.20		0.172		0.061	bd to 0.07		bd		bd to 0.11	
Sm	bd to 0.12		bd to 0.14		bd to 0.17		bd		bd to 0.08		bd to 0.06		bd to 0.08		0.058	bd to 0.04		bd		bd to 0.04	
Eu	bd to 0.06		bd to 0.01		bd to 0.02		bd		bd to 0.01		bd to 0.01		bd to 0.01		bd	bd to 0.12		0.023		bd to 0.10	
Gd	bd to 0.13		bd to 0.07		bd to 0.07		bd		bd to 0.06		bd to 0.03		bd to 0.03		bd	bd to 0.04		bd		bd to 0.07	
Tb	bd to 0.02		bd to 0.01		bd to 0.01		bd to 0.01		bd to 0.01		bd to 0.002		bd to 0.002		bd	bd to 0.02		bd to 0.01		bd to 0.02	
Dy	bd to 0.05		bd to 0.04		bd to 0.04		bd		bd to 0.02		bd to 0.03		bd to 0.001		bd	bd to 0.04		bd to 0.01		bd to 0.02	
Ho	bd to 0.02		bd to 0.01		bd to 0.003		bd to 0.01		bd to 0.01		bd to 0.01		bd		bd	bd to 0.03		0.012		bd to 0.02	
Tm	bd to 0.005		bd to 0.01		bd to 0.01		bd to 0.01		bd to 0.004		bd to 0.004		bd to 0.002		bd	bd to 0.01		0.005		bd to 0.04	
Yb	bd to 0.05		bd to 0.04		bd to 0.08		bd		bd to 0.03		bd to 0.02		bd		bd	bd to 0.03		bd to 0.02		bd to 0.06	
Lu	bd to 0.007		bd to 0.003		bd to 0.003		bd to 0.002		bd to 0.01		bd to 0.003		bd to 0.002		0.002	bd to 0.01		bd to 0.02		bd to 0.02	
Pt	bd to 0.098		bd to 0.10		bd to 0.13		bd to 0.12		bd to 0.1		bd to 0.05		bd		bd	bd to 0.09		bd to 0.07		bd to 0.04	
Au	bd to 0.06		bd to 0.06		bd to 0.02		bd to 0.01		bd to 0.05		bd to 22.7		bd		22.7	bd to 0.03		bd to 0.01		bd to 0.07	

Table Par03: Chemical Compositions of Copper-Bearing Tourmalines from Brazil
LA-ICP-MS Analysis (in µg/g). Sample No. GRS-Ref2976

Origin	Brazil																	
Sample	2976-1				2976-2													
Color	blue		yellowish green/green		yellowish-green		purple/greenish-blue		"neon"-greenish-blue		purple/greenish-blue		purple		"neon"-greenish-blue		yellowish-green	
Qty	28		53		5		1		7		1		12		13		5	
	Avg	St Dev	Avg	St Dev	Avg	St Dev	Avg	St Dev	Avg	St Dev	Avg	St Dev	Avg	St Dev	Avg	St Dev	Avg	St Dev
Al	210000		210000		210000		210000		210000		210000		210000		210000		210000	
Si	168186	2338	172002	4941	217220	8205	237800		228000	5216	221400	2962	230954	5791	241040	3988		
B	34079	567	34715	1429	34960	1412	38900		37257	1103	35400	34675	497	36385	921	36980	559	
Li	9492	251	9605	322	9074	351	10500		10087	330	9820	8633	403	9935	379	10098	278	
Na	13211	302	14762	585	13240	559	14100		13443	351	13200	13167	242	13500	515	14800	283	
Mn	189	94	11850	3736	5610	958	2660		296	123	846	1420	270	470	386	4760	1741	
Cu	7920	1027	5603	948	3920	512	8040		7879	1135	8590	3487	1780	7560	1011	6268	2000	
Be	48.4	10	34.9	10	59.20	2	75.4		46	16	28.1	8.94	7	44.3	16	54.1	14	
Mg	bd to 1.50		230	126	259	102	14.2		bd to 3.60		bd	bd to 2.44		4.64	12	161	168	
K	83.5	10	102	5	95.8	5	92.8		84	23	81.6	88.2	11	85.8	5.9	95.3	4.4	
Ca	752	220	1625	390	1113	450	769		895	386	2110	486	487	984	382	783	115	
Sc	0.440	0.06	0.439	0.07	0.357		0.430		0.435		0.36	0.348		0.304		0.333		
Ti	bd to 19.40		293	156	441	85	49.4		bd to 9.67		1.09	bd to 2.91		bd to 16		307	261	
V	0.45	0.1	2.13	0.80	1.10	0.35	0.440		0.376	0.1	0.28	0.286	0.1	0.428	0.23	0.763	0.35	
Fe	bd to 36.40		1787	803	2550	459	379		27.4	34	7.29	bd to 8.01		bd to 70		1799	1464	
Zn	12.2	12	1564	671	1564	311	428		26.6	27	11.5	14.8	7	112	312	1234	795	
Ge	111	8.6	153	33	160	13	114		121	8	124	143	6	124	12	142	31	
Ge	33.7	4.5	33.3	10	42.5	3.3	40.1		34.5	5	n/a	0.00		0.000		0.000		
Sr	0.078	0.07	0.189	0.2	0.059		0.166		0.110	0.2	0.127	bd to 0.22		0.097	0.06	0.125	0.07	
Nb	0.120		0.918	0.2	0.566	0.11	0.309		0.149	0.1	0.544	0.229	0.1	0.211	0.15	0.668	0.45	
Sn	bd to 0.94		bd to 0.70		bd to 0.40		bd		bd to 0.29		0.188	bd to 0.48		bd to 2.08		0.323	0.11	
Sb	7.35	2.9	13.65	2	7.87	0.79	14.4		5.31	1.5	4.14	6.80	11	7.81	3.6	9.82	2.2	
Ta	1.03	0.3	0.449	0.1	0.406	0.06	0.412		1.32	0.7	2.32	1.01	0.4	1.40	0.68	0.533	0.18	
Pb	33.66	7	17.2	11	7.31	3.3	23.3		34.2	5.6	51.5	8.67	11	35.2	5.3	16.12	10.4	
Bi	3600	1207	2702	1250	3428	383	3860		2441	1085	1390	285	385	2455	1201	3524	632	
Th	bd to 2.03		bd to 0.46		0.776	0.43	0.308		1.26	0.6	0.53	0.07	0.1	1.16	0.61	0.33	0.15	
U	0.132	0.1	bd to 0.67		0.292	0.41	0.020		0.094	0.1	0.080	bd to 0.17		0.115	0.10	0.027		
Cr	bd to 20		bd to 43.1		bd to 2.23		bd		bd to 2.46		bd	bd to 188		12.5	13	7.62	9.9	
Co	bd to 0.44		0.468	0.3	0.838	0.42	0.242		bd to 0.12		0.035	bd to 0.38		bd to 0.23		bd to 1.08		
Rb	bd to 0.28		bd to 3.65		bd to 0.14		bd		bd to 0.02		0.079	bd to 8.16		bd to 0.78		bd to 0.47		
Zr	bd to 0.04		bd to 0.07		bd to 0.03		0.021		bd to 0.02		bd	bd		bd		bd		
Mo	bd to 0.98		bd to 1.18		bd to 0.15		0.059		bd to 0.09		n/a	n/a		n/a		n/a		
Ag	bd to 0.27		bd to 0.62		0.073		0.154		bd to 0.14		0.223	0.15		bd to 0.26		0.097		
Cs	bd to 13.90		bd to 0.65		bd to 0.05		0.066		bd to 1.11		0.140	bd to 1.1		1.59	3.1	0.114	0.1	
Ba	bd tp 3.90		bd to 2.00		bd to 0.02		bd		bd to 0.01		bd	bd to 1.23		bd to 0.26		bd to 0.05		
La	bd to 0.04		0.360	0.3	0.119	0.09	0.023		bd to 0.03		0.063	bd to 0.04		bd to 0.10		0.052	0.1	
Ce	bd to 0.34		0.816	0.6	0.301	0.30	0.014		bd to 0.11		0.043	bd to 0.03		bd to 0.17		bd to 0.37		
Pr	bd to 0.13		bd to 0.25		bd to 0.03		0.002		bd to 0.003		0.021	bd to 0.01		bd to 0.14		bd to 0.04		
Nd	bd to 0.04		bd to 0.49		bd to 0.15		bd		bd		bd	bd to 0.03		bd to 0.05		bd to 0.10		
Sm	bd to 0.06		bd to 0.32		bd to 0.13		bd		bd		0.044	bd to 0.04		bd to 0.02		bd to 0.09		
Eu	bd to 0.09		bd to 0.19		bd to 0.04		bd		bd to 0.03		0.022	bd to 0.04		bd to 0.07		bd to 0.01		
Gd	bd to 0.06		bd to 0.28		0.057		bd		bd to 0.03		bd	bd to 0.04		bd		bd		
Tb	bd to 0.02		bd to 0.09		bd to 0.02		0.008		bd to 0.006		n/a	n/a		n/a		n/a		
Dy	bd to 0.08		bd to 0.09		bd to 0.06		bd		bd to 0.01		bd	bd to 0.02		bd to 0.02		bd		
Ho	bd to 0.03		bd to 0.10		bd		bd		bd to 0.02		n/a	n/a		n/a		n/a		
Tm	bd to 0.03		bd to 0.04		bd		0.004		bd to 0.001		n/a	n/a		n/a		n/a		
Yb	bd to 0.07		bd to 0.07		bd to 0.01		0.008		bd to 0.01		bd	bd to 0.03		bd to 0.01		bd to 0.01		
Lu	bd to 0.04		bd to 0.07		bd		0.006		bd to 0.01		bd	bd to 0.004		bd to 0.003		bd		
Pt	bd to 0.07		bd to 0.11		bd		bd		bd to 0.04		n/a	n/a		n/a		n/a		
Au	bd to 0.04		bd to 0.08		bd to 0.03		bd		bd		bd	bd to 0.05		bd to 0.04		bd to 0.04		

**Table Par05: Chemical Compositions of Copper-Bearing Tourmalines from Mozambique
LA-ICP-MS Analysis (in µg/g). Sample No. GRS-Ref2939, 2942, 2943, 3138, 3143**

Origin Sample Color	Mozambique																	
	2939 Violet			2942 Green			2942.2 Yellowish-Green			2943 Blue Green			3138 Vivid Green			3143 Purple		
	Avg	St Dev	Qty	Avg	St Dev	Qty	Avg	St Dev	Qty	Avg	St Dev	Qty	Avg	St Dev	Qty	Avg	St Dev	Qty
Al	210000		3	210000		3	210000		3	210000		3	210000		6	210000		6
Si	164967	1966		164467	1498		161867	1401		165967	1069		169633	2038		164767	2482	
B	34400	529		35200	300		34233	306		34967	513		34783	850		33233	843	
Li	10167	231		8837	110		8197	35		8527	238		7698	187		8442	135	
Na	13933	208		18600	173		16967	153		17000	361		16133	398		13750	266	
Mn	11333	208		37500	346		34867	1747		30367	814		28133	258		7777	1234	
Cu	3237	95		2490	35		2427	416		3350	401		1945	69		1802	141	
Be	32.6	5.5		28.7	1.7		18.0	2.9		17.5	3.2		7.69	2.9		7.94	2.3	
Mg	2.16	0.7		3.05	1.0		4.46	6.0		9.95	9.5		2.34	1.5		bd to 142		
K	134	8.0		196	7.5		175	5.0		160	17		171	2.3		131	8.5	
Ca	4917	90		1860	46		1620	122		1417	170		561	18		780	36	
Sc	0.421	0.09		9.76	0.21		2.82	0.39		1.04	0.13		2.06	0.12		0.679	0.06	
Ti	44.0	12		224	9.7		216	85		103	7.8		267	11		bd to 3.15		
V	0.542	0.29		2.35	0.41		1.09	0.15		2.51	1.1		1.54	0.14		0.570	0.45	
Fe	56.3	66		355	55		181	45		287	232		189	12		bd to 40.7		
Zn	4.35	2.1		6.89	0.88		8.84	0.55		11.7	2.0		17.1	2.0		bd to 2.16		
Ga	343	6.1		392	6.00		404	13.6		398	4.6		435	6.8		446	12	
Ge	7.68	0.27		11.1	0.25		8.98	0.53		11.2	0.81		5.59	0.31		7.52	0.45	
Sr	0.462	0.28		1.39	0.05		0.231	0.02		0.387	0.09		0.079	0.02		0.130	0.03	
Nb	2.81	0.20		1.36	0.14		0.903	0.10		1.78	0.47		0.54	0.05		0.316	0.05	
Sn	4.44	0.13		14.7	0.51		8.80	0.16		3.85	0.21		9.17	8		2.53	1.0	
Sb	5.91	0.09		3.61	0.24		1.06	0.06		1.90	0.52		0.48	0.11		1.33	0.11	
Ta	2.36	0.09		1.63	0.10		1.00	0.17		1.32	0.08		0.41	0.05		0.404	0.03	
Pb	80.6	1.2		74.5	1.1		34.2	1.8		49.6	1.0		8.78	2.2		18.4	6	
Bi	967	12		858	4.4		258	19		467	63		27.1	0.71		151	4	
Th	0.68	0.08		0.15	0.02		0.13	0.01		0.12	0.03		bd to 0.011			bd to 0.018		
U	0.064	0.02		bd to 0.147			bd			bd to 0.066			bd to 0.047			bd to 0.081		
Cr	8.13	5.2		9.92	3.8		6.38	3.0		bd to 22.9			bd to 3.52			bd		
Co	0.073	0.05		0.079	0.01		bd to 0.05			bd			1.33	1.4		bd to 1.13		
Rb	bd to 2.24	bd		bd to 0.054			bd to 0.060			bd to 0.093			0.062	0.03		bd to 0.064		
Zr		bd		bd to 0.010			bd to 0.119			bd to 0.036			bd to 0.029			bd to 0.018		
Mo	0.185	0.07		0.473	0.22		0.387	0.25		bd to 0.567			0.301	0.08		bd to 0.272		
Ag	bd to 0.06			0.034	0.01		bd to 0.102			bd to 0.068			bd to 0.098			bd to 14.7		
Cs	bd to 0.068			bd to 0.054			bd to 0.071			0.013	0.00		bd to 9.05			bd to 0.056		
Ba	bd to 0.12			bd to 0.193			0.113	0.04		bd			bd to 0.069			bd to 0.084		
La	bd to 0.082			bd to 0.047			0.022	0.01		bd to 0.232			bd to 0.004			bd to 0.004		
Ce	0.066	0.02		0.044	0.02		bd to 0.029			0.111	0.11		bd to 0.241			bd to 0.012		
Pr	bd to 0.011			bd to 0.010			bd to 0.011			0.018	0.02		bd to 0.008			bd to 0.007		
Nd				bd to 0.088			bd to 0.073			bd to 0.163			bd			bd to 0.021		
Sm	bd to 0.086			bd to 0.053			bd			bd to 0.049			bd to 0.040			bd to 0.023		
Eu	bd to 0.015			bd			bd to 0.007			bd to 0.006			bd to 0.006			bd to 0.011		
Gd				bd			bd to 0.053			bd to 0.071			bd to 0.020			bd		
Tb				bd			bd to 0.004			bd to 0.007			bd to 0.006			bd to 0.006		
Dy	bd to 0.017	0.00		bd to 0.015			bd			0.028	0.02		bd to 0.011			bd to 0.006		
Ho				bd to 0.008			bd to 0.016			bd			bd to 0.003			bd to 0.013		
Tm	bd to 0.01			bd to 0.003			bd			bd to 0.003			bd to 0.003			bd to 0.006		
Yb	bd to 0.004			bd to 0.042			bd to 0.022			bd to 0.062			bd to 0.062			bd to 0.018		
Lu	bd to 0.007			bd to 0.007			bd to 0.008						bd to 0.003			bd to 0.003		
Pt	bd to 0.035			bd			bd						bd			bd to 0.130		
Au				bd			bd						bd to 0.022			bd to 0.071		

Ba contaminations were found in the surface layer of the following samples (concentrations in ppm)

Sample No. Ba-concentrations

2942	37.7 ppm
2942.2	65.8 ppm
2939	44.0 ppm
2343	66.8 ppm

GRS Table Par06: Chemical Compositions of Copper-Bearing Tourmalines from Nigeria
LA-ICP-MS Analysis (in µg/g)

Origin	Nigeria		Nigeria		Nigeria		Nigeria		Nigeria	
Sample	N 1533_lot 4.88		N 0671_kt 23.77		Ref. 2877		Ref. 2876		N 0441	
Qty	5		5		5		5		5	
Type	Avg	StDev	Avg	StDev	Avg	StDev	Avg	StDev	Avg	StDev
Al	210000		210000		210000		210000		210000	
Si	167860	2802	165280	2428	165480	1483	169120	1757	168380	1370
B	33560	646	32560	532	32560	181	32820	408	33420	465
Li	9810	188	10058	94	10060	89	9880	163	9952	47
Na	12820	383	11760	151	11500	18	12000	70	11580	109
Mn	6354	325	3066	73	659	35	3074	130	3292	41
Cu	3066	201	1634	59	1966	36	2534	65	1736	27
Be	33.0	4.8	30.2	7	29	4	36	3.2	35.2	6
Mg	bd to 0.23		bd		2.0	1	bd to 4.72		6.7	1.1
K	109	2.7	100	2.2	102	2	103	1.1	113	1.1
Ca	5208	118	5726	118	4786	136	5120	86	5746	66
Sc	bd to 0.48		bd to 0.47		bd to 0.43		bd to 0.47		0.3	0.1
Ti	bd		bd to 1.52		bd to 2.46		bd to 2.58		bd to 1.92	
V	0.4	0.1	0.4	0.3	bd to 0.53		0.3	0.1	bd to 0.34	
Fe	79.4	5.3	20.4	3.4	48.9	6	bd to 14.6		58.7	6
Zn	1360	86	10.1	0.8	9.3	2.1	36.6	2.3	17.1	1.2
Ga	105	3.6	103	2.5	133	3.8	98	1.5	105	3.2
Ge	24.3	0.7	22.6	1.2	33.8	1.5	26.3	1.1	24.2	0.4
Sr	20.6	0.7	119	2.6	138	3.7	21.8	0.4	117.4	0.9
Nb	2.8	0.1	3.8	0.1	1.0	0.1	2.6	0.1	4.0	0.2
Sn	0.9	0.1	1.3	0.1	1.9	0.4	1.8	0.4	1.3	0.1
Sb	9.8	0.6	12.2	0.5	55.4	1.6	13.9	0.5	12.8	0.6
Ta	20.0	1.0	13.7	1.2	8.9	0.5	15.8	0.3	15.1	0.2
Pb	1102	39	1102	37	487	17	1222	25	1156	1
Bi	273	6	348	12	323	12	379	6	368	3
Th	1.1	0.1	1.3	0.2	2.0	0.1	0.7	0.1	1.7	0.1
U	bd		bd		bd to 0.004		bd to 0.004		bd to 0.003	
Cr	bd		bd		bd to 2.04		bd		bd to 2.19	
Co	bd		bd to 0.06		bd		bd to 0.06		bd to 0.03	
Rb	bd to 0.97		bd to 0.14		bd		bd		bd to 0.10	
Zr	bd to 0.06		bd to 0.02		bd to 0.03		bd to 0.03		0.11	0.03
Mo	bd to 0.05		bd		bd		bd to 0.10		bd	
Ag	bd to 0.03		bd to 0.11		bd to 0.11		bd to 0.12		bd to 0.06	
Cs	bd to 0.89		bd to 0.13		bd		bd to 0.02		bd to 0.01	
Ba	bd to 0.06		bd to 0.11		bd to 0.06		bd		0.17	0.10
La	0.08	0.02	bd to 0.01		0.03	0.01	bd to 0.10		bd to 0.02	
Ce	bd to 0.01		bd to 0.20		0.11	0.16	bd		0.02	0.01
Pr	bd to 0.002		bd to 0.00		bd to 0.005		bd to 0.002		bd to 0.002	
Nd	bd to 0.01		bd to 0.02		bd to 0.03		bd to 0.01		bd to 0.02	
Sm	0.01	0.01	bd to 0.17		bd to 0.02		bd		bd to 0.03	
Eu	bd to 0.01		bd to 0.14		bd		bd to 0.005		bd to 0.00	
Gd	bd to 0.04		bd		bd to 0.04		bd to 0.02		bd to 0.04	
Tb	bd		bd		bd		bd		bd	
Dy	bd to 0.01		bd to 0.01		bd to 0.01		bd to 0.01		bd to 0.01	
Ho	bd		bd to 0.004		bd		bd to 0.004		bd to 0.004	
Tm	bd to 0.004		bd to 0.01		bd to 0.003		bd to 0.01		bd to 0.003	
Yb	bd to 0.02		bd		bd		0.01	0.01	bd	
Lu	bd		bd to 0.009		bd to 0.005		bd to 0.009		bd to 0.004	
Pt	bd to 0.03		bd to 0.03		bd to 0.03		bd		bd	
Au	0.10	0.03	bd to 0.09		bd to 0.07		bd to 0.09		bd to 0.29	

Copper-bearing tourmaline with “Paraiba”-type color are considered the most valuable gems in the world of tourmalines. A documentation of recent and historical pictures of the mines in Brazil is presented in this report together with statistics on size and color of the most valuable tourmalines from different localities.

This study also derives a more simple and inexpensive chemical fingerprinting useful for origin and authenticity analysis of these tourmalines. For this purpose, color-zoned copper-bearing tourmalines from Brazil (such as from Paraiba) and from Mozambique have been analyzed by different chemical testing methods (EMPA, LA-ICP-MS, ED-XRF and LIBS).

Tourmalines from different origins can be separated, because they developed a different pattern of “Chemical Variations” during their growth.

